INVESTIGATION OF THE POSSIBLE ONCOGENIC ROLE OF NLRP7 IN HUMAN ENDOMETRIUM CANCER

by

Gizem Olay Artık

B.S., Molecular Biology and Genetics, Istanbul Technical University, 2016

Submitted to the Institute for Graduate Studies in
Science and Engineering in partial fulfillment of
the requirements for the degree of
Master of Science

Graduate Program in Molecular Biology and Genetics

Boğaziçi University

2019

ACKNOWLEDGEMENTS

Firstly, I would like to thank my supervisor Prof. Nesrin Ozoren for giving me the opportunity to work in her laboratory. She always supported me to follow my curiosity throughout my master project. I am also thankful to my thesis committee members Assoc. Prof. Ceren Cıracı and Assoc. Prof. Umut Sahin for spending their valuable time to evaluate my thesis.

I would like to thank Bogazici University and TUBITAK for their financial support during my master thesis. This project was supported by the funds of TUBITAK project number 217Z131.

I also want to thank all current and former AKİL lab members and MBG department for their help during my master studies and writing the thesis.

I want to thank specially İlke Süder, Özen Kaya, Farukcan Tolunay and Harun Öztürk for their friendship and amazing work relationship in every situation between us. They have kept my motivation at high level even in hard times and give me a second family.

My special thanks go to my parents Betül and Hüseyin Artık for their love and support.

ABSTRACT

INVESTIGATION OF THE POSSIBLE ONCOGENIC ROLE OF NLRP7 IN HUMAN ENDOMETRIUM CANCER

NLRP7 is an innate immune protein that is involved in the activation of pro-inflammatory caspases by participating in inflammasome oligomerization. So far, mutations in NLRP7 have been associated with Hydatidiform Mole disease, characterized by excessive trophoblastic proliferation and lack of embryo development. Besides, NLRP7 is proposed to have an oncogenic role since its expression levels significantly increase in testicular seminoma and endometrial cancer tissues. However, the mechanism(s) behind its oncogenic contribution is currently unknown. Here, we analyzed the protein interactome of NLRP7 to fully elucidate putative pathways and molecular mechanisms through which NLRP7 may drive oncogenesis in the context of human endometrium cancer. We conducted protein network analysis using the Ingenuity Pathway tool, which showed that the Ras pathway is at the center of the network comprised by NLRP7 interactors. Then, we validated the physical interaction between NLRP7 and selected partners using co-immunoprecipitation. Our initial results indicated that NLRP7 might be an effector protein of two Ras-related GTPases and it also may interfere with the DNA damage response pathways via ATM-Brat1-Chk1 axis. Moreover, we showed that NLRP7 is modified by Small Ubiquitin-Like Modifier (SUMO), which may explain its upregulation in human endometrium cancer. Taken together, our results illuminate a protein network of NLRP7, show novel interaction partners and a modification of the same protein, and provide new insights into the contribution of NLRP7 to oncogenesis. We expect that our results will lead to a better understanding of the role of NLRP7 in human endometrium cancer and possibly pave the way for future therapies.

ÖZET

İNSAN ENDOMETRİUM KANSERİNDE NLRP7 PROTEİNİN OLASI ONKOGENİK ROLÜNÜN ARAŞTIRILMASI

NLRP7 inflamazom oligomerizasyonuna katılarak proinflamatuar kaspazların aktivasyonuyla ilişkili olan doğal immünite proteinidir. Bügüne kadar NLRP7 üzerindeki mutasyonlar, aşırı trofoblastik çoğalma ve embriyo gelişiminin olmaması ile karakterize edilmiş Mol (Üzüm) Gebelik hastalığı ile ilişkilendirilmiştir. Üstelik NLRP7'nin ifade seviyesinin testis seminom ve endometriyal kanser dokularında dikkate değer şekilde artmasından ötürü bu proteinin onkojenik rolü olabileceği öne sürülmüştür. Fakat bu onkojenik katkının arkasındaki mekanizma(lar) halen bilinmiyor. Burada, insan endometriyal kanseri bağlamında NLRP7'nin onkojenezi tetikleyebileceği olası yolak ve moleküler mekanizmaları bütünüyle aydınlatmak için NLRP7'nin protein interaktomunu analiz ettik. Ingeunity Pathway aracını kullanarak protein ağ analizi yaptık ve Ras yolağının bu ağın merkezinde olduğunu gösterdik. Sonrasında seçtiğimiz partnerlerle NLRP7 arasındaki fiziksel etkileşimi birlikte immün çöktürme yoluyla teyit ettik. İlk sonuçlarımız NLRP7'nin Ras ilişkili GTPase enzimlerinin efektör proteini olabileceğini ve ayrıca bu proteinin DNA hasarı onarım yolağına ATM-Brat1-Chk1 ekseni yoluyla müdahil olabileceğini gösterdi. NLRP7'nin küçük ubikitin benzeri modifiye edici (SUMO) tarafından modifiye edildiğini gösterdik ki bu NLRP7'nin insan endometriyum kanserinde yüksek ifadesini açıklayabilir. Özetle, sonuçlarımız NLRP7'nin bir protein ağına ışık tutuyor, aynı proteinin yeni etkileşim partnerleri ve bir modifikasyonunu gösteriyor ve NLRP7'nin onkojenezdeki katkısına yeni bakış açıları sağlıyor. Sonuçlarımızın NLRP7'nin insan endometriyum kanserindeki rolünün daha iyi anlaşılmasını sağlayacağını ve belki de yeni terapilerin önünü açabileceğini umuyoruz.

TABLE OF CONTENTS

LIST OF FIGURES

LIST OF TABLES

LIST OF SYMBOLS

g	Gram
h	Hour
kDa	Kilodalton
L	Liter
M	Molar
ml	Mililiter
mM	Milimolar
ng	Nanogram
V	Volt
α	Alpha
β	Beta
μg	Microgram
μl	Microliter
μM	Micromolar
^{o}C	Degree Celcius

LIST OF ACRONYMS/ABBREVIATIONS

AD	Acidic Trans-Activation Domain
BIR	Baculoviral Inhibition of Apoptosis Repeat
CARD	Caspase Activation and Recruitment Domain
CDS	Cytosolic dsDNA Sensor
CLR	C-type Lectin Receptor
DAMP	Danger Associated Molecular Pathogens
DUB	Deubiquitinase
FGR	Fetal Growth Restriction
HM	Hydatidiform Mole
Hec1a	Human Endometrium Cancer Cell Line
HMGB1	High-Mobility Group Box 1
IL-18	Interleukin-18
IL-1β	Interleukin-1 Beta
IPSC	Induced Pluripotent Stem Cells
LPS	Lipopolysaccharide
LRR	Leucine-Rich Repeats
NAD	NACHT-Associated Domain
NLR	NOD-Like Receptor
NLRP	Pyrin Domain Containing NLR Protein
PAMP	Pathogen Associated Molecular Pattern
PBMC	Peripheral Blood Mononuclear Cells
PRR	Pathogen Recognition Receptor
RLR	RIG-I-Like Receptor
STAMBP	STAM-Binding Protein
SUMO	Small Ubiquitin-Like Modifier
TLR	Toll-Like Receptor

1. INTRODUCTION

1.1. Innate Immunity

In the simplest terms, our immune system is responsible for providing effectual and impressive protection against invasive pathogens and diseases such as cancer. The protection status from foreign pathogens has been divided into two general types of reactions: reactions of innate immunity and reactions of adaptive immunity. Although adaptive and innate immunity differs from each other with respect to their effector cell types, memory, speed of response and the specificity against pathogens, recent studies showed that these two reactions overlap and interact in particular concepts [1].

Innate immunity defends the organism against pathogens while tolerating the host flora which also contains various beneficial microorganisms. This defense mechanism is evolutionarily conserved among plants, invertebrates, and mammals whereas adaptive immunity emerged 500-700 million years ago only in vertebrates. The innate immune system is characterized by the rapid response (within minutes to hours) and non-specificity to particular pathogens since the innate immune recognition is based on germ-line encoded receptors. The innate immune system also primes the adaptive immunity which provides memory and long-lasting immunity [2].

Although the innate defense is ancient and found even in the simplest organisms, it has a complex structure consisting of four different elements: surface barriers, chemical barriers, cellular defenses, and pattern recognition molecules (Figure 1.1). Physical barriers contain almost all tissues, particularly skin, reproductive tract, gastrointestinal tract and respiratory tract in mammals. Despite physical defenses, pathogens can achieve to get into the body using the mechanisms they developed to overcome the first barriers of the host defense system. In this instance, there is a secondary defense mechanism, chemical barriers, that fight against the pathogens. Some of the examples of chemical barriers include gastric fluid, blood proteins, urination process, and blood-brain barrier [3]. The next element of innate defense is cellular defenses

which involve numerous cell types such as neutrophils, macrophages, dendritic cells, myeloid-derived suppressor cells, and innate lymphoid cells. These cells attack and eliminate pathogens using different strategies such as releasing toxins and engulfing pathogens. Although innate immune cells play an instrumental role, non-immune cells such as epithelial cells, endothelial cells, and fibroblasts also contribute to effector role of innate immunity [4]. Altogether, the cellular innate immune response provides a barrier to prevent pathogen infections. An essential feature of the host immune response is the discrimination of non-self molecules from self molecules using certain pattern recognition molecules. Pattern recognition receptors can be found on the cell surface, cytoplasm, cellular compartments or they can be found in their released forms in the bloodstream to activate pro-inflammatory immune signals. Another important part of innate immunity is the complement system containing a great number of proteins that operate as a cascade to activate inflammation, lysis of infected cells, opsonization, and immune clearance. In addition to the complement system, cytokines that are produced from main immune cells and some epithelial cells, also maintain and regulate innate immunity [5].

1.2. Pathogen Recognition Receptors

Pathogen recognition receptors (PRRs) immediately recognize and react to the pathogen-associated molecular patterns (PAMPs) and danger associated molecular pathogens (DAMPs). PAMPs are molecular motifs such as carbohydrate, polypeptide, LPS, peptidoglycan, flagellin, and nucleic acid parts whereas DAMPs are endogenous molecules such as ATP, heat shocked proteins, uric acid, high-mobility group box 1 (HMGB1), which are released from infected and damaged cells. PAMPs are signatures of pathogens such as bacteria, viruses, and parasites and they allow the recognition of "self" and "non-self" to avoid the host destruction since they are not produced from host cells. Upon interaction with PAMPs and DAMPs, PRRs initiate changes in the transcriptional and post-translational attitude of innate immune cells that leads to the secretion of cytokines and chemokines by the effector cells.

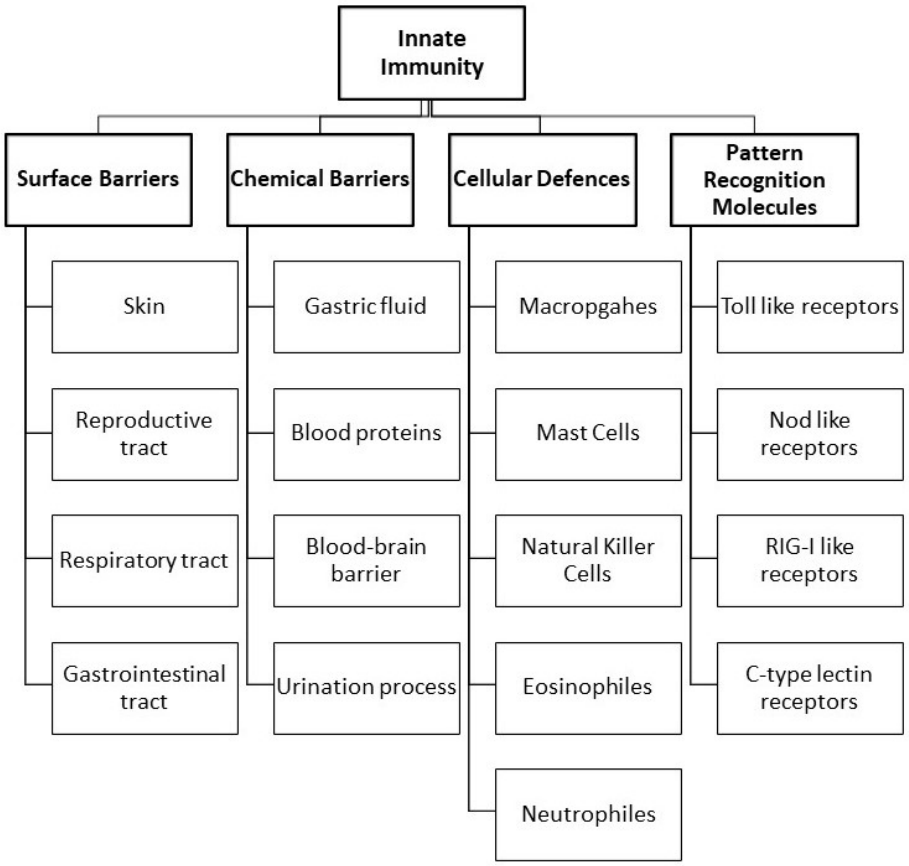

Figure 1.1. Main components of innate immunity. As a defense mechanism, the specialized components of innate immunity are comprised of surface barriers, chemical barriers, cellular defenses and pattern recognition molecules.

PRRs are divided into five subtypes: Toll-like receptors (TLRs), NOD-Like Receptors (NLRs), RIG-I-Like Receptors (RLRs), C-type Lectin Receptors (CLRs) and cytosolic dsDNA sensors (CDSs) [4]. These receptors are found in critical locations such as cell surfaces, endosomes, and cytoplasm to sense the invading pathogens.

1.3. NOD-Like Receptors

NOD-like receptors (NLRs) are the most recently discovered intracellular pathogen sensors compared to other sub-types of PRRs and they have a key role in the regulation of the innate immune response [6]. Although they are typically found in lympho-

cytes, dendritic cells, and macrophages, they can also be present in non-immune cell types like epithelial cells. All NLRs share a NACHT or NOD domain, which mediates ATP-dependent self oligomerization, at their center and an LRR domain at their C-terminal, which senses the presence of ligands. NOD-like receptor family consist of 22 cytoplasmic receptor proteins. These receptors are divided into four sub-groups based on their N-terminal effector domain that provides a unique function (Figure 1.2). NLRA contains an acidic transactivation domain (AD) domain and plays a key role in transcriptional regulation of MHC II antigen presentation. NLRB has a baculoviral inhibition of apoptosis repeat (BIR) domain and has a role in host defense. NLRC is distinguished by caspase activation and recruitment domain (CARD) through which it homo-typically interacts with other CARD domain containing proteins to trigger a signaling cascade. Pyrin domain containing NLR proteins are called as NLRP and their most known function is inducing the oligomerization of inflammasome complex by making a homotypic protein-protein interaction with ASC adaptor protein. In addition to aforementioned NLR proteins, a new intriguing member termed as NLRX has also been discovered with a mitochondria targeting sequence at the N-terminal that causes its localization to the mitochondria [7].

The major role of many NLRs is inflammasome activation. Inflammasomes are formed in myeloid cells of the innate immune system and they promote activation of procaspase-1 and maturation of pro-inflammatory cytokines like IL-1β and IL-18 by recruiting caspase-1, ASC adaptor, and NLR proteins. NLRP3, NLRP1b, and NLRC4 are the most studied and established inflammasomes. Additionally, there are other inflammasomes forming NLRs such as NLRP6, NLRP7, NLRP2, and NLRP12 but these are not well characterized. Two signals are required to trigger inflammation through a canonical pathway. The first priming signal activates NF-κB pathway, which drives the expression of pro-IL1β. The second signal leads to the assembly of the inflammasome complex. When the complex formation is achieved, procaspase-1 is cleaved into active caspase-1 enzyme which in turn causes IL-1β maturation and leads to the secretion of IL-1β. Through the canonical pathway, activation of caspase-1 results in the secretion of IL-1β which triggers pyroptosis, a form of inflammatory cell death.

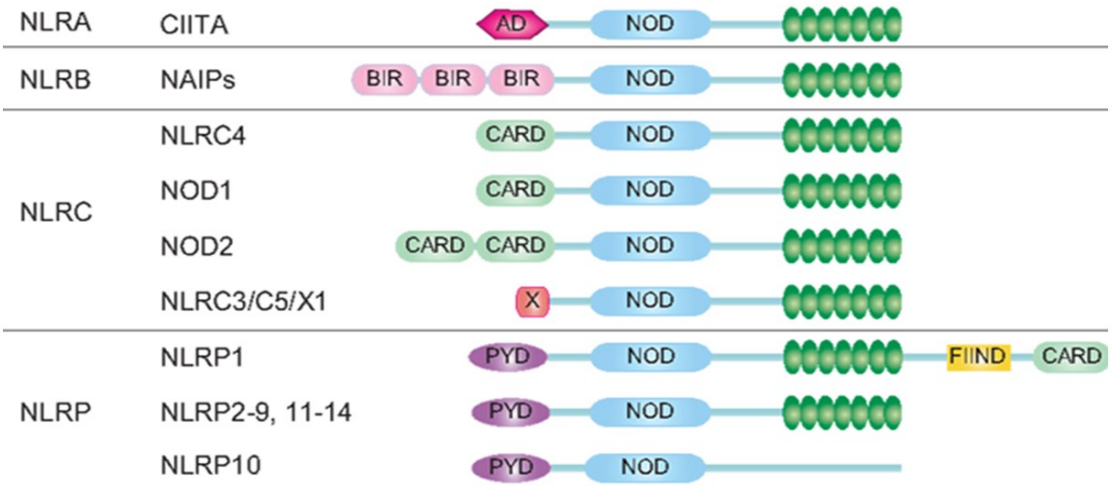

Figure 1.2. The Representation of Human NLR Family Protein Domains. CARD: Caspase recruitment domain; AD: Acidic transactivation domain, NOD: nucleotide-binding domain, BIR: Baculoviral inhibitory repeat-like domain, X: Unknown, PYD: Pyrin domain. Green circles: LRR (Leucine-rich repeat) domain.

In contrast to the caspase-1 dependent inflammasome activation, there are other underrecognized pathways to process IL-1β. For instance, some particular proteases such as caspase-8 cleave pro- IL-1β to its mature form [8]. Although inflammasomes are mostly known for their role in host defense, dysregulation of inflammasomes has been associated with diseases like cancer, autoimmune and neurodegenerative diseases [9].

1.4. NLRP7

NLRP7 is a member of the NLR family and it consists of an N-terminal pyrin domain, followed by a NACHT-associated domain (NAD), and a C-terminal leucine-rich repeat (LRR) region. Although we referred to it as NLRP7 in this thesis, various names such as NALP7, PYPAF3, PAN7, NOD12, and HYDM have been used across the scientific literature and public biological databases, which sometimes make it diffi-

cult to reach the information about this protein. In 2004, the chromosomal location of NLRP7 gene was mapped as 19q13.4 within a cluster of some other NLRP genes via genomic sequence analysis and it was determined that it contains 11 exons [10]. NLRP7 gene has appeared relatively later in evolution and it is found in primates and certain mammalians including human, chimpanzee, orangutan, gibbon, macaque, marmoset, horse, cow, and pig. Although NLRP7 does not have a true mouse orthologous gene, NLRP2 is the closest relative of it and located adjacent to NLRP7 on human chromosome 19 [11]. In light of this information, it is proposed that NLRP7 gene is originated as a consequence of a gene duplication event from NLRP2 after speciation [12].

NLRP7 is abundantly expressed in thymus, spleen and bone marrow, suggesting a role in inflammation and host defense. However, its expression is not restricted to the immune system. Kinoshita *et al.* detected the expression of NLRP7 in various tissues including placenta, ovary, spleen, lung, liver, kidney, pancreas, thymus, prostate, testis, small intestine, colon, and peripheral blood leukocytes. Conversely, they could not determine its expression in heart, brain, and skeletal muscle using RT-PCR analysis In addition, they determined NLRP7 as an anti-inflammatory protein for the first time. In that paper, it was claimed that NLRP7 is a feedback regulator of IL-1β. They observed that when THP-1 cells, which stably express NLRP7, are stimulated by lipopolysaccharide, caspase-1-dependent IL-1β secretion is revoked, therefore, NLRP7 acts like an anti-inflammatory protein [13].

The first observations had advocated NLRP7 as an anti-inflammatory protein, however, the following publications showed the opposite [14]. NLRP7 was determined as an intracellular receptor against bacterial acylated lipoproteins and its activation triggers subsequent ASC-dependent caspase-1 activation, IL-1β and IL-18 maturation. Moreover, using siRNA-based knockdown screening researchers showed that depletion of NLRP7 results in impaired IL-1β secretion against heat-killed *Mycoplasma spp.*, *Staphylococcus aureus* or *Legionella pneumophilia.* Furthermore, NLRP7 has also been found to be crucial to restrict growth of intracellular bacteria, *Staphylococcus aureus* and *Listeria monocytogenes*, in macrophages [15].

Our former lab member, Duygu Demiröz, also revealed the interaction between NLRP7, ASC, and Caspase-1 (2012, M.S. thesis). In 2016, another study showed that *M. bovis* infection activates NLRP7 inflammasome which results in IL-1β secretion, induction of pyroptosis, and upregulation of TNF-α in human THP-1 macrophages [16]. Nowadays, NLRP7 is accepted as a pro-inflammatory protein due to these observations.

Besides its role in the inflammasome formation, different roles of NLRP7 have been revealed. Messaed *et al.* observed that peripheral blood mononuclear cells (PBMCs) from patients with NLRP7 mutations secrete lower amounts of IL-1β and TNF when stimulated with LPS compared to PBMCs from control groups. However, these cells synthesize more intracellular pro-IL-1β and can process more pro-IL-1β as well. Moreover, they showed that NLRP7 colocalizes with giantin, a cis-Golgi resident protein, and γ-tubulin, a marker of the microtubule-organizing center. This observation suggested that NLRP7 may affect cytokine secretion by interfering with their trafficking [17].

Mutations in NLRP7 gene are associated with abnormal pregnancies including recurrent hydatidiform moles (HM) and fetal growth restriction (FGR) pregnancies. HM is an abnormal human pregnancy characterized by the aberrant trophoblast differentiation of non-viable fertilized egg [12]. In order to better investigate how these mutations might cause HM, our former lab member, Aybüke Garipcan, generated patient-derived induced pluripotent stem cells (iPSCs). She found that absence of NLRP7 due to mutations leads to excessive differentiation of iPSCs into trophoblast cells and this lineage commitment may arise through BMP4 pathway by altering trophoblast associated genes such as CDX2, INSL4, PGF, and NP63 (2019, PNAS, under revision).

On the other hand, a recent paper claimed that NLRP7 is a placental factor that has a major role in placental development and its dysregulation results in FGR pregnancies which are characterized by retarded fetus growth. Researchers showed that NLRP7 is produced in the human placentas during the first trimester of pregnancy and its level decreases from the early to the late points under hypoxia. Thus, they hypothesized that NLRP7 is regulated by hypoxia which is a key parameter of placental

development. They also determined that NLRP7 is able to induce trophoblast proliferation, migration, and invasion by exhibiting an anti-apoptotic role. Furthermore, using a placental explant model, they showed that NLRP7 controls the precocious differentiation of trophoblasts to syncytium and it leads to an invasive extravillous trophoblast proliferation [18].

Although a few groups investigated the functional role of NLRP7, there is only one paper available about its regulation. Researchers discovered that NLRP7 stabilization occurs with inflammation whereas in the absence of an inflammatory signal NLRP7 is ubiquitinated and degraded in lysosomes. Upon stimulation with lipopolysaccharide (LPS) and the synthetically acylated lipopeptide, Pam3CSK4, NLRP7 gets stabilized because of deubiquitinase (DUB) activity of STAM-binding protein (STAMBP), which can be reversed by BC-1471, a small molecule with an inhibiting activity on STAMBP [19].

1.5. The Connection between NLRs and Cancer

1.5.1. The Distinguishing Features of Cancer

Cancer is by definition a dysregulated cell cycle which leads to uncontrolled cellular proliferation and subsequent formation of a tumor. Hanahan and Weinberg hypothesized about the distinguishing properties of neoplastic cells, which give rise to tumorigenic and ultimately malignant cells, by merging the following characteristics under the title of hallmarks of cancer: staining proliferative signaling, evading growth suppressors, resisting cell death, enabling replicative immortality, inducing angiogenesis, and activating invasion and metastasis (Figure 1.3) [20]. The most important feature that separates cancer cells from healthy cells is their continuous proliferation, which occurs even when growth-promoting signals are dysregulated and the cellular homeostasis is damaged. Moreover, cancer cells can overcome the regulation by growth suppressors such as TP53 and RB, which are responsible for negative regulation of cellular proliferation and growth. The inactivation of tumor suppressor genes can modulate the decision of cells from senescence or apoptosis to proliferation that results in improper

reproduction of cells, eventually leading to one of human's worst nightmares, cancer.

Although NLR proteins are mostly known for their involvement in host defense, their aberrant functions have been linked to numerous cancer cases. In the following chapter, how different NLR proteins are implicated in different cancer cases will be discussed.

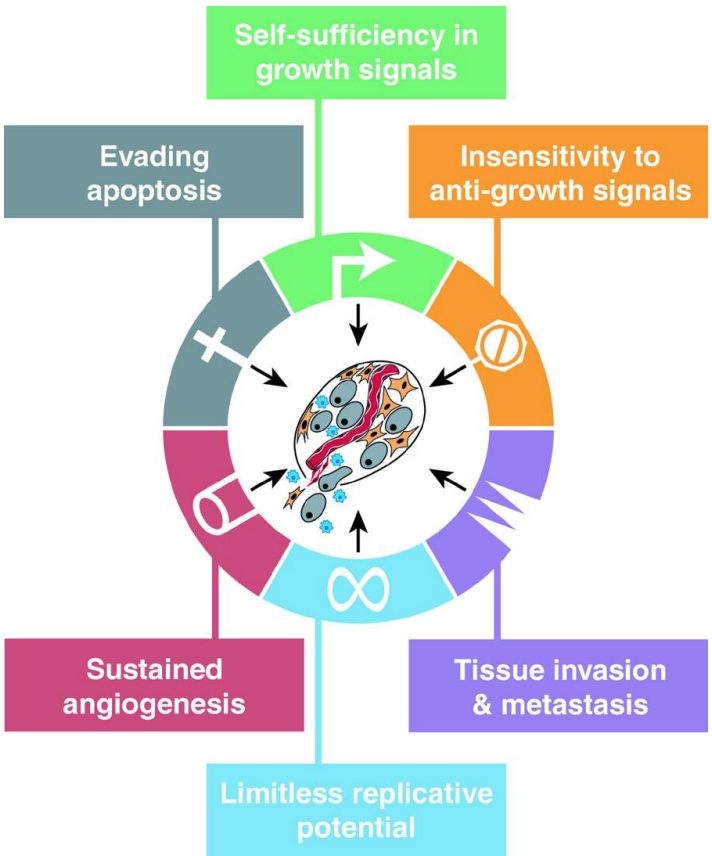

Figure 1.3. The Distinguishing Features of Cancer (Adopted from [20]).

1.5.2. NLRA's Relationship with Cancer

The presence of genetic alterations in CIITA gene, which encodes an NLR family protein called major histocompatibility complex (MHC) class II transactivator, was found to be associated with Primary mediastinal large B Cell Lymphoma (PMBCL) which is considered to appear from thymic medullary B cells, that is indicated by the

presence of immunoglobulin rearrangements and expression of B-cell antigens [21].

Mottok *et al.* showed that 53% of tumor samples and cell lines comprise missense, nonsense, and frameshift mutations in the CIITA gene. Additionally, the same group discovered that DNA lesions in CIITA cause a reduction in MHC Class II surface expression which leads to immune privilege in PMBCL patients [22]. In a similar study, it was shown that the genomic CIITA breaks are quite common in PMBCL and also classical Hodgkin Lymphoma which is the most common lymphoma of adolescents and young adults, with approximately 8500 new cases per year [23]. Moreover, CIITA is a partner of in-frame gene fusions which negatively influence survival rates of PMBCL patients [24].

1.5.3. NLRB's Relationship with Cancer

NAIP is a BIR domain containing NLR protein which functions as an apoptosis inhibitor. The expression levels of NAIP were found to be increased in the breast cancer samples while there is no NAIP expression in normal cells at all. Additionally, larger tumors with unfavorable histology have higher NAIP expression levels compared to breast cancer patients with smaller tumors and favorable histology. Although this research pointed out a link between NAIP and breast cancer, further studies should be conducted to illustrate the possible role of NAIP in breast cancer [25]. Besides breast cancer, *in vitro* experiments showed that elevated NAIP expression is also associated with increased NF-κB DNA-binding activity and survival of prostate cancer cells after androgen deprivation therapy (ADT). Furthermore, significantly elevated NAIP expression was correlated with drug resistance of prostate cancer patients who received ADT [26]. On the other hand, in 2005, Allam *et al.* proposed that NAIP may have a protective role in colonic epithelium against tumorigenesis. Mice which do not express NAIP (knockout model) show increased gene expression profile of proliferation-related genes, particularly STAT3. Moreover, p53 activation was not observed after carcinogen exposure in knockout mice hence it is concluded that NAIP has a protective role against colon cancer tumor initiation [27].

1.5.4. NLRC's Relationship with Cancer

Card domain containing NLR family proteins, especially NOD1 and NOD2, have been implicated in various cancers. For instance, polymorphisms in NOD1 and NOD2 genes were shown to be associated with the increased risk of several cancers including colorectal, breast, ovarian, lymphoma, and leukemia. It is proposed that single nucleotide polymorphisms (SNPs) in NOD1 and NOD2 may change the balance between anti and pro-inflammatory cytokines that leads to infection, chronic inflammation and cancer [28]. First insights about the involvement of NOD proteins in cancer came up in 2006. Correria *et al.* showed that overexpression of NOD1 reduces the proliferation of MCF-7 cells *in vitro* and inhibits tumor growth in immune-deficient SCID mice in an estrogen-dependent manner. Furthermore, tumor growth and proliferation were enhanced in the absence of NOD1 protein since NOD1-dependent apoptosis could not occur [29,30]. In line with this study, it was shown that overexpression of either NOD1 or NOD2 reduces cell proliferation although it increases clonogenic potential in triple negative Hs 578T breast cancer cell line which is highly invasive [31].

Using a proteomic approach where bioinformatic analysis carried out by analyzing enriched molecules and integrating them into different functional groups, researchers revealed that NF-κB, PI3K/AKT/mTOR, and MAPK signaling pathways are linked to the tumorigenesis in triple negative breast cancer. In that study, both NOD1 and NOD2 overexpressing cells were used to identify common and different proteins that may be implicated in the inception of tumorigenesis through NOD1 and NOD2. Researchers concluded that the reason behind tumorigenesis can be dysregulation of aforementioned NF-κB and MAPK signaling pathways upon overexpression of NOD1 and NOD2 proteins which causes alteration in the cell cycle, cellular adhesion, and proteasomal degradation processes [32].

One of the major cause of gastric cancer, also known as stomach cancer, is *Helicobacter pylori* infection. Interestingly, certain SNPs in NOD1 and NOD2 genes were found to be associated with *H. pylori* infection and gastric lesions [33]. Mechanistically, Asano *et al.* showed that an increase in NOD1 signaling reduces the precancerous

gastric lesion accumulation via suppressing TRAF3 activation which eventually leads to inhibition of NF-κB signaling. In addition, *H. pylori* infected NOD1 knockout mice display increment of CDX2 expression and accumulation of precancerous gastric lesions which further proves that NOD1 has a protective role against *H. pylori* induced gastric cancer [34].

There is an existing correlation between NLRC family proteins and colorectal (colon) cancer (CRC). Inflammation has a major role in CRC, therefore, it is important to understand the role of inflammasome components and how they behave in CRC. In one study, it was observed that NOD1 and NOD2 expressions are upregulated whereas the expression of NLRC3 is downregulated in CRC patient samples based on bioinformatic analysis from public data sets and samples from Chinese CRC patients compared to controls. This study emphasizes that NLRs can be a biomarker of CRC progression [35]. Uden *et al.* also demonstrated that NOD2 is a key player in intestinal inflammation via regulating it through TLR signaling pathways, thus NOD2 repress inflammation-induced tumorigenesis in the colon. Moreover, they showed that NOD2 expression induces IRF4 and suppress NF-κB and MAPK signaling pathways [36]. Another study came from Kanneganti's group in 2017. While they were investigating the signaling pathways that may drive tumorigenesis, they enlightened the relationship between NLRC3 and CRC. Using knockout NLRC3 enterocytes (epithelial cells in the small intestine), they identified that PI3K–mTOR signaling pathway is negatively regulated by NLRC3 which acts as a tumor suppressor by promoting apoptosis in CRC [37].

Other NLRC family members, NLRC4 and NLRC5, also implicated in several cancers. For instance, Kolb *et al.* showed that obesity linked-NLRC4 inflammasome expression contributes to breast cancer progression via vascular endothelial growth factor A (VEGFA) mediated angiogenesis in the obese cancer patients. This research has also elucidated the link between breast cancer and obesity through IL-1β signaling [38]. On the other hand, genetic and epigenetic changes such as mutations, polymorphisms, and methylations in NLRC5, an MHC class I transactivator, have been associated with higher cancer risk in response to dysregulation of MHC Class I signaling pathway due

to impaired CD8+ T cell activation [39].

1.5.5. NLRP's Relationship with Cancer

In the literature, it was shown that high cholesterol diet (HCD) induces colorectal cancer as a result of chronic inflammation which is associated with the activation of NLRP3 inflammasome. The activation of NLRP3 inflammasome is driven by the increment of mitochondrial reactive oxygen species (ROS) as a result of AMPKα inhibition by cholesterol. The deletion of NLRP3 leads to diminished levels of pro-inflammatory cytokines and macrophage infiltration which is induced by HCD. Therefore the cascade, that is started with oxidative micro-environment and ended with IL-1β secretion, may be regressed moderately by NLRP3 depletion [40]. Furthermore, treatment with GL-V9, an AMPKα activator, leads to an anti-inflammatory response as a consequence of autophagy and NLRP3 inflammasome degradation [41]. NLRP3 expression levels are also high in colorectal cancer (CRC) tissues which lead to an increase in the number of macrophages. It was shown that NLRP3 establishes a cross-talk between macrophages and CRC cells, which augment the migration and invasion of CRC cells. As a consequence, inhibiting of NLRP3 signaling leads to diminished migration capacity of CRC cells [42].

Although the link between NLRP3 and tumor aggressiveness was revealed, the mechanism behind is controversial. For instance, NLRP3 levels are found to be high in HCT116 and HT29 colon cancer cell lines during the epithelial-mesenchymal transition, independent from its inflammasome function [43]. In another research, it was shown that IL-18, which is found downstream of NLRP3, is important for protection against colorectal cancer since its reduction causes disruption of tumor suppressors, particularly IFN-γ and STAT1 levels decrease [44]. Moreover, the relationship between IL-18 and its tumoricidal activity was revealed by showing that deficiency of NLRP3 inflammasome components in mice causes impairment of IL-18 and exacerbates metastasis in liver and colon cancer. The activation of inflammasome-IL-18 signaling cascade revitalizes the maturation of natural killer cells, expression of Fas ligand and tumor attack activity which culminates in the suppression of liver colorectal cancer [45].

Apart from NLRP3, other proteins of the pyrin domain containing NLR family are also associated with colorectal cancer. For instance, NLRP6 diminishes inflammation and tumorigenesis through a self-renewal of colon epithelium. Absence of NLRP6 impairs the regeneration of colonic mucosa upon injury and enhance the tumor growth *in vivo* [46]. In another research, Zaki *et al.* showed that NLRP12 diminishes the inflammation and tumorigenesis in the colon. When they used NLRP12 knockout mice, they observed that cytokine production and tumorigenic factors increase dramatically, implying that susceptibility to colon inflammation and tumorigenesis improves drastically. Moreover, it was observed that NLRP12 reduces the NF-κB and ERK activation, thus it has a protective role in the maintenance of intestinal homeostasis and against tumorigenesis [47]. In a similar study, Allen *et al.* observed that NLRP12 knockout mice show a tendency to develop colon cancer through activation of non-canonical ERK, AKT and NF-κB pathways [48].

SNPs in NLRP1, NLRP3, IL-1β, and IL-18 have a protective roles against human papillomavirus persistence and consequently cervical cancer progression [49]. CD200R1 is a cell surface glycoprotein that suppress inflammation and its agonist, CD200Fc, has an anti-inflammatory effect in the autoimmune diseases. To investigate its role in cervical cancer, HPV-16 positive human cervical cell lines were treated with LPS and CD200Fc. The results indicated that CD200Fc inhibits the NLRP3 and TLR4-NFKB pathways, meaning that these inflammatory pathways indeed play a critical role in cervical cancer [50].

There are several SNPs in NLRP3 and NLRP12 genes which were found to be associated with gastric cancer (GC), as a consequence of *H. pylori* infection. Moreover, NLRP9 and NLRP12 expressions decrease whereas the canonical NF-κB pathway persistently upregulated in the infected cells as a result of *H.pylori* infection. As NLRP12 is a known NF-κB pathway inhibitor, this situation may result from the continuation of the active state of NF-κB cascade [51]. On the other hand, NLRP3 expression is found to be upregulated in GC that induces inflammasome activation and IL-1β secretion in macrophages. It also induces cyclin-D1 expression by binding to its promoter region resulting in the promotion of epithelial cell proliferation. In research by Li *et al.*,

miR-22 was discovered as the suppressor of NLRP3 in gastric mucosa. Although miR-22 suppresses NLRP3's oncogenic activity, *H.pylori* infection block miR-22 expression that triggers NLRP3 up-regulation, the proliferation of epithelial cells and progression of GC [52]. Additionally, NLRP6 expression decreases in a great majority of gastric cancer cases. Phenotypic studies showed that NLRP6 suppresses gastric cancer by stimulating senescence through p21 and cyclin D1. Indeed, researchers demonstrated that overexpression of NLRP6 with inhibition of NF-κB and MDM2 induces senescence of gastric cancer cells via $P14^{ARF}$-P53 [53].

Along with colorectal, cervical, and gastric cancer; NLRP family members, especially NLRP3, have been linked to glioblastoma multiform (GBM) whose progression is extremely affected by the tumor microenvironment. Dysregulation in NLRP3 driven processing of IL-1βB leads to STAT1 transcription activation which consequently induces cell migration and glioma progression [54]. In another study, researchers demonstrated that NLRP3 has a role in the progression of human glioma via EMT, PTEN/AKT, and inflammatory pathways. NLRP3 downregulation results in inhibition of AKT and PTEN phosphorylation, and suppression of epithelial-mesenchymal transition [55].

Furthermore, Li *et al.* proposed that NLRP3 may be the link between aging and glioblastoma since NLRP3 regulates upstream targets of brain aging including inflammation and cell death. They found that NLRP3 provides resistance against radiotherapy by inducing inflammasome formation and increasing the number of senescent cells after the ionizing radiation treatment [56]. Another intriguing research also revealed that miR-223-3p expression suppresses cell proliferation and migration by attenuating NLRP3 expression [57]. Moreover, it was shown that Beta-hydroxybutyrate (BHB), a ketone body, acts as an anti-inflammatory protein by inhibiting NLRP3 inflammasome in C6 glioma cell and decrease cell migration. Thus, these two inhibitors of NLRP3, miR-223-3p and, BHB, inflammasome were suggested as a GBM treatment [57, 58].

Another member of the NLRP family, NLRP1, has also been implicated in several cancers. In a rat model of benign prostate hyperplasia (BPH) which is characterized by the abnormal increase in the size of prostate tissue, it was observed that NLRP1 levels are upregulated. The subsequent increase in IL-1β and caspase-1 end up with the maintenance of BPH-related inflammation [59].

Human skin has high levels of NLRP1 expression compared to other NLR subfamily members and mutations in this gene causes familial keratosis lichenoides chronica (FKLC) and multiple self-healing palmoplantar carcinoma (MSPC). In these diseases, NLRP1 mutations inhibit its auto-inhibitory property since they cause self oligomerization of this protein by disrupting LRR and pyrin domains [60].

1.6. NLRP7's Relationship with Cancer

In the literature, two papers correlated NLRP7 upregulation with cancer. In one of them, researchers illustrated that NLRP7 upregulation is significantly associated with tumor invasion in human endometrial cancer tissue. Moreover, overall and relapse-free survival rates of the patients was negatively correlated with NLRP7 expression, indicating a link between higher NLRP7 expression and poor prognosis [61]. Besides, another paper suggests that NLRP7 overexpression occurs in testicular seminoma cells. Although researchers concluded that NLRP7 alone does not induce cell-growth per se, downregulation of it offers a promising target to treat testicular germ-cell tumors [10]. These findings are indeed promising but they require more in-depth studies.

During her Ph.D. studies, Aybüke Garipcan conducted tumor xenograft experiments to investigate the tumorigenic role of NLRP7. She injected mice either with an empty vector expressing human endometrium cancer (Hec1a) cells or NLRP7 overexpressing Hec1a cells, then, she monitored tumor growth once they are formed. What she observed is that NLRP7 expressing tumors grow larger compared to control cells, implying that NLRP7 may contribute to tumor cells' proliferation.

Overall, different NLR proteins have been linked to various cancer cases in the literature. Figure 1.5 illustrates how these proteins interfere with different pathways whose dysregulation may trigger diverse cancer cases.

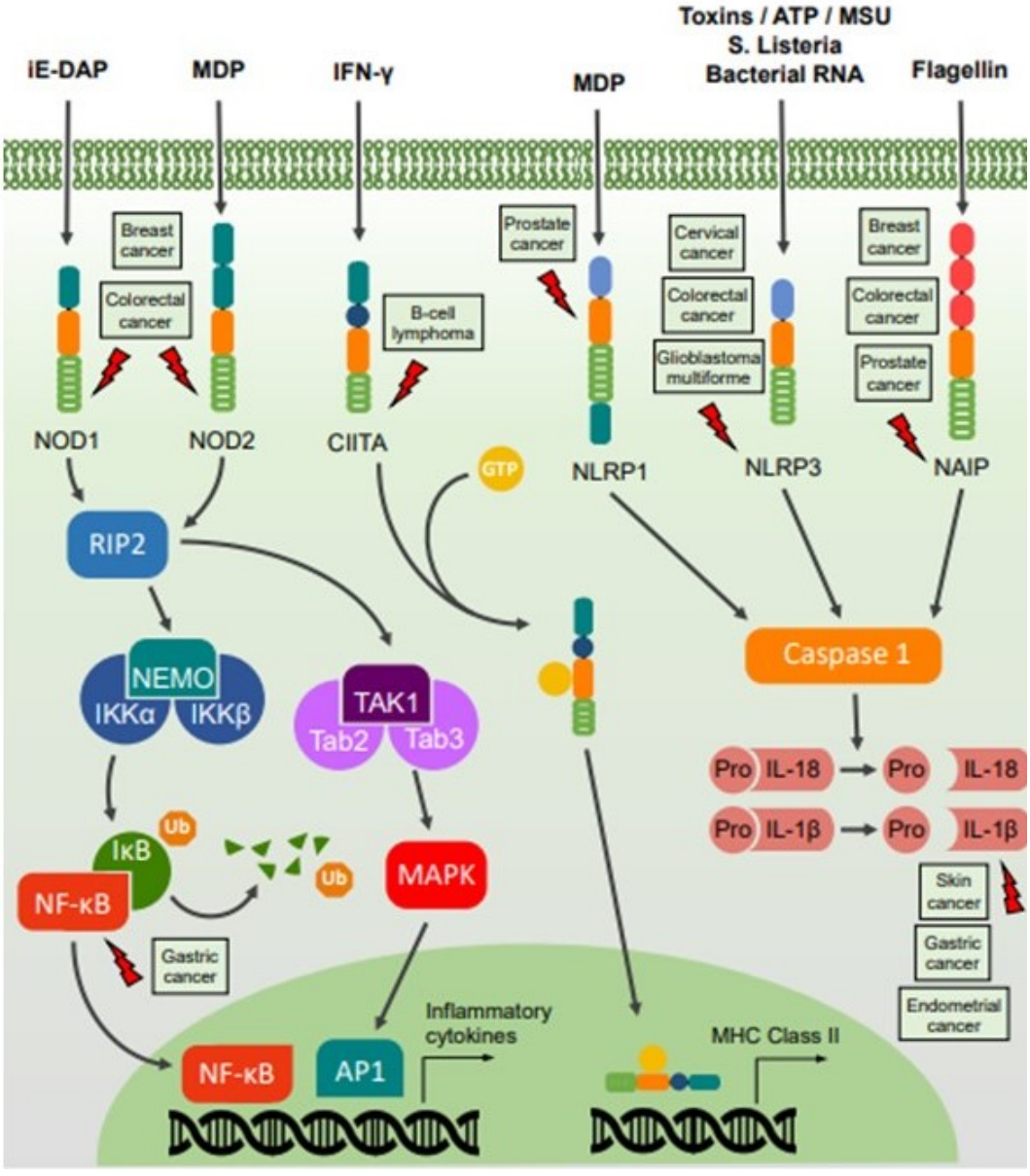

Figure 1.4. Involvement of NLRs in various cancer types through different signaling pathways (Adopted from [62].)

2. HYPOTHESIS AND PURPOSE

NLRP7 is a novel protein which from the limited data so far appears to be important for early human embryonic development, inflammatory signaling during pathogen recognition, as well as oncogenesis. Although NLRP7 upregulation has been associated with human endometrium cancer, the mechanism behind NLRP7 driven oncogenesis remains unknown. To shed light on the possible oncogenic role of this multi-functional protein, Aybüke Garipcan performed mass spectrometry analysis to reveal protein interactome of NLRP7. In this study, our first specific aim was to determine the putative pathways through which NLRP7 upregulation may trigger tumorigenesis using MS data. Our second aim was to generate NLRP7 knockout cell line using the CRISPR-Cas9 system to observe the effect of the absence of NLRP7 on cancer cells via phenotypic assays. Lastly, we aimed to generate both polyclonal and monoclonal antibody against NLRP7 to be able to detect its endogenous levels in cancer cells. In general, these study aims to provide an understanding of the functions of NLRP7 in oncogenesis which can be significant for therapeutic targets.

3. MATERIALS

3.1. Equipment

Following table contains equipments used in this project.

Table 3.1: Equipment.

Equipment	Supplier
Agarose Gel Electrophoresis System	BIO-RAD, USA
Autoclaves	Midas 55, Prior Clave, UK ASB260T, Astell, UK
Carbon dioxide Tank	Genc Karbon, Turkey
Cell Culture Dishes	TPP, Switzerland
Cell Culture Incubator	Hepa ClassII Forma Series, Thermo, USA
Cell Scraper	TPP, Switzerland
Cell Sorter	Sony, Japan
Centrifuges	Ultracentrifuge J2MC, Beckman, USA Himac CT4200C, Hitachi Koki, Japan Allegra X-22, Beckman USA
Centrifuge Tubes	CAPP, Denmark
Cold room	Birikim Elektrik Soğutma, Turkey
Cryovial Tubes (2ml)	CAPP, Denmark
Deepfreezers	(-20) Ugur, UFR 370 SD, Turkey (-80) ULT deep freezer, Thermo, UK (-150) Sanyo MDF-1156, UK
Dish Washer	Mielabor G7783, Miele, Germany
Documentation System	Gel Doc XR System, Bio-Doc, ITALY G-BOX Chemi XX6, Syngene, UK
Electrophoresis Equipments	Mini-Protean III Cell, Bio-Rad, USA

Table 3.1. Equipment (cont.).

Equipment	**Supplier**
Heat blocks	Block heater analog, VWR, USA
Ice Maker	Scotsman Inc. AF20, Italy
Laboratory Bottles	VWR, USA
Laminal Flow Cabinet	Class II B, Tezsan, Turkey
Magnetic Stirrer	VWR, USA
Microfuge Tubes	CAPP, Denmark
Micropipettes	Axygen, Axypipettes, USA
Micropipette Tips	Axygen, USA
Microscopes	Zeiss, Acio Observer, Germany Nikon, Eclipse TS100, Netherlands, Zeiss, Axio Observer Z1, Germany
Microwave Oven	Arçelik, Turkey
Multiwell Plates	TPP, Switzerland
PVDF Membrane	Merck Millipore, Germany
Oven	Gallenkamp 300, UK
PCR Tubes (0.2ml)	Axygen, USA
Petri Dishes	Fırat Plastik, Turkey
pH Meter	Hanna Instruments, USA
Pipettor	VWR, USA
Pippette Tips (Bulk)	CAPP, Denmark
Plate Reader	VersaMax, Molecular Devices, USA
Power Supply	Power Pac Universal, BIO-RAD, USA
Real-Time Quantitative PCR System	Bioneer Exicycler, Republic of Korea
Refrigerators	2021D, Uğur, Turkey 4250T, Uğur, Turkey
Rotator	Isolab, Germany
SDS-PAGE Transfer System	Trans-Blot Semi-Dry, Thermo, USA

Table 3.1. Equipment (cont.).

Equipment	**Supplier**
Serological Pipettes	CAPP, Denmark
Shakers	Polymax 1010, USA Polymax 1040, USA Heildophl, Germany
Softwares	Quantity One, Bio-Rad, ITALY ImageJ, Image Analysis Software, NIH, USA XStella 1.0, Stella, GERMANY FlowJo, USA, Syngene-Genetools, UK Leica LASX, USA
Sonicator	SonoPlus, Bandelin, USA
Spectrophotometer	Nanodrop ND-100 Thermo, USA
Syringes	Set Medikal, Turkey
Syringe Filter Units	EMD Millipore, USA
Test Tubes	CAPP, Denmark
Thermal Cycler	Bio-Rad, USA
Vortex	VWR, USA
Water Bath	GFL, Germany
Water purification system	UTES, TURKEY
Watmann Filter Paper-Extra Thick	Thermo Scientific, USA

3.2. Cell Lines

Table 3.2: Cell Lines.

Cell line	Supplier
F0 Myeloma cells	ATCC CRL 1646, USA
Hec1a	Thermo, USA
HEK293	ATCC, USA
Jar	ATCC, USA
Macrophages	Balb/c mouse
Spleen cells	Balb/c mouse
Swan	ATCC, USA

3.3. Plasmids and Primers

Plasmids were purchased from Addgene. SUMO plasmids were gifts from Umut Sahin, Boğaziçi University. Rab5A plasmid was kindly provided by Batu Erman. Primers were ordered form Macrogen (South Korea).

Table 3.3: Plasmids.

Construct	Origin	Backbone
Ago2	provided by Umut Şahin, Boğaziçi University	pIRESneo
ASC	AKİL	pcDNA3
Brat1	Addgene	pcDNA3
Cas9	provided by Tolga Emre, Boğaziçi University	pCW
His-SUMO1	provided by Umut Şahin, Boğaziçi University	Unknown
His-SUMO2	provided by Umut Şahin, Boğaziçi University	Unknown
Myc-N7	AKİL	pcDNA3

Table 3.3. Plasmids (cont.).

Construct	**Origin**	**Backbone**
Lentiviral empty	AKİL	plex307
Lentiviral GFP	AKİL	plex307
Lentiviral N7	AKİL	plex307
pet30a-N7	AKİL	pet30a
RalB	Addgene	pLA
Rab5A	provided by Batu Erman, Sabancı University	pCFP
sg5,6,7	AKİL	pLKO

Table 3.4: Sequences of Primers.

Oligo ID	**Sequence (5'-3')**	**Application**
Ralb-G23V-F	CATGGTTGGCAGCGTAGGCGTTG GCAAGTC	SDM
Ralb-G23V-R	GACTTGCCAACGCCTACGCTGCC AACCATG	SDM
Rab5a-Q79L-F	GGATACAGCTGGTCTAGAACGAT ACCATAG	SDM
Rab5a-Q79L-R	CTATGGTATCGTTCTAGACCAGC TGTATCC	SDM
GAPDH-qPCR-F	GGAGCGAGATCCCTCCAAAAT	qPCR
GAPDH-qPCR-R	GGCTGTTGTCATACTTCTCATGG	qPCR
Nlrp7-F	UUCUCCGAACGUGUCACGUTT	qPCR
Nlrp7-R	AAGAGTCGGCCGACTTCTGGT	qPCR

3.4. General Kits and Enzymes

Following tables indicate kits, enzymes and chemicals used in this study.

Table 3.5: Kits and Enzymes.

Name	Supplier
Complete Mini Protease Inhibitor Cocktail	Roche, Switzerland
Direct-zol™ RNA MiniPrep Plus	Zymo Research, USA
DNA Ladder (1 kb)	NEB, USA
DpnI restriction endonuclease	NEB, USA
ECL-Sirius	Advansta, USA
ECL-Sirius	Advansta, USA
Nucleobond Xtra Plus EF Plasmid Isolation Kit	Macherey Nagel, Germany
Nucleospin Plasmid Kit	Macherey Nagel, Germany
PageRuler Prestained Protein Ladder	Thermo, USA
Q5 High-Fidelity DNA Polymerase	NEB, USA
SensiFAST™ cDNA Synthesis Kit	Bioline, UK
SensiFAST™ SYBR® No-ROX Kit	Bioline, UK

3.5. Chemicals and Buffers

3.5.1. Cell Culture

Table 3.6: Cell culture chemicals and buffers.

Chemicals/Buffers	Supplier/Recipe
$CaCl_2$	Merck, USA
DMSO	Applichem, Germany

Table 3.6. Cell culture chemicals and buffers. (cont.).

Chemicals/Buffers	**Supplier/Recipe**
Dulbecco's Modified Eagles Medium	Gibco, USA
Fetal Bovine Serum	Gibco, USA
HEPES	Gibco, USA
McCoy's Medium	Gibco, USA
Non-essential amino acid	Gibco, USA
Penicillin/Streptomycin	Gibco, USA
Polybren	Sigma, USA
Puromycine	Sigma, USA
2X HBS Buffer	50 mM HEPES ph=7 280 mM NaCl 1.5 mM NaH_2PO_4
10X PBS	80 gr NaCl 2 gr KCl 2.4 gr KH_2PO_4 14.4 gr NaH_2PO_4 add ddH20 up to 1 lt final pH=7.2
Trypsin (0.05%) with EDTA	0.154 gr EDTA 0.5 gr Trypsin 8 gr NaCl 0.4 gr KCl 0.06 gr KH_2PO_4 1 gr Glucose 0.048 gr NAH_2HCO_3 add ddH_20 up to 1 lt final ph=8

3.5.2. Western blot

Table 3.7: Western blot chemicals and buffers.

Chemicals/Solutions	**Supplier/Recipe**
Acrylamide	Bio-Rad, USA
Agarose beads	Thermo, USA
Ammonium Persulfate (APS)	AppliChem, Germany
β-Mercaptoethanol	Merck, Germany
Blocking Solution	5% Non-fat milk in TBS-T
Bovine Serum Albumin Fraction V	Roche, Germany
Bromophenol Blue	Sigma-Aldrich, USA
Isopropanol	Merck, Germany
Methanol	Merck, Germany
Sodium Chloride (NaCl)	Merck, Germany
Sodium Dodecyl Sulfate (SDS)	Applichem, Germany
TEMED	Merck, Germany
Tris-Base	Sigma-Aldrich, USA
Tween 20	Sigma-Aldrich, Germany
Co-IP Buffer	137 mM NaCl 0.2% NP40 2 mM EDTA 50 mM Tris-HCl pH 7.4 Protease inhibitor cocktail
4X Laemmli Buffer	200mM TrisHCl pH 6.8 8% (w/v) SDS 40% (w/v) 100% Glycerol 4% (w/v) β-mercaptoethanol 50 mM EDTA 0.08% (w/v) Bromophenol Blue

Table 3.7. Western blot chemicals and buffers (cont.).

Chemicals/Solutions	**Supplier/Recipe**
8% Resolving Gel	375 mM TrisHCl pH 8.8 0.1% (w/v) SDS Acrylamide:Bisacrylamide (8% w/v) 0.05% (w/v) APS 0.005% (w/v) TEMED
4% Stacking Gel	0.125 mM TrisHCl pH 6.8 0.1% (w/v) SDS Acrylamide:Bisacrylamide (4% w/v) 0.05% (w/v) APS 0.0075% (w/v) TEMED
10X SDS Running Buffer	1% (w/v) SDS 3.03% (w/v) Tris Base 14.41% (w/v) Glycine
10X Transfer Buffer	3.03% (w/v) Tris Base 14.41% (w/v) Glycine
1X Transfer Buffer	10% (w/v) 10X transfer buffer 20% (w/v) Methanol
1X Tris Buffered Saline with Tween-20 (TBS-T)	50 mM TrisHCl pH 7.4 150 mM NaCl %0.05 Tween-20

3.5.3. Antibodies

Table 3.8: Antibodies.

Antibody	Supplier	Source	Dilution
Actin	Cell Signalling Technologies, USA	Rabbit	1:1000
Flag	Cell Signalling Technologies, USA	Rabbit	1:1000
GFP	Torrey Pines Biolab, USA	Rabbit	1:1000
HA	Cell Signalling Technologies, USA	Rabbit	1:1000
His	Santa Cruz Biotechnology, USA	Mouse	1:1000
Mouse IgG, HRP	Cell Signalling Technologies, USA	Horse	1:5000
Myc	Cell Signalling Technologies, USA	Mouse	1:1000
Rabbit IgG, HRP	Cell Signalling Technologies, USA	Goat	1:5000

3.5.4. ELISA

Table 3.9: ELISA solutions and their contents.

Solution	Content
Reagent Solution	1% BSA in 1X PBS
Stop Solution	2N H_2SO_4
Substrate Solution	Color Reagent A and B mix (1:1 ratio)
Wash Buffer	0.05% Tween-20 in 1X PBS

3.5.5. Protein Purification

Table 3.10: Protein purification buffers.

Buffer	**Content**
Coomassie Blue Solution	0.1% Coomassie Brilliant Blue R-250 10% Acetic Acid 50% Methanol
Destaining Solution	40% Methanol 10% Acetic Acid
Elution Buffer	50 mM Tris-HCl 150 mM NaCl 0.1 mM EDTA pH=7.5
IPTG	Roche, Germany

4. METHODS

4.1. Maintenance of Cell Lines

HEK293FT and SWAN cells were cultured in DMEM (Gibco, Thermo Fisher Scientific, USA) which supplemented with 10% FBS (Thermo Fisher Scientific, USA) and Penicillin (100U/mL)-Streptomycin (100μg/mL) (Lonza, Switzerland) and 1% non-essential amino acid solution. Hec1a cells were grown in McCoy's 5A (Modified) Medium (Gibco, Thermo Fisher Scientific, USA), supplemented with 10% FBS (Thermo Fisher Scientific, USA) and Penicillin (100U/mL)-Streptomycin (100μg/mL) (Lonza, Switzerland) and 1% non-essential amino acid solution. Jar and THP-1 cells were grown in RPMI Media 1640 (Gibco, Thermo Fisher Scientific, USA), supplemented with 10% FBS (Thermo Fisher Scientific, USA) and Penicillin (100U/mL)-Streptomycin (100μg/mL) (Lonza, Switzerland) and 1% non-essential amino acid solution. All cells were maintained in T75 cell culture flasks at 37 ^{o}C, 5% CO_2 and humidified atmosphere. They were sub-cultured every 2 or 3 days except THP-1 cells. For cell passage, old media were aspirated and cells were washed with 1X PBS. After that, 0.05% trypsin-EDTA was put to the cells and the cells were incubated at 37 ^{o}C for 2 to 5 minutes depending on the cell line. After incubation, media which belongs to the particular cell line was added onto the cells twice as much amounts to trypsin in order to inactivate its activity. After inactivation, cells were centrifuged at 2000 rpm for 2 minutes and media aspirated. Finally, appropriate media was added to the cell pellet and cells were seeded depending on the surface area of the plates or flasks.

For long-term storage of the cells, cell pellet was resuspended in filtered cell freezing medium, containing 10% DMSO and 20% FBS and the cell suspension was aliquotted into 1 ml cryovials and stored at -80 ^{o}C for short term, -150 ^{o}C freezer for longterm storage. Approximately one million cells were freezed in each of the cryovials. In order to thaw a cell, cryovials were quickly transferred to 37 ^{o}C water bath. After it was defrozen completely, 4 ml culture media was put on a a 15 ml falcon tube and cell suspension was transferred into the falcon tubes and centrifuged at 2000 rpm for 2

minutes. Then, the freezing medium was aspirated and the cell pellet was resuspended in regular medium that is used for the maintenance of the cells. After that, the cell suspension was transferred to T25 flasks.

4.2. Site-directed Mutagenesis

Site-directed mutagenesis experiments was performed using the primers which were purchased from Macrogen. For polymerase chain reaction (PCR) 250-500 ng template DNA was used and amplified. Components and conditions of PCR were showed below in the table. Dpn1 (6 μl Cut Smart Buffer + 1 μl DpnI enzyme) digestion was performed for 3 hours at 37 °C after PCR. Then, 1 μl sample was transformed into *Escherichia coli* Stbl3 strain which is thaw on ice approximately 10 minutes and competent cells were incubated on ice for 30 minutes. Then, heat shock of each transformation tube was performed by placing the bottom 1/2 to 2/3 of the tube into a 42 °C water bath for 45 seconds. After that, tubes were put back on ice for another 2 minutes. Next, 950 μl LB was added to the bacteria which were grown at 37 °C with shaking for 1 hour. Subsequently, competent cells were centrifuged and 900 μl LB was discarded. Remaining 100 μl was resuspended and spread to LB agar plate containing the appropriate antibiotic, which is followed by overnight incubation at 37 °C. Later, single colonies were selected and incubated in antibiotic containing LB-Broth at 37 °C overnight with shaking. Then, plasmid DNA was isolated using Plasmid DNA isolation Miniprep kit (Macherey Nagel, Germany) according to the manufacturer's recommendation. Finally, samples were sent to Macrogen for sequencing to validate the change in double stranded plasmid DNA.

Table 4.1: PCR Components.

Component	**Volume (μl)**
Q5 reaction buffer (NEB)	5
dNTP (10 mM)	1
Forward primer (10 μM)	1.25
Reverse primer (10 μM)	1.25

Table 4.1. PCR Components (cont.).

Component	**Volume (μl**
DMSO	3
template DNA	1
Q5 high-fidelity DNA polymerase (NEB)	1
dH_2O	31.5
Total	**50**

Table 4.2: PCR Conditions.

Temperature^{o}C	**Time**	**Cycle**
98	30 sec	1
98	10 sec	25
55-65	30 sec	
72	5 min	
72	2 min	1

4.3. Plasmid Transfections into HEK293FT Cells via Calcium Phosphate Method

In order to express plasmids transiently, particular vectors were transferred into HEK293FT cells via Calcium Phosphate method. For transfection, cells were seeded at 80% confluency 1 day prior to the transfection. Next day, appropriate amount of plasmids diluted in ddH_2O and 62,5 μl of 2M CaCl2 (125 mM) was added as the volume of the solution was completed to 500 in eppendorf tubes. Then, 500 μl of 2X

HBS solution very added slowly and drop wise. This mixture was mixed very well until bubbles were observed and incubated at room temperature for 7 to 9 minutes. After incubation, transfection mixture was added onto the cells drop wise. The amount of reagents and plasmid amounts can be changed depending on the experiments.

4.4. Lentivirus Harvest and Lentiviral Transduction

Lentivirus containing media of HEK293FT cells were harvested 48 hours later from the transfection. Lentivirus containing media was filtered through a 0.45 μm filter into a 15 ml falcon tube and divided into eppendorf tubes as 1 ml aliquottes which are used directly for lentiviral transduction or stored at -80 ^{o}C for later use. For lentiviral transduction, 150.000 cells were seeded into 6-well plates one day before the transduction. It is important to have low confluency to be able to have successful transduction efficiency. On the next day, lentivirus aliquottes were thawn from -80 ^{o}C and mixed with polybrene at a final concentration of 4 μg/ml. The media of the cells were aspirated and 1 ml lentivirus-containing medium was added onto the cells. After 6-8 hours, lentivirus containing medium was aspirated and fresh regular medium was added onto the cells.

4.5. Single Cell Sorting with SH800 Cell Sorter

In order to achieve single cell sorting after transduction of sgRNA constructs, which have the GFP marker, cells were tyripsinized and half of the cells were transferred into 15 ml falcons. Other half of the cells were seeded as a backup. Then, cells were centrifuged at 2000 rpm for 2 minutes and supernatant was discarded. Cell pellet was washed with 1X PBS and centrifuged again. This step was repeated for 2 times. After that, supernatant was discarded and cell pellet was resuspended in 2 ml 1X PBS. Cells were vortexed and the cell sample was put through a 40 micron cell strainer before sorting well to obtain single cells. For cell sorting experiments Sony SH800 cell sorter with 100 μm sorting chip was used. Untransduced cells were used as negative control. Cells were collected into 96 well plates in 100 μl regular medium containing 20% FBS and 2% P/S to avoid contamination.

4.6. Stable Cell Line Generation by Antibiotic Selection and Doxycycline Treatment of Inducible Stable Cell Lines

For the generation of stable cell lines, cells were treated with 2 μg/ml puromycin after 3 days of transduction with corresponding lentiviruses and selection continued until all untransduced cells were dead. Expression of target proteins were checked with western blotting. Since we used Dox inducible Cas9 vector, stable cell lines were treated with 2 μg/ml doxycycline for the induction of Cas9. Doxycycline was refreshed every 24 hours and treatment was performed in dark since it is light sensitive.

4.7. Co-Immunoprecipitation

HEK293 cells were transfected with 10 μg Myc-NLRP7 and 5 μg plasmids encoding putative interactor proteins since it was determined that the NLR expressing plasmids produce lower amount of proteins than the other plasmids. After 48 hours of transfection, the cells were lysed as explained below. During immunoprecipitation experiments, Pierce Protein A/G Agarose beads were used. As a first step, agarose beads were blocked by adding 1 ml PBS containing 0.1%, which was mixed using an eppendorf rotator for 1 hour at RT. After blocking step, beads were washed with PBS for two times. Then, the supernatant was aspirated and 400 μl lysis buffer was added. The ready beads can be stored at 4 °C if not used in the same day.

For the lysis step, briefly, the cell culture dishes were placed on ice and washed with ice-cold PBS. Then, the PBS was drained and 1 ml lysis buffer added to 100 mm2 dish. Adherent cells were scraped using a cold plastic cell scraper and gently transferred into a pre-cooled micro-centrifuge tube. The samples were maintained at constant agitation for 30 min at 4 °C then centrifuged in a micro-centrifuge at 4 °C 20 min at 12,000 rpm. The tubes were placed on ice, the supernatant was collected and the pellet was discarded.

After preparing samples, approximately 50 μl beads were put into micro-centrifuge tubes. 1-5 μl antibody (depending on antibody affinity) was added. The antibody-bead mixture was incubated for 1–4 h at 4 °C by gently mixing the mixture on an eppendorf shaker. After conjugation of antibody and agarose beads, the samples were centrifuged at 2,000 x g for 2 min at 4°C and the supernatant was discarded. 1 mL lysis buffer was added to the mixture and centrifuged at 3,000 x g for 2 min at 4 °C. This washing step was repeated in twice. After washing antibody and bead mixture, the cell lysate was added to the mix. The lysate-bead/antibody conjugate mixture is incubated at 4 °C on an eppendorf shaker for 8 h. At the end of the incubation, the tubes were centrifuged at 3,000 g for 2 minutes at 4 °C and the supernatant was discarded. At this point, the protein of interest should be specifically bound to the antibody coating the beads. The beads were washed with lysis buffer for three times to remove non-specific binding. All centrifuges were done at 4 °C. After last washing step, the wash buffer was removed carefully using an insulin needle. After washing steps, the beads were eluted using 50 μl 2x Laemmli buffer and boiled for 5 minutes at 95 °C. Then the samples were analyzed using Western Blotting.

4.8. Cell Lysis

Medium of the cells was aspirated and cells were washed with 1X PBS. Then, cells were tyripsinized and collected in 15 ml falcon tubes and centrifuged at 2000 rpm for 2 minutes. After that, supernatant was discarded and cell pellet was washed with cold 1X PBS and centrifuged again. Supernatant was discarded and cell pellet was resuspended in approximately 150-200 μl cold RIPA buffer which contains protease inhibitor coctail. Resuspended cell pellet was vortexed and incubated on ice for 30 minutes. Vortexing was repeated for each 10 minutes. After 30 minutes incubation, cells were centrifuged at 14000 g for 20 minutes and the supernatant was transferred into new 1,5 ml eppendorf tubes. If not used in the same day, total protein samples were stored at -20 °C.

4.9. Western Blotting

Before loading the samples, protein samples were mixed with 5X laemmli loading dye buffer and boiled at 95 °C for 5 minutes. After boiling, they were loaded onto the SDS-PAGE gels. 70 V for approximately 20 minutes and 120 V for approximately 1.5 hours were applied in 1X Running Buffer to run proteins on stacking and resolving gels, respectively. After separation step, proteins were transferred to PVDF membrane via wet transfer which was performed at 100 V for 3 hours or Trans-Blot Turbo Transfer System depending on expected transfer efficiency. Pierce Western Blotting Filter Papers (Thermo-fisher) and Immobilon-PSQ PVDF Membrane (Millipore), which were cut in the equal sizes with the gel, was used. Following the transfer part, membrane was rinsed with TBS-T and was incubated with 5% skim milk in TBS-T for 1 hour at room temperature on an orbital shaker. After blocking, the membranes were washed with TBS-T and incubated with primary antibodies which was 1:1000 diluted with 5% BSA in TBS-T for overnight at 4 °C. Next day, membranes were washed with TBS-T 3 times for 5 minutes and were incubated with secondary antibodies 1:2000 diluted in blocking solution for 1.5 hour at RT. After secondary incubation, membranes were washed with TBS-T 3 times for 5 minutes. Finally, WesternBright ECL-HRP Substrate (Advansta) was used to visualize the protein bands. The substrate was prepared by mixing two solutions in 1:1 ratio, then the membrane was incubated with the substrate for 1 minutes at dark. Visualization of the membrane was performed with at chemiluminescence visualization system (GBox Chemi, Syngene, UK). Genetools and Image J software packages were used to analyze protein data.

4.10. Immunofluorescence Experiments

For immunofluorescence experiments, coverslips were placed to 12 mm culture dishes and following, HEK293 cells were seeded onto coverslips in 60% confluency. At the beginning, cells were fixed using 4% cold PFA in PBS for 20 minutes at RT and rinsed with cold PBS, then cells were incubated with PBS containing 0.25% Triton X-100 for 15 minutes to permeabilize cell membranes. After that, cells were washed with PBS 3 times for 5 minutes. After washing steps, cells were blocked using 1%

BSA in PBS-T for 1 hour at RT. After blocking, cells were incubated with primary antibodies which were prepared in blocking solution in a humidified chamber overnight at 4 °C. Next day, cells were washed with PBS-T 3 times for 5 minutes. Then, cells were incubated with fluorescent-dye conjugated secondary antibodies 1:500 diluted in blocking solution for 1 hour at RT in dark. After that, cells were washed with PBS-T 3 times for 5 minutes. Next, cells were incubated with DAPI (1 μg/ml) for 3 minutes on an orbital shaker which was followed by PBS rinsing. Next, coverslips were mounted with fluoroshield mounting medium to the slides and sealed with nail polish. Images were acquired using the fluorescence microscope (Leica TCS, USA) and they were analyzed using Image J.

4.11. RNA Isolation, Synthesis of cDNA and qPCR

In order to obtain total RNA, Direct-zol^{TM} RNA MiniPrep Plus kit was used (Zymo Research, USA). Briefly, the media of cells were aspirated and the cells were washed with cold 1X PBS and lysed with appropriate volumes of Trizol. Then, the following steps were proceeded according to the instructions of manufacturer's. During the procedure, optional DNaseI treatment was performed to remove DNA contaminants. At the end, RNA samples were eluted with nuclease free water and the concentration of them was measured using nanodrop. After RNA isolation, 1 μg of total RNA was converted to cDNA by using SensiFAST^{TM} cDNA Synthesis Kit (Bioline, UK). The amount of components and PCR condition is described below. The cDNAs were stored at -20 °C. After PCR, cDNA was diluted 1:5 fold. In order to determine expression levels of several genes, SensiFAST^{TM} SYBR® No-ROX Kit (Bioline, UK) was used. PCR conditions and components are described below. PCR was carried out using Exicycler 96 (Bioneer) machine. Detected Cq values were used to calculate the relative expression of genes and the expression of each gene was normalized to HPRT house-keeping gene. Then, the data analyzed by using $2^{-\Delta\Delta Ct}$ method [63].

Table 4.3: cDNA Synthesis Components.

Component	**Volume (μl)**
total RNA (1 ug)	vary
5x TransAmp Buffer	4
Reverse Transcriptase	1
DNase/RNase free-water	up to 20
Total	**20**

Table 4.4: cDNA Synthesis PCR Conditions.

Temperature^{o}C	**Time**	**Cycle**
25	10 min	1
42	15 min	1
48	15 min	1
85	5 min	1

Table 4.5: qPCR Components.

Component	**Volume (μl**
SensiFast SYBR Mastermix (Bioline)	5
Forward primer (10 μM)	0.25
Reverse primer (10 μM)	0.25
Diluted cDNA	1
dH_2O	3.5
Total	**10**

Table 4.6: qPCR Conditions.

Temperature°C	**Time**	**Cycle**
95	2 min	1
95	5 sec	40
61	10 sec	
72	10sec	

4.12. Purification of NLRP7

NLRP7 was purified for the production of monoclonal and polyclonal antibodies against NLRP7. Gel extraction method was used for purification of NLRP7 since NLRP7 is a big and hydrophobic protein.

4.12.1. IPTG Induction

PET30(a+) vector containing NLRP7 coding sequence was transformed into *E. coli* Rosetta stain via heat shock method. Competent cells were taken from -80 °C and incubated on ice for 10-15 minute. 50 ng plasmid was given to competent cells. Cells were incubated on ice for 30 min, then shacked via incubation on 42 °C water bath for 45 second and incubated on ice for 2 minutes. Then, 1 ml was added to cells and cells were incubated on shaker at 37 °C for 1 h. Cells were pulled down, supernatant was removed and cells were spread on LB agar plate containing kanamycin and chloromphenicol. The plate was incubated overnight at 37 °C. On the next day; a colony was selected and streaked on a second plate containing kanamycin and chloromphenicol. After overnight incubation at 37 °C, a colony was picked and growth overnight in starter culture. On the next day, bacterial culture was diluted 1:50 with modified LB containing kanamycin

and chloromphenicol and shaked at 37 °C. When OD_{600} was 0.8, 1 mM IPTG was given to bacterial culture and shaken overnight at room temperature.

4.12.2. NLRP7 Protein Purification from Polyacrylamide Gel Pieces

Previously, purification of NLRP7 using His Bind Columns was not achieved due to high molecular weight and making an insoluble inclusion body. Therefore, gel extraction method was used. Bacterial culture was centrifuged at 7500 g for 10 minutes. Bacterial pellet was suspended with 1X PBS containing 1 Triton X-100. Then, it was sonicated 10 times, 3 secs 3 x 50 power on ice and centrifuge at 4500 g for 10 minutes. The sonication and centrifugation steps were repeated for 3 time. The pellet was dissolved at the end with PBS. The 5x laemmli buffer was added and boiled at 95 °C for 10 min.

4.12.3. Identify and Excise the Band of Interest

The sample was loaded to 10% SDS-PAGE gel. After gel electrophoresis, a strip was cut off on the left of the gel to include the molecular weight marker lane and the first lane of protein sample. The cut strip was stained with Coomassie Reagent and used as a reference. The stained strip of gel was aligned with the unstained gel portion and cut out the band of gel. The region presumed to contain the protein of interest. After determined the exact place of target protein, following times were done without staining.

4.12.4. Elute the Protein from the Gel Matrix

After cutting of the gel strips, elution buffer was added on them to 750 μl per strip. The gels were smashed and crushed then transferred to micro-centrifuge tubes. The tubes were incubated overnight at 37 °C on a shaker.

4.13. Polyclonal Antibody Production

Purified His-tagged NLRP7 was injected to one New Zealand rabbit. First injection was done with Complete Freund's Adjuvant (CFA) and subsequent injections were performed with Incomplete Freund's Adjuvant (IFA). All injections were done with 200 μg protein and subcutaneously except the last injection, which was applied intramuscularly with 400 μg antigen. Injections were performed every two weeks. Blood was collected 10 days after injection using 1:1 sodium citrate to impede coagulation. The samples were centrifuged at 6000 rpm 10 min to remove the blood cells. The plasma samples were tested with ELISA and Western Blot to verify disposition of the rabbit and decide to continue or terminate.

4.14. Monoclonal Antibody Production

4.14.1. Immunization

100 μg NLRP7 was dissolved in PBS and mixed with equal volumes of Complete Freund's Adjuvant (CFA) was given by subcutaneous injection to three-five weeks old three BALB/c mice. Subsequent injections were done with 100 μg antigen in every two weeks using Incomplete Freund's Adjuvant (IFA) instead of CFA. The last injection was performed intravenously and without adjuvant. Blood was collected 10 days after injection using 1:1 sodium citrate to impede coagulation. The samples were centrifuged at 6000 rpm 10 min to remove the blood cells. Blood samples were tested with ELISA to track disposition of the mice. The blood was collected in a micro-centrifuge tube containing sodium citrate. Plasma from a non-immunized mouse in PBS was used as the control. A mouse was successfully immunized against NLRP7 was selected as the spleen donor for fusion.

4.14.2. ELISA

96 well ELISA plate was coated with 50 μg/well NLRP7 antigen in 100 μl PBS and incubated overnight at 4 °C. On the next day, each well was aspirated and washed with 300 μl wash buffer three times. After the last washing, the remaining drops were removed by patting the plate on a paper towel. The remaining protein-binding sites were blocked in the coated wells with 200 μl blocking buffer and the plate was incubated at 37 °C for one hour. After blocking, the plate was washed for three times with wash buffer. 100 μl of diluted primary antibody or serum samples in certain ratios were added to each well and the plate was incubated at 37 °C for one hour. Then, the plate was washed for 3 times. 100 μl of conjugated secondary antibody in blocking buffer, 1:2000 diluted concentration, were added to each well and the plate was incubated one hour at 37 °C. Then, the plates was washed 5 times with washing buffer. 100 μl of the substrate solution per well was added with a multichannel pipette. After addition of substrate, the plate was kept in dark at room temperature. After 20 minutes, 100 μl of stop solution was added to the wells. The absorbance (optical density) of each well was read with a plate reader. The readings at 540 nm or 570 nm were subtracted from the readings at 450 nm to eliminate optical imperfections in the plate.

4.14.3. Fusion

4.14.3.1. Preperation of Peritoneal Macrophage Feeder Cells. Feeder layer plates were prepared with peritoneal macrophages cells to provide growth factors to support the growth of the hybridoma cells one day before the fusion. Peritoneal macrophages were collected from female animals of the same strain as the immunized animal. For this purpose, the syringe with a 25 G needle was fill with 5 ml serum free DMEM. The mouse was anesthetized and sacrificed with CO^2. The abdomen was swabbed with 70% alcohol. After pulling the skin to expose the peritoneal wall, the needle was inserted to peritoneal membrane by inserting needle into guts or bladder avoidably. Then, 5 ml of serum free DMEM was injected into peritoneal cavity. Massage was applied to abdomen for approximately 10-15 sec to spread evenly. After that, the fluid was withdrawn from peritoneum trying to draw as much fluid as possible. The content was

dispensed into a centrifuge tube on ice. The cells were counted and distributed into 96 well plates to be approximately 6000 cells and 100 μl in each well.

4.14.3.2. Preperation of F0 Myeloma Cells. F0 myeloma cells were prepared 10 days before fusion. At the moment of fusion myeloma cells were at least 95% viability. At the beginning of the expansion of the myeloma cells, Azoguanin (20 μg/ml) was added to remove HGPRT positive cells from the environment. In fusion day, the cells were washed twice in PBS at 900 rpm 10 minutes and the pellet was solved in 10 ml PBS to determine cell count.

4.14.3.3. Obtaining Splenocytes for Fusion. At the fusion day, the spleen cells from immunized mice were removed under sterile conditions and placed into a petri dish containing PBS. The foreign tissues around the spleen were cleared and the cells were crushed to reveal the cells. Then, the cells were washed twice in PBS at 900 rpm 10 minutes and the pellet was solved in 10 ml PBS to determine cell count.

4.14.3.4. Fusion. The counted F0 and spleen cells were combined in 1:5 and centrifuged at 900 rpm 10 minutes. After discard 1 ml supernatant PEG 4000 which is heated at 37 ^{o}C was added on the pellet quite slowly in one minute to cellular and nuclear membrane fusion and the cell mixture was waited at 37 ^{o}C for one minute. Then, FBS and antibiotic free 4 ml DMEM was added to quite slowly in 2-3 minutes and 20 ml DMEM was added again in 2-3 minutes and at the end 15% FBS containing 20 ml DMEM was added again 2-3 minutes. The mixture was waited in incubator for one hour and centrifuged. Then the pellet was dissolved in selection medium and distributed to the plates as 150 μl per well. After 10 days, 100 μl supernatants were removed and 100 μl HAT medium was added on the cells.

4.14.4. Screening

The HAT selection was completed after 10 d, and the cultures were passed into HT medium to remove the drug aminopterin. 13 days after the fusion step, colonies were screened with ELISA and the "best" clones are saved.

4.14.5. Isotyping of mAb

For the isotyping of mAb, supernatants of determined colonies were collected and sent to TUBİTAK, MAM.

5. EXPERIMENTS AND RESULTS

5.1. Bioinformatic Analysis of NLRP7 Interaction Partners Using Mass Spectrometry Data

The major aim of this study was to identify novel interaction partners of NLRP7 to elucidate possible pathways through which NLRP7 may drive tumorigenesis, particularly in human endometrial carcinoma. To achieve this goal, immunoprecipitation and subsequent LC-MS/MS analysis were performed to identify proteins that interact with NLRP7 at significantly higher levels in human endometrium carcinoma cell line (Hec1a) by our former lab member Aybüke Garipcan. This strategy included three steps: a) pulling down of NLRP7 from NLRP7 overexpressing Hec1a cells using an anti-NLRP7 antibody, b) SDS-PAGE separation and gel digestion and c) LC-MS/MS analysis to identify NLRP7's possible interactors. In parallel, IgG beads (without antibody conjugation) was used as a control. Two biological replicates were conducted, and the data were normalized to the proteins detected in control groups to eliminate non-specifically enriched proteins. To this end, common mass contaminants, such as keratin and trypsin, were removed. Then, possible interactor proteins were identified based on their fold changes. Finally, 80 common candidate proteins which were enriched in both biological replicas were selected.

5.1.1. Panther Software Analysis of Mass Spectrometry Data for NLRP7 Interaction Partners

Then, we classified the protein class of NLRP7's interaction partners using the PANTHER software to obtain a general view about these interactors. It turned out that NLRP7 interactors show aggregation into different groups including nucleic acid binding, transferase, enzyme modulator, hydrolyze, transcript factors, cytoskeletal proteins, cell adhesion molecules, extracellular matrix proteins, and receptors. Furthermore, cellular localization of these putative interactors was determined to get an initial understanding of where NLRP7 may interact with these proteins and possibly helps in

tumor formation.

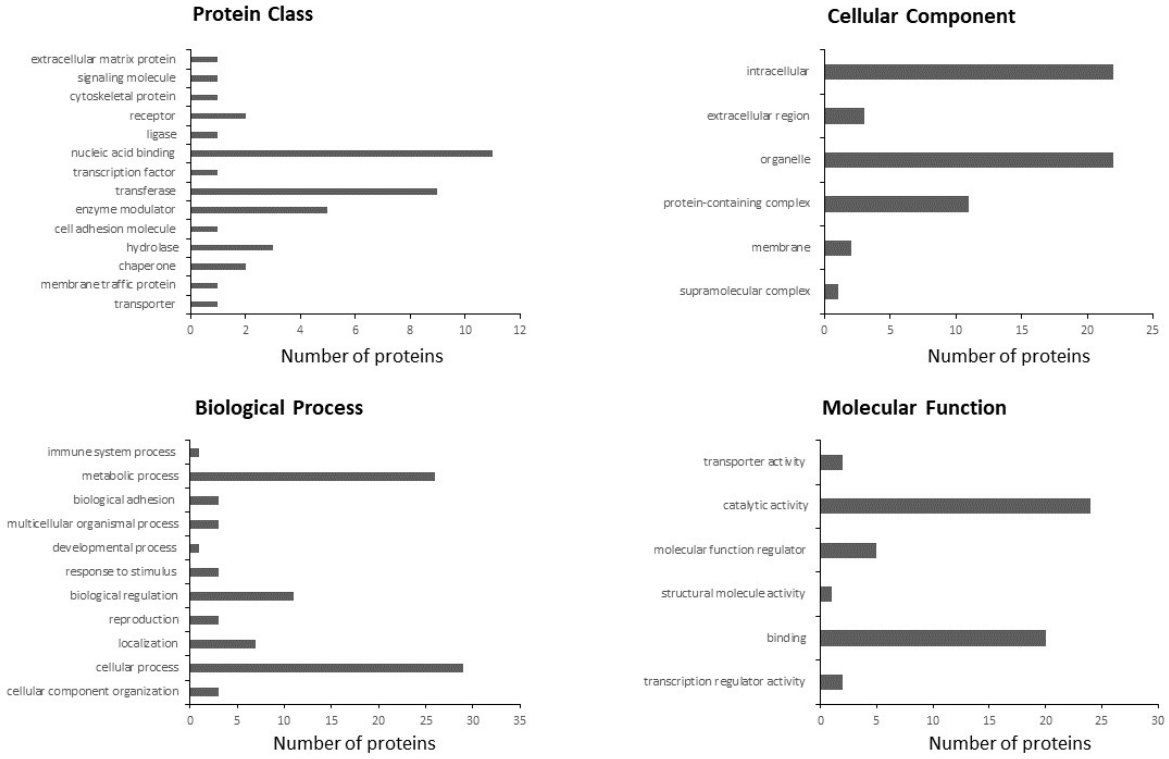

Figure 5.1. Classification of NLRP7's interaction partners using Panther software. Enriched proteins in MS data were uploaded to Panther software. Graphs show the number of proteins for the indicated categories in four different classification.

5.1.2. Determination of Top Canonical Pathways using Ingenuity Pathway Analysis Tool

Next, interaction partners of NLRP7 were analyzed via Ingenuity Pathway Analysis (IPA) tool to determine the biological pathways through which NLRP7 may contribute to human endometrial carcinoma. To this end, the previously determined 80 proteins from two different biological replicates were uploaded to IPA software with their fold changes. Remarkably, NLRP7's possible interaction partners were found to be associated with crucial pathways including cell proliferation and cell death pathways which gave the first hints about the role of NLRP7 in tumorigenesis. Table 5.1 describes the proteins that were revealed by the IPA tool and their related pathways.

Note that Brat1, RalB, and Rab5A were mostly studied in this thesis work (Figure 5.2).

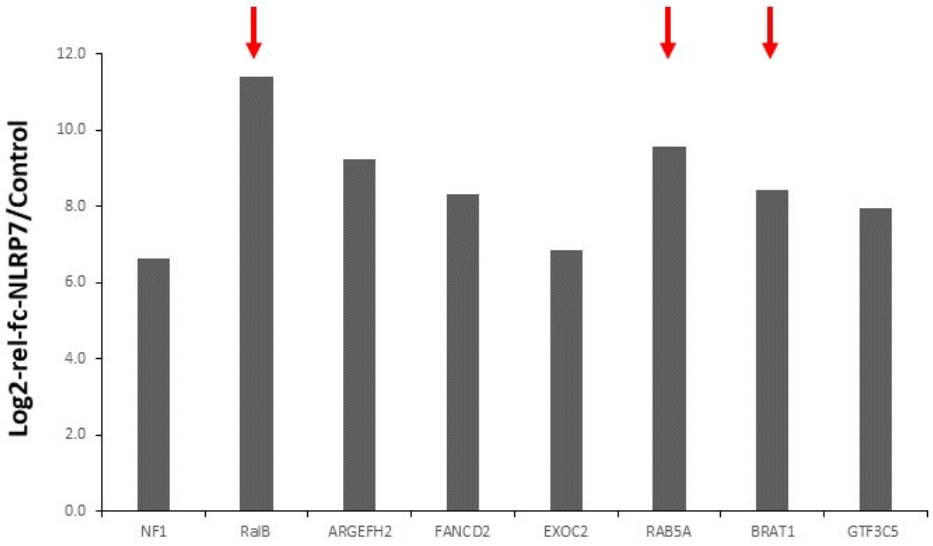

Figure 5.2. Mass Spectrometry data revealed the most possible NLRP7 interactors. Bar graph shows the most enriched proteins compared to the control group. Target proteins were basically normalized intensities of proteins, which are enriched in both replicates, taken into account the molecular weight, theoretical peptides and the actual found peptides. Red arrows indicate proteins which are further investigated.

Table 5.1: IPA results of proteins.

Gene	**Protein**	**KEGG Pathway**
NF1	Neurofibromin	MAPK signaling pathway
RalB	Ras-related protein Ral-B	Ras-related pathway
ARGEFH2	Rho guanine nucleotide exchange factor 2	Tight junction, *E.coli* infection
FANCD2	Fanconi anemia group D2 protein	Fanconi anemia pathway
EXOC2	Exocyst complex component 2	Ras signaling pathway
Rab5A	Ras-related protein Rab-5A	Endocytosis
BRAT1	BRCA1-associated ATM activator 1	Streoid biosynthesis Meatabolic pathways

Table 5.1. IPA results of proteins and their top canonical pathways (cont.).

Gene	Protein	KEGG Pathway
GTF3C5	General transcription facotr 3C polypeptide 5	Transfection factor TFIIC complex

5.1.3. NLRP7 upregulation might interfere with Ras signaling pathway

We also used IPA to conduct a network analysis using the 80 interactors that were described earlier. Intriguingly, we found that Ras and its downstream ERK (highlighted with the red circle) is at the center of this protein network (Figure 5.3A). For this reason, we decided to check whether ERK phosphorylation status is affected when NLRP7 is upregulated. To assess this idea we used different Hec1a cell lines including WT, Hec1a-empty (transduced with empty vector), and Hec1a-NLRP7 which stably produces NLRP7 protein. Remarkably, we observed significant ERK phosphorylation (much stronger p-ERK band in lane 3, Figure 5.3B) when the cells simply have more NLRP7, implying that NLRP7 may activate Ras signaling pathway to drive unwanted cell proliferation (Figure 5.3B).

5.2. Validation of NLRP7 Interaction Partners Using Co-Immunoprecipitation

On the basis of the bioinformatic analysis, three potential NLRP7 binding proteins (RalB, Brat1, and Rab5A) categorized in three groups in pathway analysis were picked out for further validation. The reason we chose these proteins is that they have the highest log value for their enrichment in the Mass Spectrometry (MS) data. In addition, 2 of them, RalB and Rab5A, are Ras-related proteins which may explain the ERK phosphorylation phenomenon that we observed. To validate the putative interac-

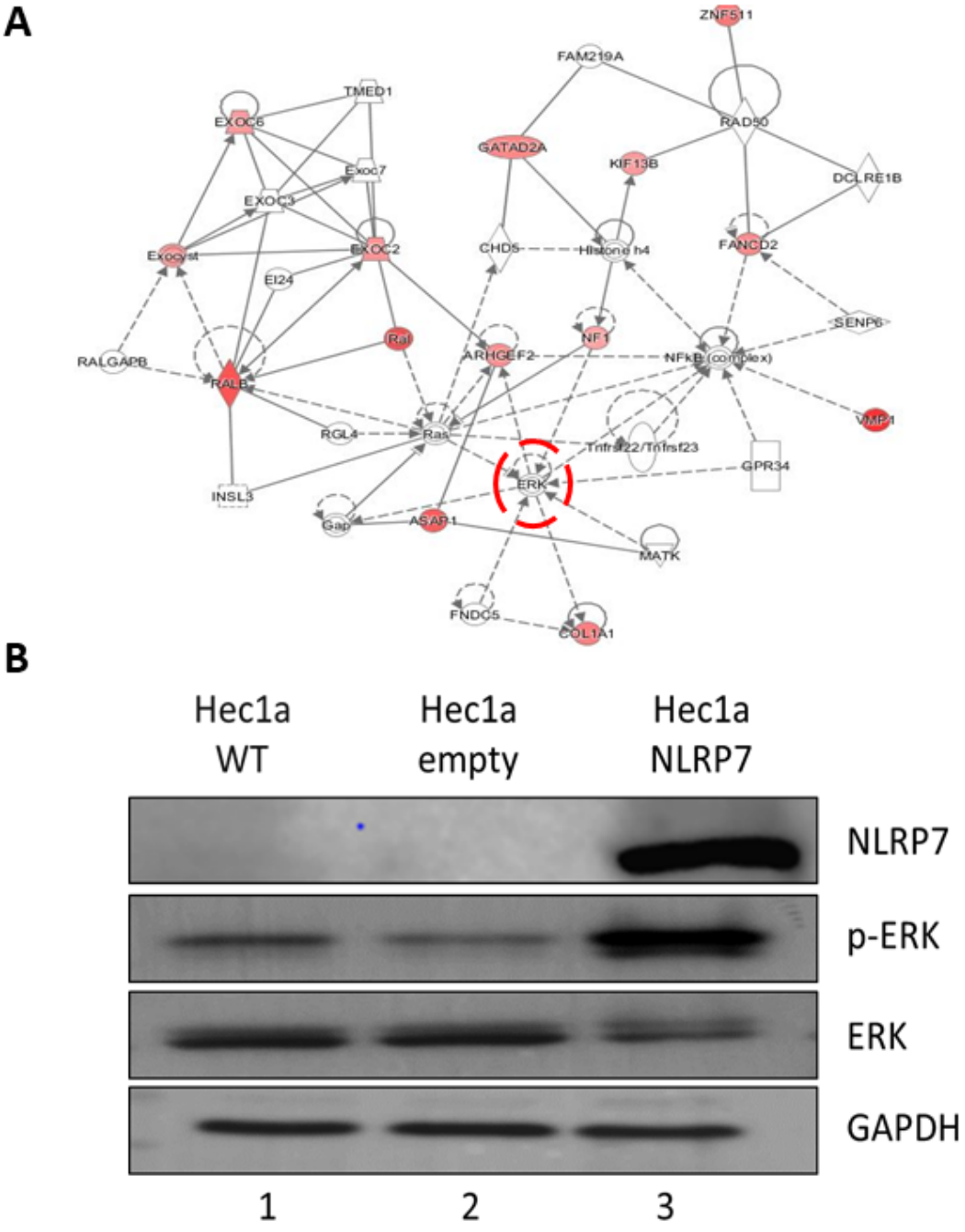

Figure 5.3. NLRP7 upregulation drives ERK phosphorylation. A) Protein network showing RAS and ERK (red circle) at the center. B) WT, empty transduced (Hec1a-empty) and NLRP7 stably expressing (Hec1a-NLRP7) Hec1a cells lysed and western blot was performed using indicated antibodies. GAPDH serves as loading control.

tions, we used Co-Immunoprecipitation (Co-IP) method. In this method we followed a simple strategy, a-) transfection of HEK293 cells with the plasmids encoding NLRP7 and its candidate interactor, b-) pulling down of NLRP7, and c-) Western blotting using antibodies against putative interactor proteins (Figure 5.4A). At the beginning, we determined a known NLRP7 interactor and a protein which negatively regulated in the Mass Spectrometry data to use them as positive and negative controls, respectively. An adaptor protein which functions in inflammasome formation, ASC, served as a positive control since the interaction between NLRP7 and ASC has previously been reported. As a negative control, Ago2, a catalytic protein functions in RNA interference, was chosen depending on its decreasing fold change in Mass Spectrometry Data. If you look at line 3 of Figure 5.4B, there is no interaction band for AGO2. However, in line 3 of Figure 5.4C, it can be clearly seen that ASC has an interaction band. In these figures, bottom panels also show protein expressions from the transfected plasmids (input). In conclusion, we observed that ASC interacts with NLRP7 (Figure 5.4B) while we didn't detect an interaction between AGO2 and NLRP7 (Figure 5.4C), which demonstrated that our Co-IP strategy is a reliable tool to detect NLRP7's interactors.

5.2.1. RalB interacts with NLRP7

RalB, a Ras-related GTPase protein, was chosen as the first putative interaction partner because of its highly increased fold change in the MS data and its relation with the aforementioned Ras signaling pathway. However, RalB and other GTPases interact with their targets transiently, therefore it is difficult to detect interactions between these proteins. In order to circumvent this problem, we generated a constitutively active RalB mutant by converting its 23rd Glycine residue into Valine using Site-directed mutagenesis (Figure 5.5A). Due to this mutation, RalB cannot hydrolyze GTP, therefore it becomes constitutively active which significantly elevates our chances to catch an elusive interaction between RalB and its effector (target), in this case, NLRP7. Afterwards, HEK293 cells were transfected with Myc-NLRP7, Flag-RalB and Flag-RalB G23V plasmids and then Co-IP was performed as previously described. We observed a faint interaction band for RalB (see lane 3 in Figure 5.5B), however, this interaction

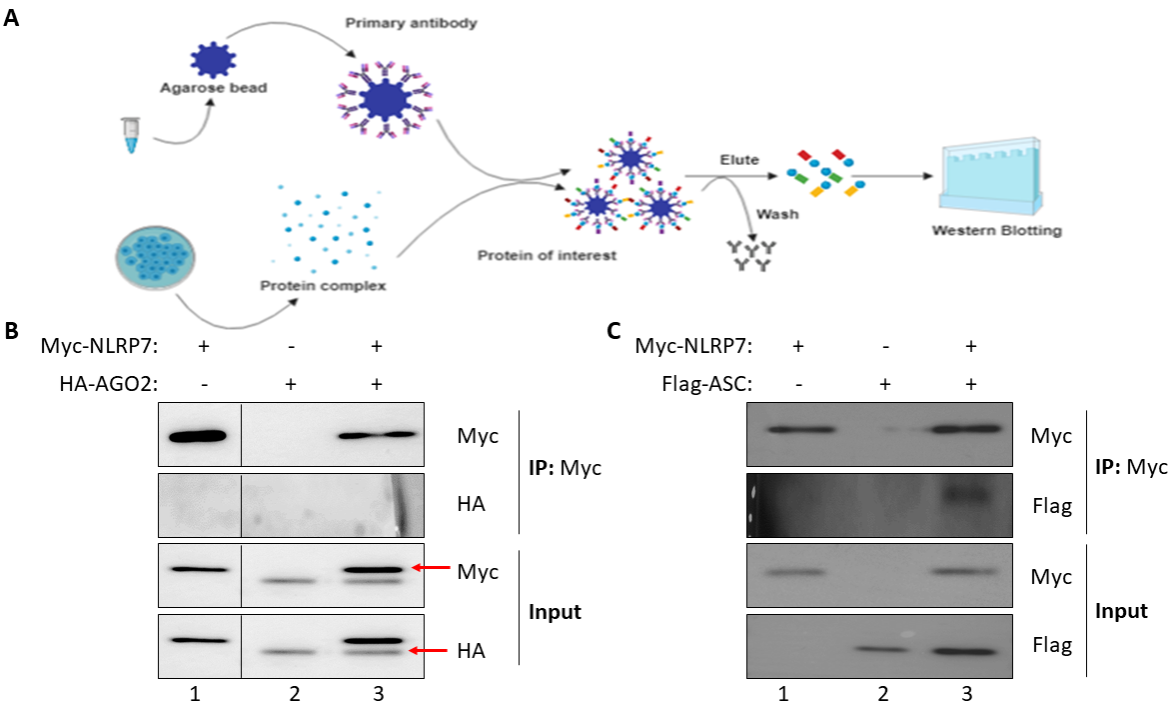

Figure 5.4. Using of Co-IP approach for the validation of NLRP7's possible interactors. A) Overview of Co-IP experiments. B) Myc-NLRP7, HA-AGO2 or C) Flag-ASC, Myc-NLRP7 expressing HEK293 cells were lysed and NLRP7 was precipitated using Myc antibody. Upper red arrow indicates NLRP7 while bottom one shows AGO2.

band was robust for the mutant RalB form (lane 4). In total, our results showed that NLRP7 physically interacts with RalB and this interaction is stronger with the mutant form, implying that NLRP7 might be an effector protein of RalB (Figure 5.5B).

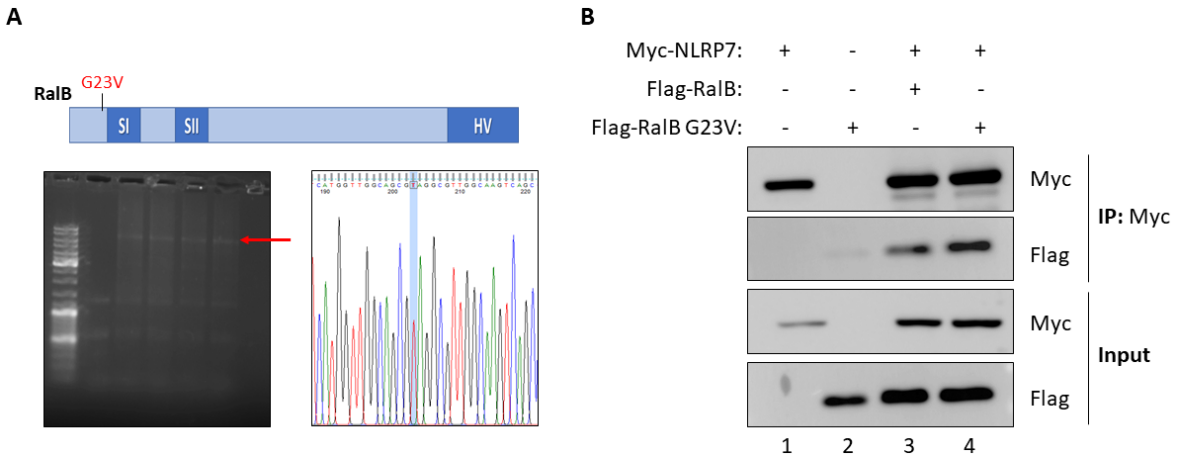

Figure 5.5. RalB is a novel interactor of NLRP7. A) Indicated mutation on RalB protein scheme (G23V) was introduced. Agarose gel shows amplified DNA band which have the desired mutation (red arrow) which confirmed by sequencing. B) HEK293 were transfected with indicated plasmids. 48 hours upon transfection, Co-IP was performed as previously described.

5.2.2. Rab5A interacts with NLRP7

After determining the NLRP7 and RalB interaction, we wanted to assess the putative interaction between NLRP7 and the other Ras-related protein Rab5A. Interestingly, the relationship between these two proteins was already being assessed by our previous lab member before we conducted MS analysis (Duygu Demiröz, 2011). She was able to show that NLRP7 colocalizes with Rab5A in the endosomes (data not shown) but she didn't show if these two proteins physically interact. Here, we again generated a constitutively active Rab5A mutant (Rab5A Q79L) using Side-directed mutagenesis since Rab5A is another GTPase like RalB (Figure 5.6A). To determine whether NLRP7 interacts with Rab5A, HEK293 cells were transfected with plasmids encoding Myc-NLRP7, CFP-Rab5A, and CFP-Rab5A-Q79L and subsequently Co-IP

was performed. As in the case of RalB interaction, we observed a mild interaction between NLRP7 and RaB5A (lane 3 in Figure 5.6B), reflecting a transient interaction between a GTPase and its effector. However, constitutively active Rab5A displays a potent interaction with NLRP7 (lane 4). In total, we observed that these two proteins physically interact and this interaction dramatically increases with the active Rab5A mutant which strengthen our notion that NLRP7 might be an effector of Ras-related GTPases Rab5A and also RalB (Figure 5.6B).

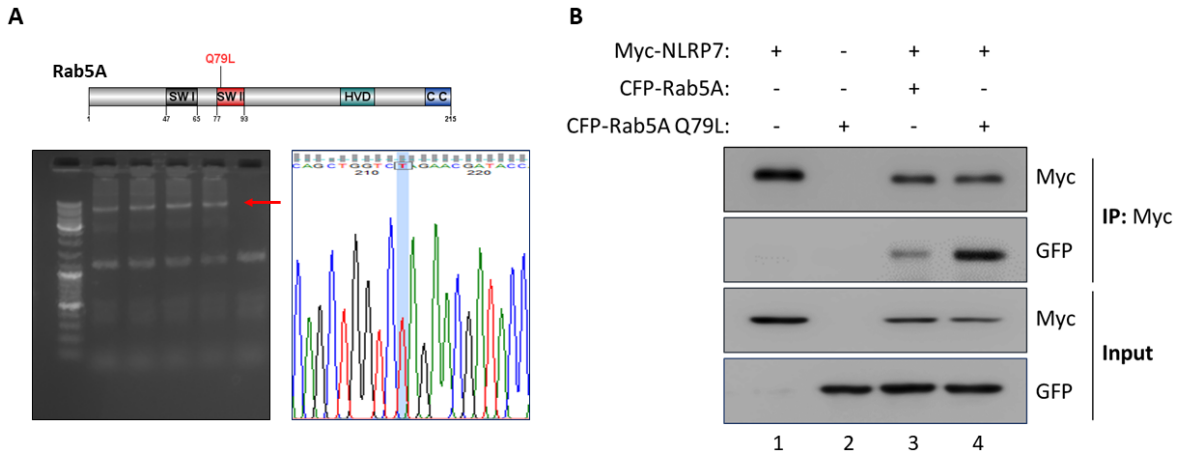

Figure 5.6. Rab5a interacts with NLRP7. A) Constituvely active Rab5A (Q79L) was generated using Side-Directed Mutagenesis. B) HEK293 cells were transfected with indicated plasmids. Pull down of NLRP7 was performed with Myc antibody. Western blotting was conducted using indicated antibodies. GFP antibody was able to detect CFP tagged Rab5A (CFP antibody wasn't available at that time).

5.2.3. Brat1 interacts with NLRP7

After showing the possible involvement of NLRP7 in the Ras signaling pathway, we decided to assess NLRP7's implication in another crucial pathway, which was revealed by our MS data. The candidate interactor is Brat1 and it functions in the DNA damage response pathway. To check whether NLRP7 physically interacts with Brat1, HEK293 cells were transfected with Myc-tagged NLRP7 and HA-Brat1 plasmids and subsequently NLRP7 immunoprecipitated using the anti-Myc antibody. Then, sam-

ples were analyzed using SDS-PAGE by performing immunoblots with HA and Myc antibodies. Only Brat1 and NLRP7 transfected HEK293 cells were used as controls separately to see whether both proteins may bind non-specifically to agarose beads. Our results showed that NLRP7 interacts with Brat1 (Figure 5.7A, lane 3). In addition, we also conducted a reciprocal Co-IP procedure by immunoprecipitating Brat1 (instead of NLRP7) using anti-HA antibody. In line with our previous finding, again, we observed an interaction band in the Western blot which strengthing our result that Brat1 is an interactor of NLRP7 (Figure 5.7B, lane 3). In total, our results revealed a novel interaction between NLRP7 and Brat1.

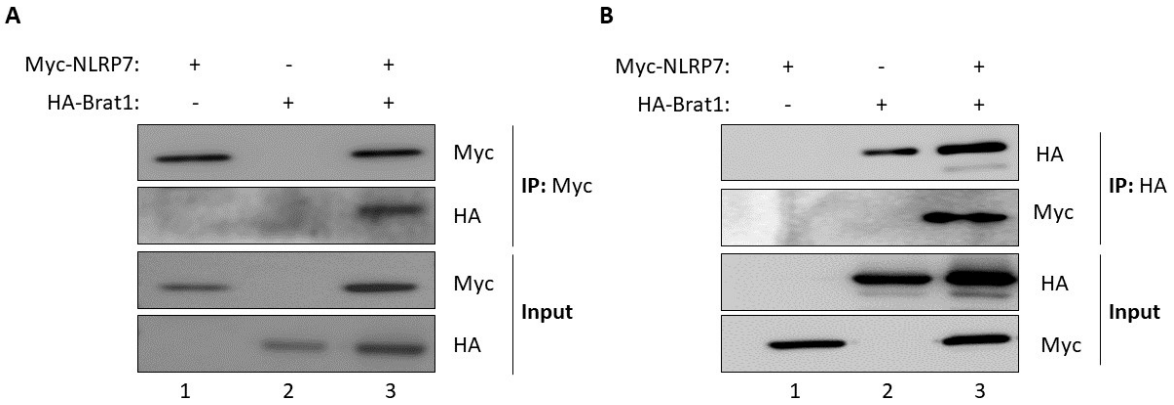

Figure 5.7. Brat1 is a new binding protein of NLRP7. Reciprocal co-immunoprecipitation from HA-Brat1 and Myc-NLRP7 transfected HEK293 cells. A) NLRP7 was immunoprecipitated using anti-Myc antibody. B) Brat1 was pulled down using anti-HA antibody. Western blotting was performed using indicated antibodies.

5.2.3.1. Sub-cellular Localization of Brat1 and NLRP7. Next, we wanted to monitor Brat1 and NLRP7's sub-cellular localization. To this end, HEK293 cells were transfected with Myc-NLRP7 and HA-Brat1 plasmids and they were stained with proper antibodies using the immunofluorescence protocol described in methods section. We observed that NLRP7 was predominantly found in the cytoplasm whereas Brat1 showed a dominant nuclear localization with a slight cytoplasmic expression which can be an artifact of transient expression (Figure 5.8).

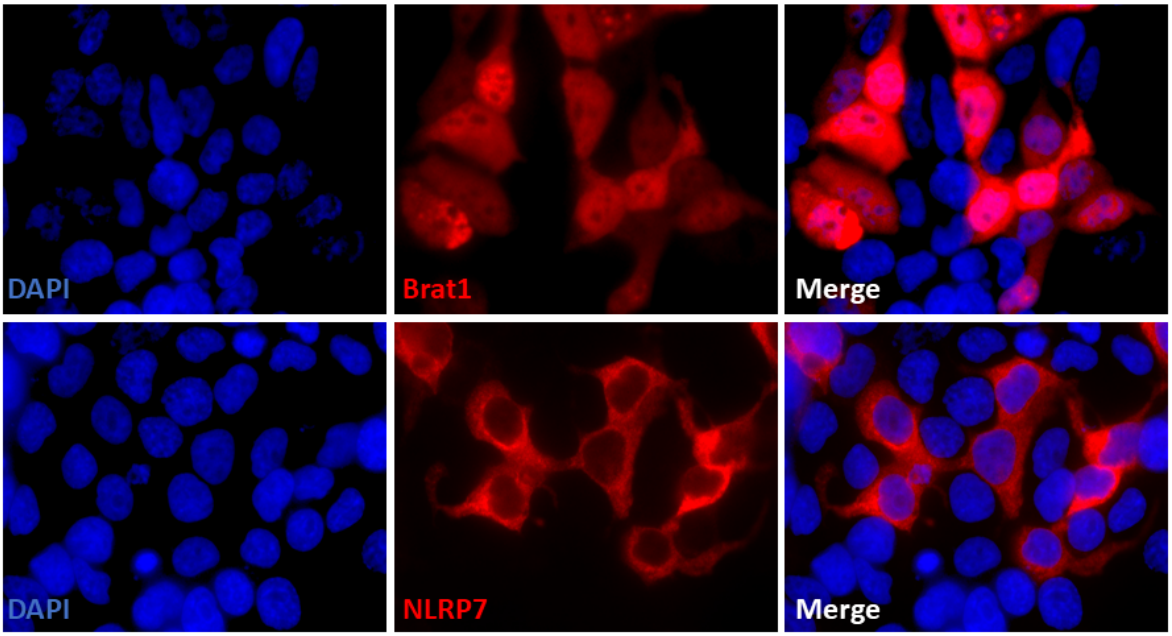

Figure 5.8. Sub-cellular localizations of NLRP7 and Brat1 differ. HEK293 cells expressing either Brat1 or NLRP7 plasmids were stained using corresponding antibodies (red). Nuclei were stained using DAPI (blue). Samples were visualized using fluorescence microscopy.

5.2.3.2. Prediction of Nuclear Localization Signals. Although we observed NLRP7 and Brat1 interaction, our IF data clearly showed that these two proteins are located in the different parts of the cells. Then we hypothesized that some portion of NLRP7 may migrate into the nucleus especially under certain conditions. To assess this idea, we checked if NLRP7 has nuclear localization signals (NLS) using bioinformatic tools. NLS represents specific sequence motifs which are required for the transport of proteins into the nucleus. NLS sequences vary in length and characteristics from protein to protein. When there is a single NLS on the sequence, which provides the import of that protein into nucleus, it is called as monopartite. On the other hand, if there is more than one monopartite signal bound with a linker sequence, it is named as bipartite NLS sequence [64]. We uploaded the protein sequence of NLRP7 into cNLS Mapper software to predict NLS of our protein. This software predicts the NLS on the protein of interests and interprets their sub-cellular localization based on their scores.

There are four possible outcomes: a-) score 8-10 indicates exclusive localization in the nucleus, b-) score 7-8 suggests partial localization in the nucleus, c-) score 3-5 points to localization in both nucleus and cytoplasm, and d-) score 1-2 indicates localization in the cytoplasm. As expected, NLRP7 does not contain strong NLS peptides, however, its score varies between 3-5, meaning that it can be transported between cytoplasm and nucleus (Figure 5.9).

A

Predicted NLSs in query sequence

```
MTSPQLEWTLQTLLEQLNEDELKSFKSLLWAFPLEDVLQKTPWSEVEEAD 50
GKKLAEILVNTSSENWIRNATVNILEEMNLTELCKMAKAEMMEDGQVQEI 100
DNPELGDAEEDSELAKPGEKEGWRNSMEKQSLVWKNTFWQGDIDNFHDDV 150
TLRNQRFIPFLNPRTPRKLTPYTVVLHGPAGVGKTTLAKKCMLDWTDCNL 200
SPTLRYAFYLSCKELSRMGPCSFAELISKDWPELQDDIPSILAQAQRILF 250
VVDGLDELKVPPGALIQDICGDWEKKKPVPVLLGSLLKRKMLPRAALLVT 300
TRPRALRDLRILAQQPIYVRVEGFLEEDRRAYFLRHFGDEDQAMRAFELM 350
RSNAALFQLGSAPAVCWIVCTTLKLQMEKGEDPVPTCLTRTGLFLRFLCS 400
RFPQGAQLRGALRTLSLLAAQGLWAQMSVFHREDLERLGVQESDLRLFLD 450
GDILRQDRVSKGCYSFIHLSFQQFLTALFYTLEKEEGEDRDGHAWDIGDV 500
QKLLSGEERLKNPDLIQVGHFLFGLANEKRAKELEATFGCRMSPDIKQEL 550
LQCKAHLHANKPLSVTDLKEVLGCLYESQEEELAKVVVAPFKEISIHLTN 600
TSEVMHCSFSLKHCQDLQKLSLQVAKGVFLENYMDFELDIEFERCTYLTI 650
PNWARQDLRSLRLWTDFCSLFSSNSNLKFLEVKQSFLSDSSVRILCDHVT 700
RSTCHLQKVEIKNVTPDTAYRDFCLAFIGKKTLTHLTLAGHIEWERTMML 750
MLCDLLRNHKCNLQYLRLGGHCATPEQWAEFFYVLKANQSLKHLRLSANV 800
LLDEGAMLLYKTMTRPKHFLQMLSLENCRLTEASCKDLAAVLVVSKKLTH 850
LCLAKNPIGDTGVKFLCEGLSYPDCKLQTLVLQQCSITKLGCRYLSEALQ 900
EACSLTNLDLSINQIARGLWILCQALENPNCNLKHLRLWSCSLMPFYCQH 950
LGSALLSNQKLETLDLGQNHLWKSGIIKLFGVLRQRTGSLKILRLKTYET 1000
NLEIKKLLEEVKEKNPKLTIDCNASGATAPPCCDFFC 1037
```

B

Predicted bipartite NLS

Pos.	Sequence	Score
164	RTPRKLTPYTVVLHGPAGVGKTTLAKKCMLD	3.1
164	RTPRKLTPYTVVLHGPAGVGKTTLAKKCMLD	3.3
164	RTPRKLTPYTVVLHGPAGVGKTTLAKKCMLDW	4.4
286	LLKRKMLPRAALLVTTRPRALRDLRILA	4.8
371	TTLKLQMEKGEDPVPTCLTRTGLFLRFLC	4
528	EKRAKELEATFGCRMSPDIKQELLQCKAHLH	3.2
701	RSTCHLQKVEIKNVTPDTAYRDFCLAFIGKKTLT	3.4
791	LKHLRLSANVLLDEGAMLLYKTMTRP	3.9
791	LKHLRLSANVLLDEGAMLLYKTMTRPKH	5.2
792	KHLRLSANVLLDEGAMLLYKTMTRPKHFL	3.5
814	TRPKHFLQMLSLENCRLTEASCKDLAAVLV	3.5
853	LAKNPIGDTGVKFLCEGLSYPDCKLQTL	4.2
860	DTGVKFLCEGLSYPDCKLQTLVLQQCSITKL	3.2

Figure 5.9. NLRP7 may be transported into nuclues. A) Predicted NLS (highlighted with red) of NLRP7 on amino acid sequence. B) Positions and scores of NLS peptides of NLRP7 by cNLS software.

5.2.3.3. NLRP7 interferes with DNA damage response pathway. There is not much about Brat1 in the literature besides its function in DNA damage response [65]. For this reason, we hypothesized that NLRP7 may dysregulate proper DNA damage response by interfering with Brat1. Here we co-transfected HEK293 cells with NLRP7, Brat1, and combination of these two plasmids. Subsequently, we treated the cells with hydrogen peroxide (H_20_2) at different time points to induce DNA damage and we analyzed the phosphorylation levels of two instrumental proteins, Chk1 and Chk2, which coordinate DNA damage response. Our results revealed a dramatic difference for p-Chk1 levels especially at 6 h time points (Figure 5.10). Brat1 expressing cells quickly respond to DNA damage (see lane 6) while this response sharply delayed when NLRP7

is expressed (see lanes 3 and 9). On the other hand, we didn't observe significant changes for p-Chk2.

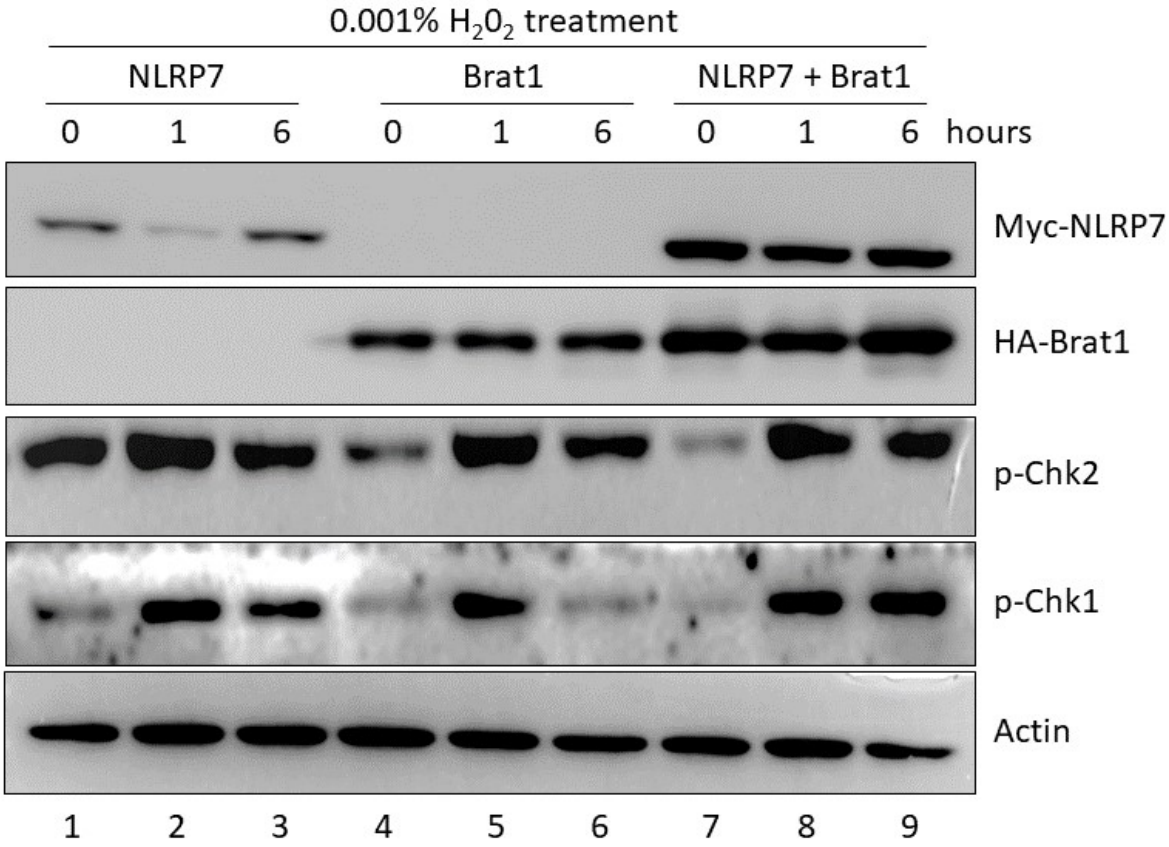

Figure 5.10. NLRP7 overexpression delays DNA damage response. HEK293 cells transfected with NLRP7, Brat1 or combination of these two plasmid. 24 hours after transfection, DNA damage was induced using 0.001% H_20_2 for 1 to 6 hours. Lane 3 and 9 indicate persistent Chk1 phosphorylation (p-Chk1) whereas lane 6 shows quickly reversed p-Chk1.

5.2.4. NLRP7 gets modified by both SUMO paralogs

So far, we revealed three novel interactors of NLRP7 based on our MS data. Intriguingly, our MS data also indicated that NLRP7 might be modified by Small Ubiquitin-Like Modifier (SUMO). Briefly, humans have three functional SUMO paralogs; SUMO1, SUMO2 and SUMO3. SUMO2, and SUMO3 are quite similar and they cannot be distinguished by antibodies, therefore they are referred to as SUMO2. These

peptides covalently attach to their substrates through a process known as SUMOylation. Proteins get modified by SUMO on lysine residues found within a consensus motif. SUMOylation regulates different basic properties of proteins such as their enzymatic activity, stability, interactions, and solubility. Moreover, this modification is reversible by SUMO-specific proteases, which makes it a highly dynamic modification [66]. In the literature, it has been shown that NLR proteins are subjected to SUMOylation. For example, a crucial NLR protein, NLRP3, gets modified by SUMO, which inhibits inflammasome activation [67]. Furthermore, many articles showed that misregulation of the SUMO pathway is implicated in cancer cells [68].

To investigate whether NLRP7 is modified by SUMO, firstly we did an in silico analysis to determine if NLRP7 has any lysine residues within a consensus motif. Our analysis revealed two lysine residues onto which SUMO may covalently be attached (Figure 5.11A). Next, we transfected HEK293 with Myc-NLRP7, His-SUMO1, and His-SUMO2 plasmids. Then, we pulled down His-tagged SUMOs using Nickel-NTA beads and performed Western blot using anti-Myc antibody. This method enabled us to detect only the SUMO-modified NLRP7 proteins. We observed ladder-like bands which reflects SUMOylated forms of NLRP7, although some portion of it non-specifically bound to beads. Consequently, in line with our MS data and in silico discovery, we observed that NLRP7 gets modified by both SUMO paralogs (Figure 5.11B, lanes 7 and 8).

5.3. Knockdown of NLRP7 using CRISPR/Cas9 Technology

After demonstrating the novel interactors and modifiers of NLRP7, we also wanted to assess the role of NLRP7 in tumorigenesis using phenotypic assays. Previously, Hec1a cells which stably express NLRP7 (Hec1a-NLRP7) were generated by our former lab members. To complement this, we decided to generate NLRP7 knockdown Hec1a cell line using CRISPR/Cas9 technology. In this approach, our single guide RNAs were used to target the first exon of NLRP7 to downregulate NLRP7 expression. To achieve this, firstly we produced lentiviruses by transfecting HEK293 cells with P-VSV-G (envelope vector), PSPAX2 (packaging vector) and Flag-tagged Cas9 plasmids.

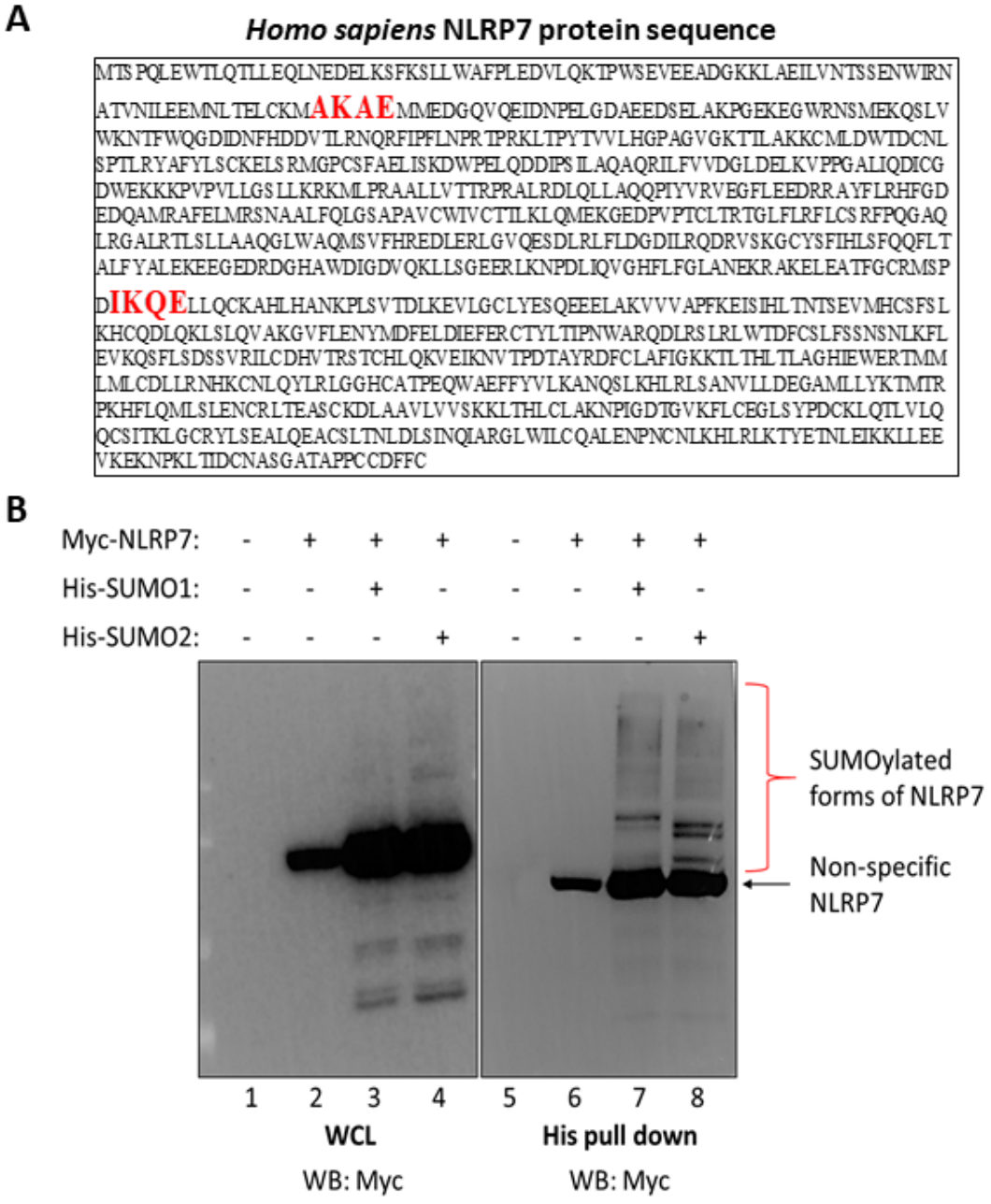

Figure 5.11. NLRP7 gets modified by both SUMO paralogs. A) In silico discovery of two SUMOylation sites on NLRP7 protein sequence. B) HEK293 cells were transfected with indicated plasmids. His-tagged SUMO proteins were precipitated using Nikel beads and Western blotting was performed using indicated antibodies. The ladder like structure represents SUMOylated forms of NLRP7.

Afterwards, Hec1a cells were transduced with these lentiviruses to insert Cas9 into the genome of Hec1a cells (Figure 5.12A). Since Cas9 plasmid also carries an antibiotic marker (puromycin), we treated the cells with puromycin to eliminate untransduced cells from the population (Figure 5.12B). Finally, we validated Cas9 expression using Western blotting (Figure 5.12C). Note that in our system Cas9 expression is doxycycline (dox) inducible, and we also determined that 24 hours treatment with 2 μg/ml dox treatment yields with the optimal Cas9 expression.

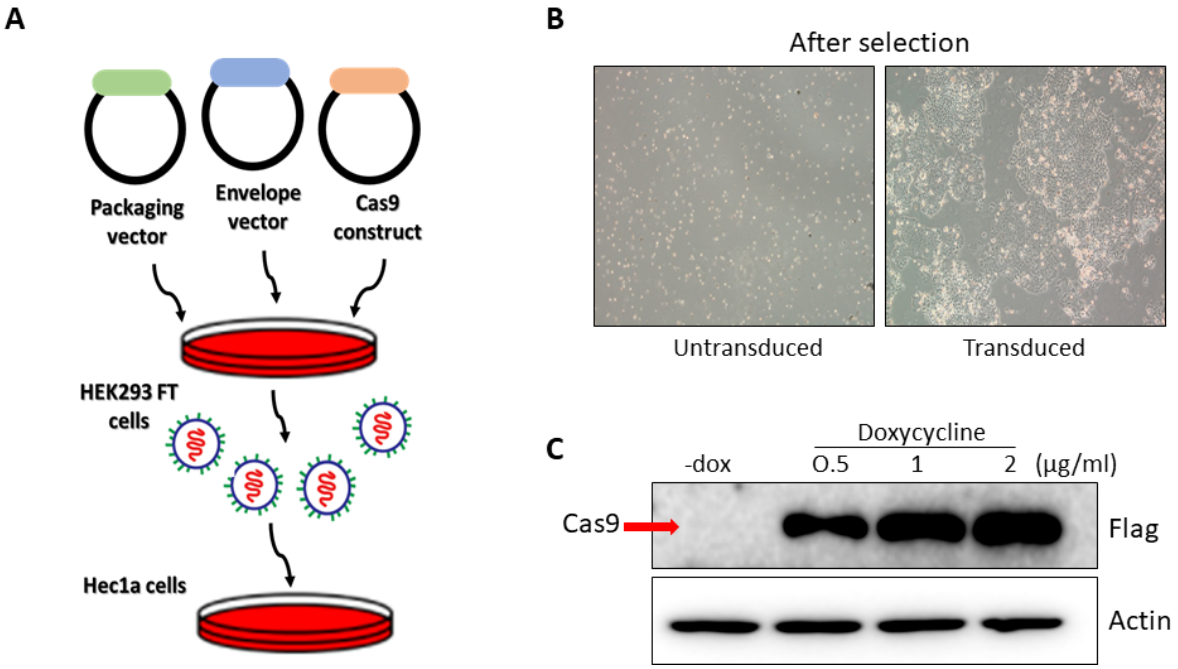

Figure 5.12. Generation of Cas9 stable Hec1a cells. A) Diagram showing transduction procedure. B) Bright field images of transduced and untransduced Hec1a cells after puromycin selection. C) Cells were treated with indicated doxycycline concentrations. Anti-Flag antibody was used to detect Flag tagged-Cas9 (red arrow) levels and actin was used as a loading control.

Next, using the same strategy described earlier, we produced two separate sgRNA (sg6 and sg7) carrying lentiviruses in HEK293 cells (Figure 5.13A). sgRNA plasmids have a fluorescent marker GFP which is used to determine transduction efficiency of these plasmids into Hec1a cells. Flow cytometry analysis showed that nearly half of the cells are transduced with sgRNAs (Figure 5.13B). Then, to get the same population of cells (having the same genetic background), we sorted the population of transduced cells and got single cells having GFP expression (Figure 5.13C). Finally, we performed Q-PCR to validate successful downregulation of NLRP7 by checking its mRNA levels. Our results demonstrated that NLRP7 downregulated significantly by both sgRNAs, although sg7 worked slightly better (Figure 5.13D). Interestingly, we observed NLRP7 downregulation in the absence of dox induction which possibly due to leaky expression of Cas9 plasmid.

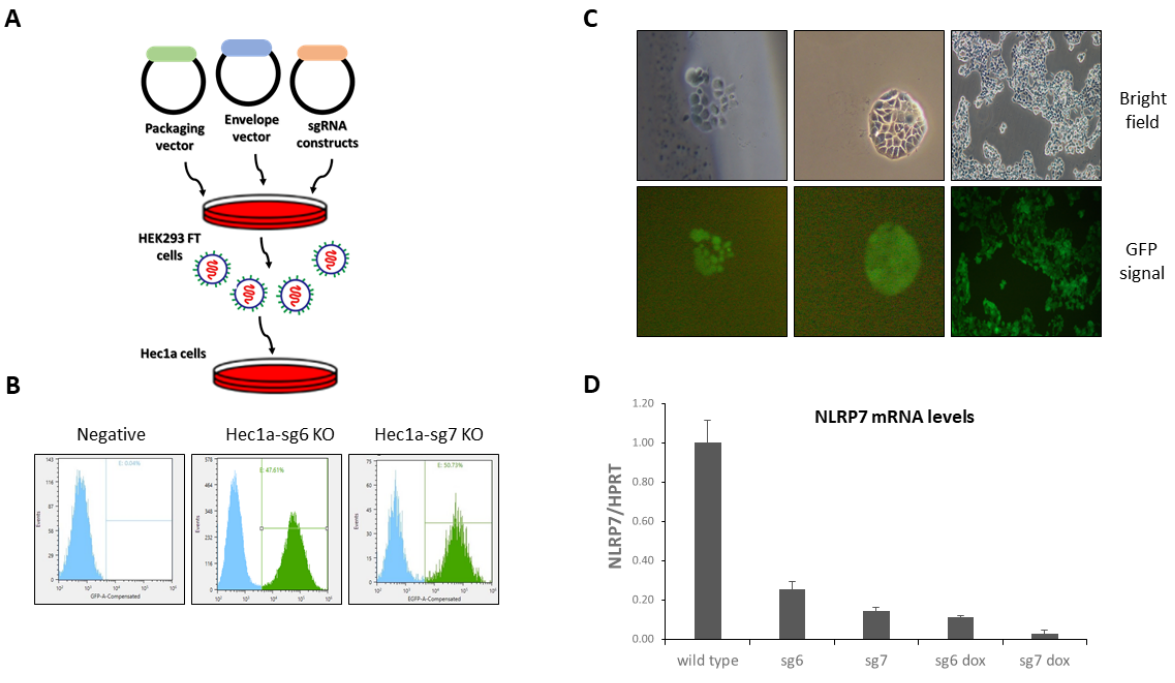

Figure 5.13. Downregulation of NLRP7 using CRISPR system in Hec1a cells. A) Diagram showing sgRNAs' transduction procedure. B) Lentiviral transduction efficiency was determined via Flow cytometry. C) Images of single cell colonies having GFP expression after sorting procedure. D) NLRP7 mRNA levels were detected with Q-PCR with and without DOX induction.

5.4. Generation of Stable Cell Lines

In order to understand whether the oncogenic effect of NLRP7 is specific to human endometrium, we wanted to generate other cell lines with stable NLRP7 expression. Firstly, trophoblast-like Swan71 stable cell lines were generated since NLRP7 is abundantly expressed by trophoblast cells and it was shown that NLRP7 downregulation causes a significant decrease in the proliferation rate of these cells and furthermore researchers claimed that NLRP7 controls trophoblast proliferation, migration, and invasion by showing an anti-apoptotic role [18]. In addition, human choriocarcinoma stable cells (JAR) were generated since choriocarcinoma is placental cancer that develops upon abnormal pregnancies named Hydatidiform Moles (HMs) and there is a strong connection between recurrent HMs and mutations in Nlrp7 gene revealed by genetic studies and by iPSC disease modeling in our lab [12]. GFP was inserted into both cell's genome to use it as a negative control. Expression of NLRP7 was analyzed in both cell line via Western blotting (Figure 5.14).

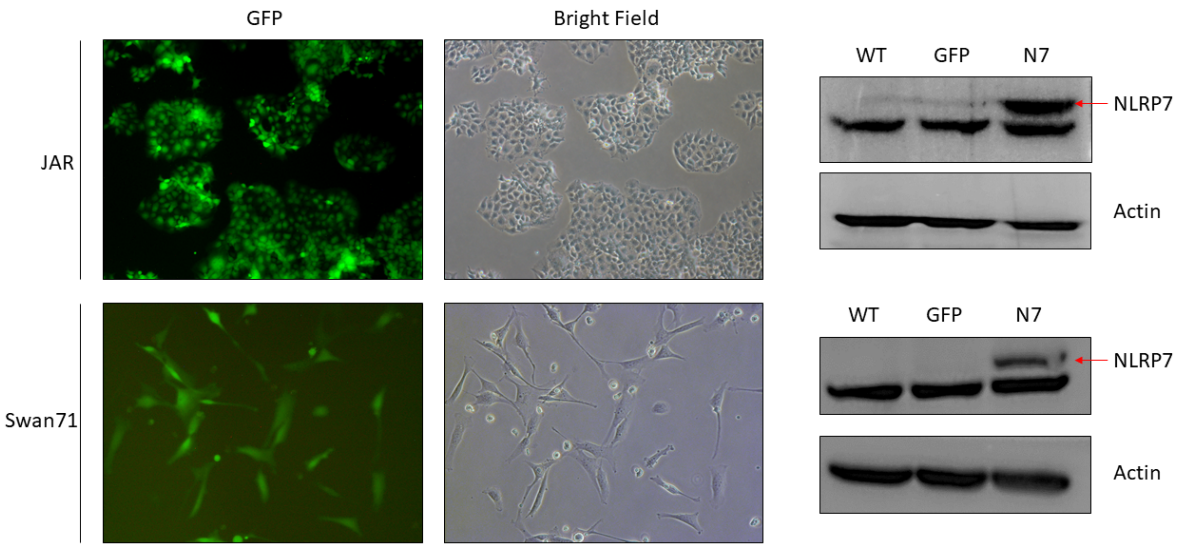

Figure 5.14. Generation of NLRP7 expressing stable cell lines. JAR and SWAN stably expressing GFP and NLRP7 cell lines were generated by lentiviral transduction method. GFP signaling was observed with fluorescence microscope. NLRP7 levels were checked via western blotting. Actin was used as loading control.

5.5. Antibody Production Against NLRP7

In our experiments, we had difficulties to detect endogenous NLRP7. For instance, after validating NLRP7 knockdown in Hec1a cell line at the mRNA level, we wanted to show it at the protein level. Unfortunately, our commercial antibody could not detect endogenous NLRP7 protein due to some unknown reasons. Since NLRP7 is not studied intensely around the world, there are not many options for us to buy and use commercial antibodies. For this reason, we decided to produce our own antibody.

5.5.1. Purification of NLRP7

The first step of antibody production was the purification of NLRP7. To start with, PET30(a+)-NLRP7 plasmid was transformed into Rosette- pLysS *E.coli* strain, then IPTG induction was applied to produce His-tagged NLRP7 in these bacteria. After successful induction, cells were disrupted and lysed using Triton-X containing buffer and sonication. Next, samples were centrifuged to remove soluble proteins from insoluble proteins, which contain NLRP7. After discarding supernatant, the pellet was dissolved in PBS, which subsequently was mixed with Laemmli buffer and analyzed with Coomassie staining.

After obtaining sufficient amount of NLRP7, we wanted to purify it before immunization. Previously, purification of NLRP7 using His bound columns was not achieved due to precipitation of NLRP7 into inclusion bodies. Thus, NLRP7 was purified by gel extraction method from the polyacrylamide gel. The concentration of purified NLRP7 was determined as 700 μg/ml using BSA standards (Figure 5.15A). Additionally, the specificity of bands was checked with anti-His and commercial anti-NLRP7 antibodies (Figure 5.15B). His antibody showed a single band whereas commercial NLRP7 antibody detected both NLRP7 as a single band and a smear pattern that can be explained by some degradation of NLRP7 and also non-specific proteins come from gel extraction procedure.

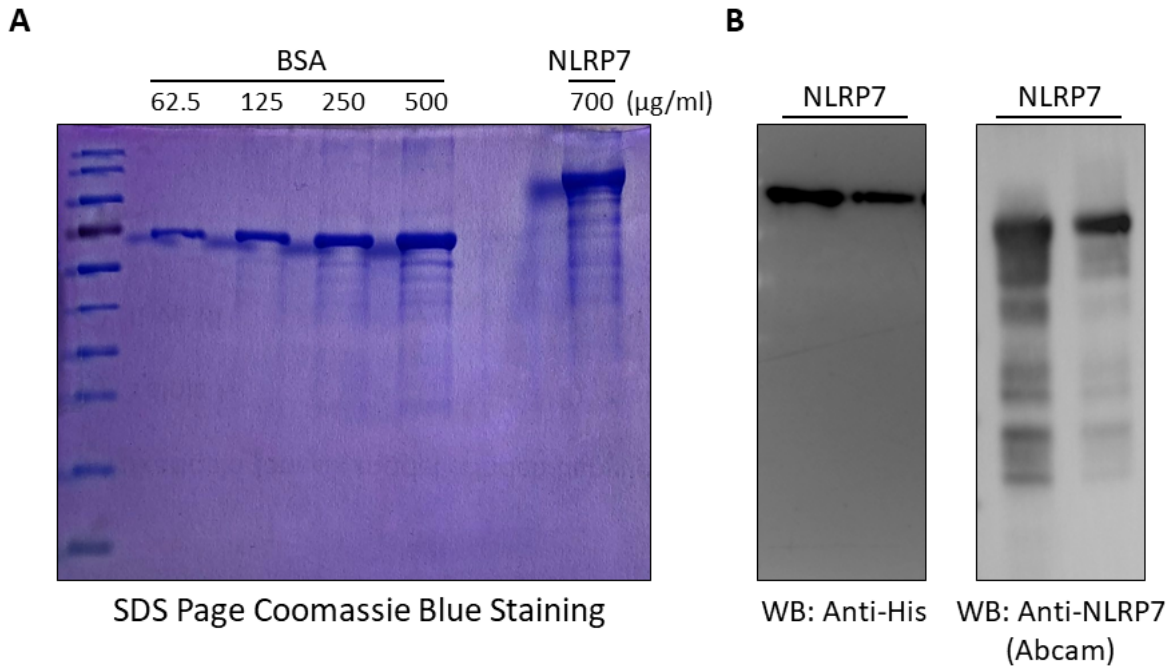

Figure 5.15. NLRP7 was purified from Polyacrylamide Gel. A) NLRP7 amount was controlled with Coomassie Staining by comparing it with the BSA standarts and subsequently it was quantified with Image J software. B) NLRP7 levels were detected via Western blot with indicated antibodies. Duplicate lanes were shown.

5.5.2. Monoclonal Antibody Production Against NLRP7 Protein using Hybridoma Technology

We performed the following steps to generate monoclonal antibody against NLRP7: immunization, fusion, selection, hybridoma production, screening, cloning, expanding and freezing down hybridomas, and antibody validation (Figure 5.16). These steps were briefly described here in this thesis.

Immunization is necessary to introduce an antigen to induce the humoral immune response in the mice. This essential step results in the production of B cells which secrete antibody against NLRP7. Figure 5.17A summarizes the timeline of immunizations. Immunizations were carried out with 100 ng protein which is diluted in PBS and mixed with equal volumes of adjuvants, which injected into five weeks old

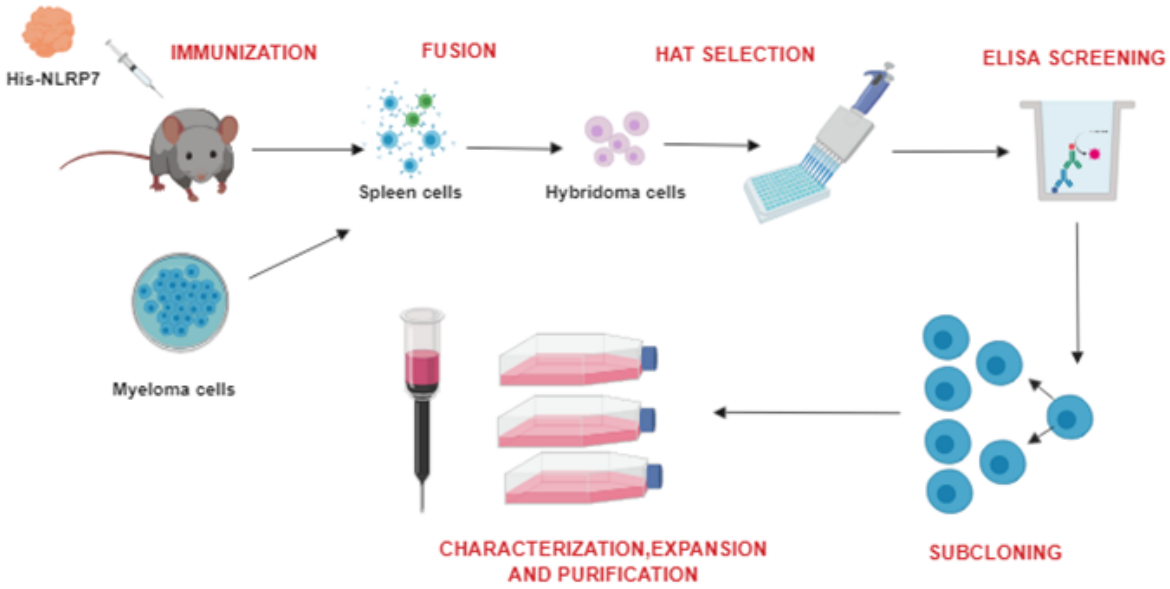

Figure 5.16. Diagram illustrating the flow chart of the production of monoclonal antibodies. Purified NLRP7 antigen introduced to a mouse and then, B cells collected from the mouse spleen and fused with myeloma cells. The resulting hybridoma cells are selected with HAT medium. After ELISA screening, hybridomas producing the desired monoclonal antibodies cultured and expanded.

three BALB/c mice. Blood was collected 10 days after injection using 1:1 sodium citrate to impede coagulation and subsequently, ELISA was performed to assess the antibody response against NLRP7 after immunization. Our results indicated that all three mice were successfully immunized against NLRP7 (Figure 5.17B). After the third immunization, one of these mice was selected as the spleen donor for the fusion step.

One day before the fusion, feeder layer plates were prepared with peritoneal macrophages to provide growth factors to support the growth of the hybridoma cells. Peritoneal macrophages were collected from female animals of the same strain as the immunized animal. Then, cells were counted and distributed into 96 well plates.

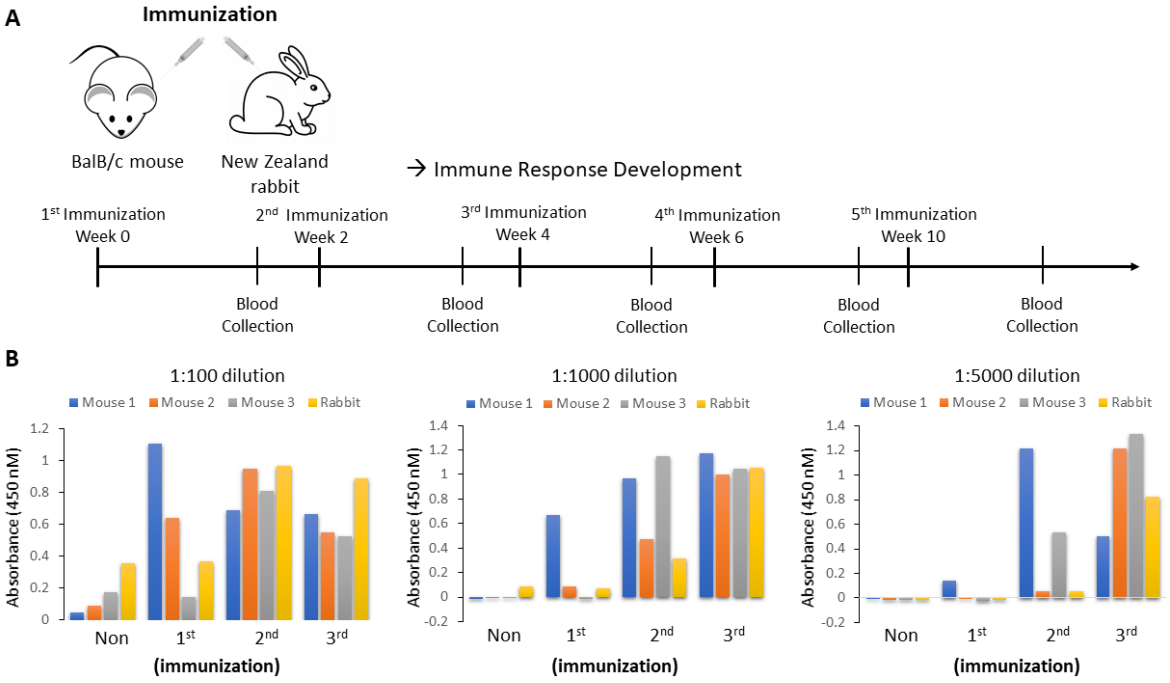

Figure 5.17. Verification of antibody responses against NLRP7. A) Immunizations were performed with 100 ng and 200 ng protein for five weeks old three BALB/c mice and a New Zealand rabbit, respectively. Blood was collected 10 days after injections using a 1:1 sodium citrate buffer. B) Serum responses of mice and the rabbit against NLRP7 were determined via indirect ELISA with indicated dilutions.

On the day of the fusion, the spleen cells from immunized mice were removed under sterile conditions and placed into a petri dish containing PBS. Then, the foreign tissues around the spleen were cleared and the spleen was crushed to reveal the cells. F0 myeloma cells which are at least 95% viability were prepared 10 days before fusion. The counted F0 and spleen cells were combined in a 1:5 ratio. After 10 days, 100 μl supernatants were removed and 100 μl HAT medium was added onto the cells.

In Figure 5.18, the diagram shows the possible outcomes of the fusion step. We separated Myeloma – Spleen Hybrid cells from others and selection was carried out based on their ability for nucleotide synthesis. Briefly, cells can use two pathways for nucleotide synthesis. Myeloma cells are deficient for HPGRT protein, which is essential for Salvage pathway so that their survival depends on the de novo pathway. Aminopterin in HAT medium blocks de novo pathway so when HGPRT deficient cells were planted in HAT medium, both of their DNA synthesis pathways were blocked, thus they are being eliminated from the population. Furthermore, spleen cells cannot live longer than four to five days in cell culture conditions after plantation. So, in HAT medium, the only myeloma–spleen hybridoma cells survive and reproduce to form colonies. The HAT selection was completed after 10 days, and the cultures were passed into the HT medium to remove the drug aminopterin.

Thirteen days after the fusion step, colonies were screened by ELISA to determine the NLRP7 antibody secreting colonies. After detecting positive colonies, serial dilutions were made to obtain the exact single cell to grow a colony. After plantation of fusion samples to 96-well plates, we observed colony formations in around 350 wells. We screened those samples using ELISA and narrowed down the number of colonies to 65 based on their OD values.

In the second round of ELISA, we observed that only 27 of these colonies maintained their positive response to NLRP7. After serial dilutions of these promising colonies, we ended up with 4 candidate hybridoma colonies which still secreted antibody against NLRP7.

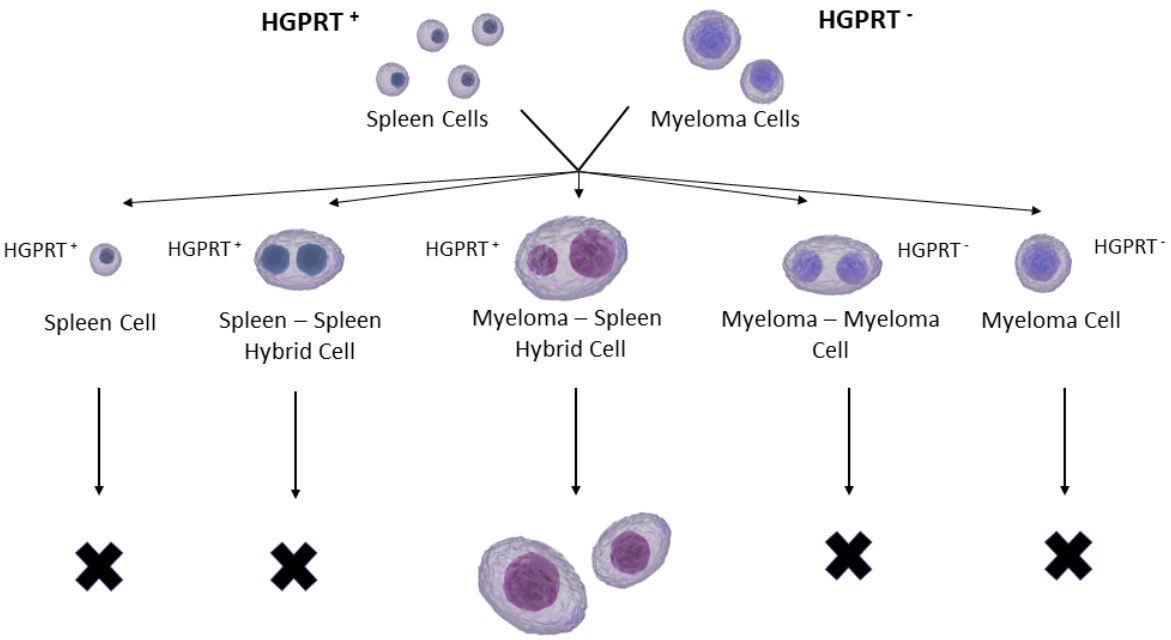

Figure 5.18. Selection of hybridoma cells using HAT medium. Illustration shows the possible outcomes of HAT medium selection. Aminopterin in HAT medium prevents the growth of Myeloma cells by blocking de novo DNA synthesis whereas spleen cells can not survive in cell culture conditions. Therefore, only Myeloma-Spleen hybrid cells can grow on this medium.

We also assessed the cross-reactivity with the blocking, BSA, solution during serial dilutions because there is a possibility that samples could detect the blocking solution instead of NLRP7. Indeed, one of our samples did react with the blocking solution, therefore, we discarded it. Finally, five colonies, obtained by serial dilutions of previously determined 4 candidates, continuously detected NLRP7 during serial dilutions in ELISA experiments and these samples were determined as strong candidates for providing monoclonal antibody against NLRP7 (Figure 5.19). In order to check their specificity and efficiency in Western blotting, we run HEK293 lysates which contain NLRP7 on SDS-PAGE. During Western blotting, we incubated membranes using the aforementioned colonies' supernatants. Our results showed that one of our colonies, termed as 3-F2, successfully detects NLRP7 (Figure 5.20).

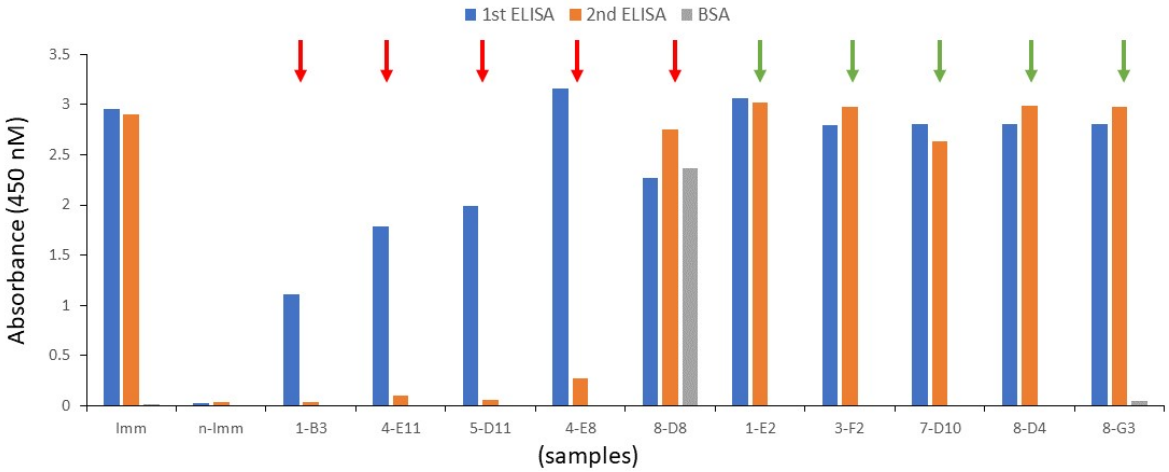

Figure 5.19. Five hybridoma colonies retains their response against NLRP7. After serial dilutions, supernatants of various colonies were analyzed using ELISA. The figure represents: four colonies lost their pre-existing response (red arrows), one colony's (8-D8) BSA cross-reactivity (red arrow), and response retaining colonies (green arrows).

Then, to be further sure that these cells are coming from the same origin, we performed serial dilutions again to get single colonies and we used their supernatants for Western blotting, which showed that all colonies produce antibodies against NLRP7 (Figure 5.21).

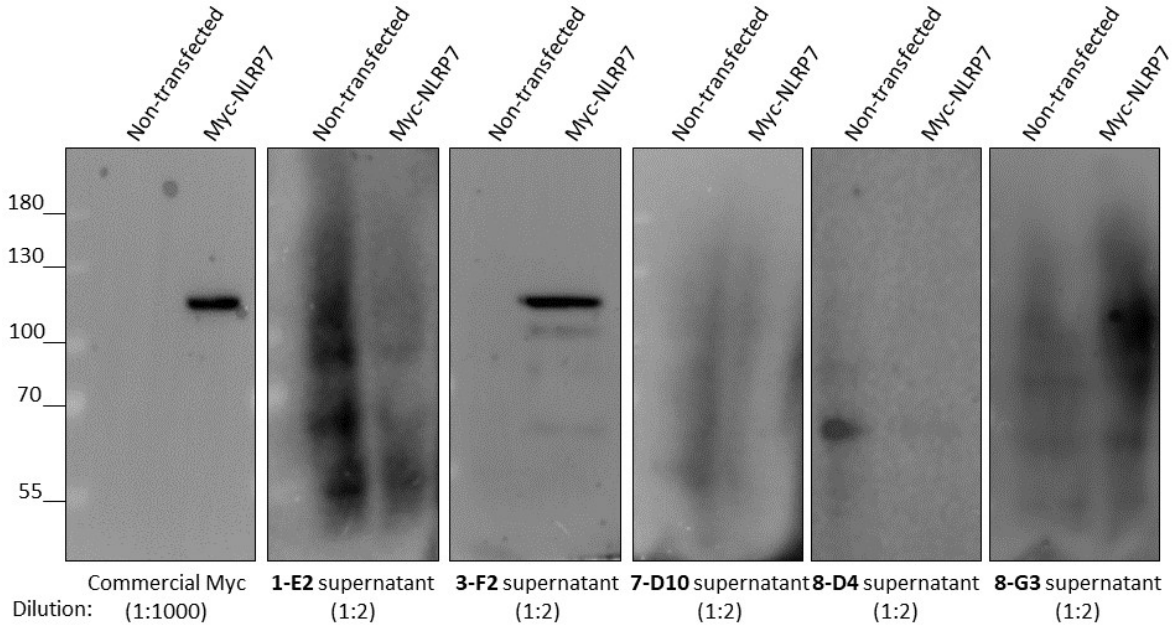

Figure 5.20. A hybridoma colony, termed as 3-F2, successfully detects NLRP7. Myc-NLRP7 transfected HEK293 cell lysates were checked via western blotting using Myc antibody and different colony supernatants (1E2, 3F2, 7D10, 8D4, and 8G3) in 1:1000 and 1:2 dilutions, respectively.

5.5.3. Cross-reactivity Trial

Detection of the target antigen does not exclude the possibility that the antibody might be cross-reactive to other proteins, especially ones that share significant sequence identity with NLRP7. Therefore we decided to test 3-F2 supernatant if it can recognize other NLR related proteins. To achieve this goal, using the lysates of HEK293 cells which were transfected with Myc-NLRC3, Myc-NLRP13, and Myc-NLRP7 plasmids, we performed Western blot using Myc antibody and 3-F2 supernatant. Our results revealed that 3-F2 supernatant does not have any cross-reactivity to either NLRC3 or NLRP13 proteins since it only detected NLRP7 whereas Myc antibody was able to recognize all of them (Figure 5.22). In total, we have produced a hybridoma cell line which continuously secretes a monoclonal antibody that specifically recognizes NLRP7 in both ELISA and Western blotting.

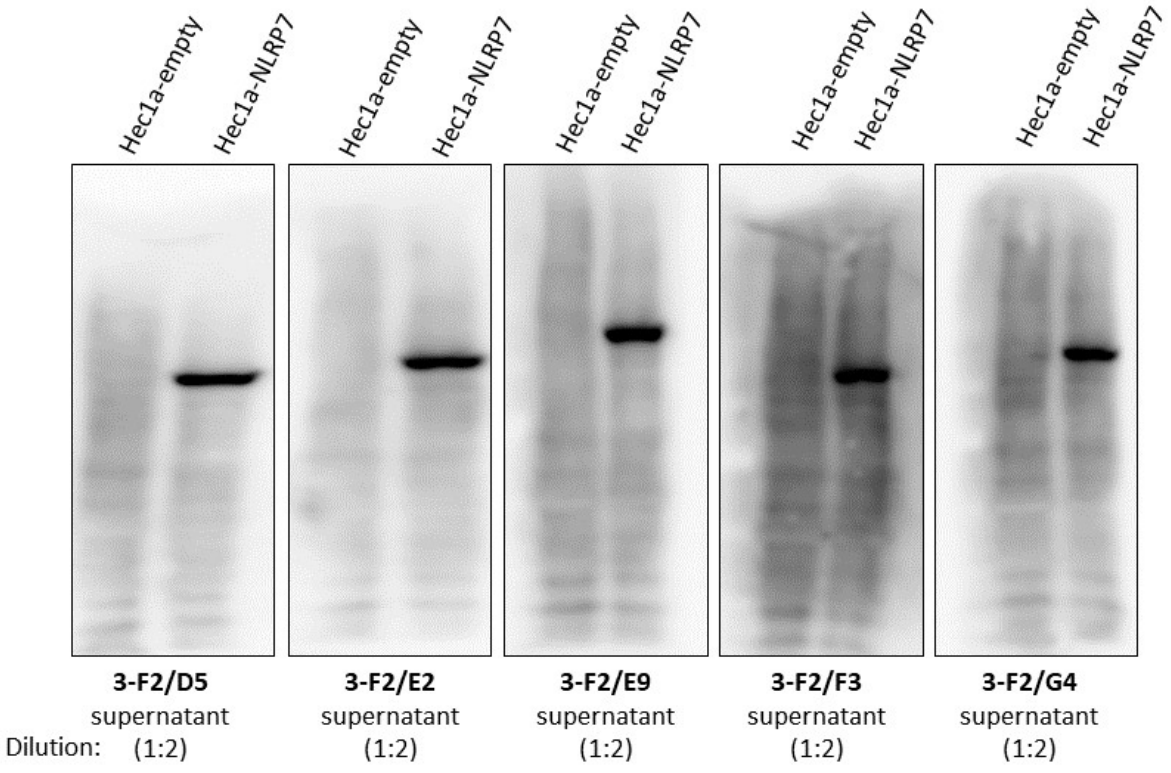

Figure 5.21. All 3F2 sub-colonies continue to produce antibodies against NLRP7 after serial dilutions. Hec1a cell line stably expressing NLRP7 and empty vector was tested by western blot using supernatants of single 3F2 sub-colonies (D5, E2, E9, F3 and G4) in 1:2 dilution.

5.6. Polyclonal Antibody Production Against NLRP7

Polyclonal antibody represents a collection of antibodies from different B cells that secrete antibodies which recognize multiple epitopes on the same antigen. Each of these individual antibodies recognizes a unique epitope that is located on that antigen (Figure 5.23A). Because we think this can be advantageous for us to detect endogenous NLRP7, we also decided to generate a polyclonal antibody. For this purpose, purified His-tagged NLRP7 was injected into a four-five months old New Zealand rabbit. Then, the plasma samples were tested with ELISA and western blot to verify the successful immunization of the rabbit. As it is shown in Figure 5.23B, our polyclonal antibody was able to recognize Myc-NLRP7 protein produced in HEK293 cells.

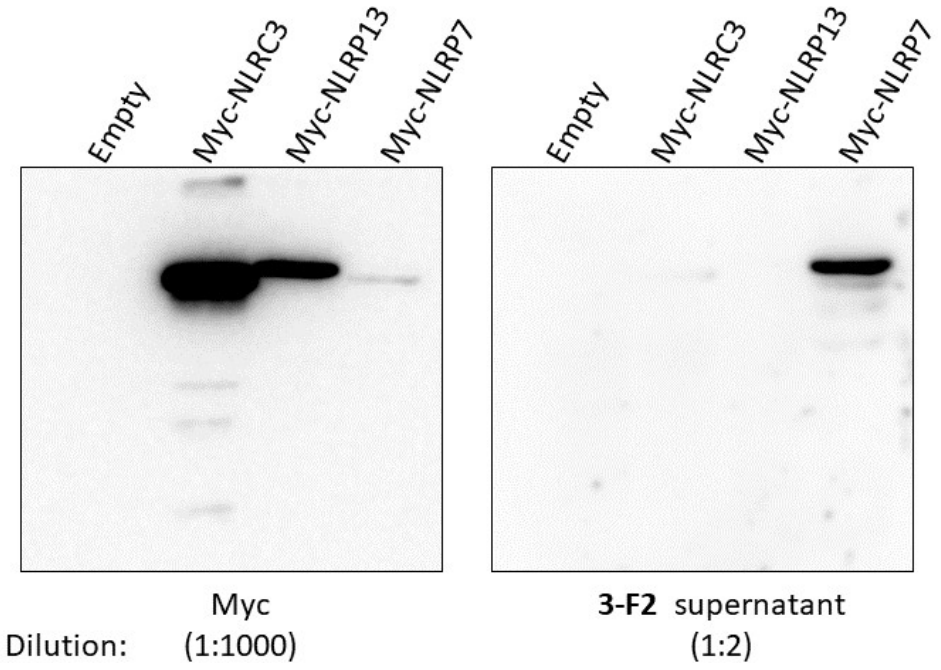

Figure 5.22. Homemade monoclonal antibody did not give cross-reactivity with NLRP13 and NLRC3 proteins on SDS-PAGE. Myc-NLRP7, Myc-NLRP13, and Myc-NLRC3 plasmids were transfected into HEK293 cells and protein levels were checked with Myc (left panel) and homemade monoclonal antibody (right panel) in 1:1000 and 1:2 dilution, respectively.

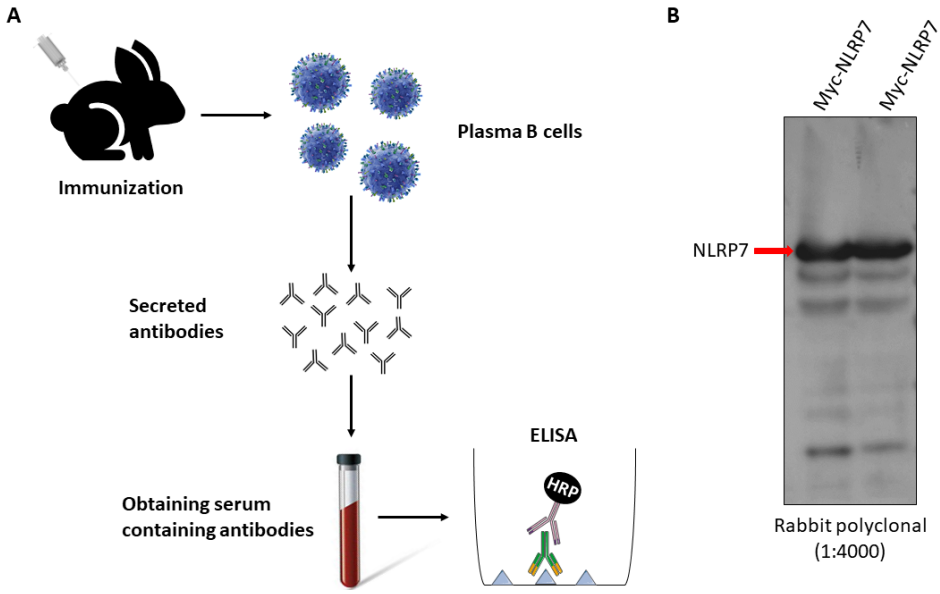

Figure 5.23. Polyclonal rabbit antibody is succesfully generated against NLRP7. A) Diagram shows the production steps of polyclonal antibodies against a desired antigen. B) Myc-NLRP7 transfected HEK293 cell lysates were blotted against NLRP7 using homemade polyclonal rabbit antibody in 1:4000 dilution.

6. CONCLUSION AND DISCUSSION

Our study revealed three novel interactors of an innate immune protein NLRP7 and here we also showed for the first time that it gets modified by SUMO. Furthermore, we observed a dramatic increase in ERK phosphorylation when NLRP7 is upregulated in Hec1a cells. Our initial results indicate that NLRP7 might be an effector protein of two Ras related GTPases, RalB and Rab5A, and it also may interfere with DDR pathways via ATM-Brat1-Chk1 axis. However, more detailed studies are required to pursue NLRP7' oncogenic role in human endometrium cancer (Figure 6.1).

6.1. Analysis of LS-MS/MS Data

Recent studies in our laboratory have demonstrated that NLRP7 may have a tumor promoting role in the progression of human endometrial carcinoma. However, the underlying molecular mechanism behind this phenomenon is hitherto unknown, thus determining with which proteins NLRP7 interacts in Hec1a cells (human endometrium cancer cell line) may provide a possible explanation. Therefore, the major aim of this M.Sc. thesis was to identify novel interaction partners of NLRP7 in Hec1a cells using LC-MS/MS data, previously obtained by our former lab member Aybüke Garipcan. These putative interactor proteins of NLRP7 can be important for its regulation, function and stability or perhaps they can be regulated by NLRP7 itself or vice versa.

Gene ontology analysis of the discovered putative interactors using Panther software revealed that "cellular process" and "metabolic process" have the highest score in the biological process segment. Cellular process refers to any process that occurs at cellular level but not restricted to single cell. Subgroups of cellular process category includes cell cycle, cell adhesion, cell communication, and cell death categories. Changes in cell to cell junctions and morphological disruption of tight junctions have been described in endometrial adenocarcinoma. The cell communication category consists of RalB and Rab5a GTPases and NLRP7 upregulation may cause their dysregulation that results in aberrant cell to cell interactions. On the other hand, metabolic process related

proteins have a role in the chemical reasctions and pathways including anabolism and catabolism resulting in cell growth. In addition to transformation of small molecules, metabolic processes also include processing of macro molecules such as DNA repair and replication, protein synthesis, and degredation. Subgroups of metabolic process category includes bio-synthetic process, catabolic process, cellular metabolic process and small molecule metabolic process.

In order to analyze the link between NLRP7 and its interactors; canonical pathways and interaction networks were generated using IPA tool which regularly updates its databases that combines interaction between proteins from published literature. The mostly enriched canonical pathways were molecular mechanism of cancer, remodelling of epithelial junctions and ATM signaling based on their p-values. The mitogen-activated protein kinase (MAPK) pathway, also known as RAS-RAF-MEK-ERK signaling pathway, can be activated by upstream growth factors and their receptors. Interestingly, RAS and ERK proteins were shown to behave as a regulatory hub, which is related to most of the modulated proteins, as evident from the network analysis. RAS is an oncogene whose mutations are associated with numerous cancers as they disrupts crucial signal transduction pathways which regulates cellular proliferation, differentiation and survival [69]. The activating oncogenic mutations in KRAS (member of Ras superfamily) are also observed in endometrial carcinoma [70]. Remarkably, we revealed that ERK phosphorylation (therefore MAPK pathway activation) is eminently increased in stably NLRP7 expressing Hec1a cell line (Figure 5.3B). Therefore, it is reasonable to speculate that dysregulation of MAPK kinase activation in the presence of NLRP7 may drive abnormal cellular proliferation, eventually leading to cancer. These findings led us to study the mostly enriched Ras related GTPases, RalB and Rab5A, in the MS data to further delineate the implication of NLRP7 in MAPK pathway.

6.2. NLRP7: Putative Effector of Two Small GTPases

Ral (Ras-Like) GTPases belong to Ras superfamily of small GTPases, which have crucial roles in the regulation of diverse cellular functions such as vesicular trafficking, actin organization, tumor formation, metastasis and gene expression [71]. The two Ral GTPases, RalA and RalB, have decisive roles downstream of Ras oncoproteins in oncogenesis and particularly it is known that RalB is involved in invasion and metastasis [72].The mutations of three genes of RAS subfamily HRAS, KRAS, and NRAS have been shown to drive different human cancers such as pancreatic, lung, and colorectal cancers [73]. Moreover, it was observed that 10 to 30 percent of endometrioid endometrial carcinomas includes K-RAS mutations that lead to dysregulation in signal transduction pathways between cell surface receptors and the nucleus [70]. In addition, an unexpected link between inflammation and cancer was found through RalB signaling pathway. Chien *et al.* identified a signaling pathway mediated by the RalB GTPase that promotes both tumor survival and inflammation. They showed that RalB/TBK1 pathway supresses apoptosis in tumor cells whereas the same pathway induces innate immune response in non-tumorogenic cells [74]. In our research, we showed that NLRP7 physically interacts with RalB and this interaction is stronger with the active mutant version which can not hydrolyze GTP (Figure 5.5B). Strong binding with the mutant form indicates that NLRP7 might be an effector protein rather than an activator of RalB. Furthermore, we observed that NLRP7 interacts with endogenous RalB in stably NLRP7 expressing THP-1 cells (human monocytic cell line) which can be interesting to elucidate if NLRP7 and RalB interaction have a role in both oncogenesis and inflammation (Figure A.2, supplementary information).

Rab5A is also a member of the small GTPase superfamily. Although its most known functions are related to endocytosis and vesicle transport, Rab5A upregulation has been shown to contribute cancer progression particularly in breast and ovarian cancers [75]. Furthermore, a recent publication showed that Rab5A regulates cell cycle-associated proteins such as cyclin D1 and matrix metalloproteinase-2 (MMP-2) via inducing the ERK signaling pathway. Their results were also confirmed with ERK inhibitor PD98059 which is partially blocked the role of Rab5A on MMP-2, cell

cycle associated proteins, cell proliferation, and migration. In the end, they claimed that Rab5A induces the malignant phenotype in oral cancer through EMT and the ERK/MMP-2 signaling pathway [75]. In our Co-IP experiment, we observed that these two proteins physically interact and this interaction dramatically increases with the active Rab5A mutant, implying that NLRP7 is an effector protein in a Rab5A regulated pathway (Figure 5.6B). Interestingly, our former lab member Duygu Demiröz has assessed the interplay between these two proteins using IF before we even conducted MS analysis. She found that NLRP7 colocalizes with Rab5A in early endosomes where they probably interact.

6.3. Implication of NLRP7 in DNA damage response

DNA damage occurs continuously in every organism with a number of endogenous and exogenous factors such as harmful radiation like UV, oxidation and chemical carcinogens. If not repaired, damaged DNA accumulates mutations which make diseases like cancer inevitable. Therefore, robust DNA repair systems have evolved to maintain and preserve intact DNA. 2015 Nobel Laureates Aziz Sancar, Tomas Lindahl and Paul Modrich won the Nobel Prize in Chemistry for their excellent contribution to how cells repair DNA damage and protect their genomic integrity [76]. In our MS data, appearing of a protein, Brat1, with a function in DNA damage response (DDR) pathway was interesting since dysregulation of DDR pathway is closely associated with cancer. Although our current knowledge about Brat1 protein is limited, it is known that Brat1 is recruited to DNA double-strand break sites. Briefly, when double-strand breaks occur, ATM kinase localizes to the damaged sites where it gets activated by phosphorylation and triggers downstream signaling pathways. Aglipay *et al.* showed that Brat1 functions in ATM activation by impeding ATM's dephosphorylation via blocking the activity of Protein phosphatase 2A [65]. After ATM activation, additional kinases, Chk1 and Chk2, are also activated through phosphorylation, resulting in P53 phosphorylation and its accumulation. Subsequently, p21 gets stimulated that causes cell cycle arrest in G1 by inactivating G1/S-Cdk and S-Cdk complexes. Our results revealed a novel interaction between NLRP7 and Brat1 via mass spectrometry

and Co-IP (Figure 5.7). However, localization of these proteins are quite different as our IF experiments suggest (Figure 5.8). NLRP7 is predominantly found in the cytoplasm whereas Brat1 showed a dominant nuclear localization with a slight cytoplasmic expression, which raises this question: where and when can NLRP7 and Brat1 be together in the cell? At first, we claimed that NLRP7 may migrate into the nucleus particularly under specific conditions such as DNA damage and predicted the NLS peptides on NLRP7 sequence. Although NLRP7 does not contain strong NLS peptides as expected (Figure 5.9), it contains some peptides that may lead its transportation from cytoplasm to nucleus. On the other hand, the possibility of interaction between two proteins occurs at cytoplasm should be considered. The interaction of these two proteins should be investigated in more detail to assess it occurs where and under which conditions. Since, there is not much known about Brat1 in the literature besides its function in DNA damage response, we hypothesized that NLRP7 may dysregulate proper DNA damage response by interfering with Brat1. Our results indicated that Brat1 expressing cells quickly respond to DNA damage while this response sharply delayed when NLRP7 is expressed upon H_20_2 induced DNA damage depending on the dramatic difference for p-Chk1 levels especially at 6 h time points (Figure 5.10).

6.4. NLRP7 gets modified by both SUMO paralogs

Post-Translational Modifications regulate different aspects of proteins including their enzymatic activity, localization, and stability. So far, scientist revealed that NLRP7 is subjected to ubiquitylation, which negatively regulates its stability through lysosomal degradation. Intriguingly, our MS data suggested that NLRP7 may undergo another modification known as SUMOylation. Our in silico analysis revealed two lysine residues on NLRP7 onto which SUMO may covalently be attached (Figure 5.11A). Indeed, we observed that NLRP7 is modified by both SUMO paralogs (Figure 5.11B). Although SUMOylation cannot be considered as tumour promoting or tumour suppressing modification by itself, it is important for signalling pathways and an essential mechanism in cellular responses to stress. Furthermore, it was observed that global SUMOylation is upregulated in many cancers [68]. Although we showed that NLRP7

may undergo SUMOylation, we don't know the biochemical consequences of this modification on our protein. One of the outcomes might be the stabilization of SUMO modified NLRP7 since SUMOylation can increase protein stability via competing with ubiquitylation which triggers NLRP7 degradation. Dysregulated balance of SUMO and ubiquitin modified NLRP7 may explain why there are more NLRP7 protein in the endometrium carcinoma cells. To test this, the two aforementioned lysine residues can be converted into arginines, which ultimately blocks SUMOylation of this protein. Afterwards, cycloheximide chase experiment can be conducted to assess whether the stability of the NLRP7 is affected.

6.5. Knockdown of NLRP7 using CRISPR/Cas9 Technology

Manipulating the expression of a gene is one of the most powerful way to study its role. We previously tried shRNA based approach to downregulate NLRP7 expression in different cell lines but we could not achieve continuous and complete knockdown. Therefore, we decided to use CRISPR based technologies to obtain stable cell lines and more consistent results. Additionally, after demonstrating the novel interactors and modifiers of NLRP7, we wanted to assess the role of NLRP7 in tumorigenesis using phenotypic assays. For this purpose, we tried different sgRNAs which targets different parts of NLRP7 gene sequence and our preliminary results demonstrated that NLRP7 is downregulated significantly by two sgRNAs, although one of them (termed here as sg7) worked slightly better (Figure 5.13D). After validating NLRP7 knockdown in Hec1a cell line at the mRNA level, we wanted to show it at the protein level to further be sure that these cell are lack of NLRP7 protein. Unfortunately, our commercial antibody could not detect endogenous NLRP7 protein due to some reasons. In addition, since we obtained single cells after DOX induction (note that our system our system is DOX inducible), Sanger sequencing can be performed to validate NLRP7 knockout.

6.6. Antibody Production Against NLRP7

Since our commercial antibody does not work well and there are not many alternatives in the market, we decided to produce both polyclonal and monoclonal homemade anti-NLRP7 antibodies. Polyclonal antibodies are a heterogeneous mix of antibodies since they are derived from the immune response of multiple B-cells and therefore they recognize various epitopes of a single antigen. The advantage of using polyclonal antibodies can be the detection of proteins whose expression levels are low since they amplify the signal by binding more than one epitope. Before the discovery of hybridoma technology, only the polyclonal antibody production methods had been used. Although polyclonal antibodies have thier own advantages, development of the hybridoma technology provided some further advantages, such as less cross-reactivity with other proteins since they come from a single B-cell parent and only recognize a single epitope, generating identical monoclonal antibodies. Both polyclonal and monoclonal NLRP7 antibodies that we produced were able to recognize NLRP7 in Western blotting experiments (Figure 5.21 and 5.23B) and monoclonal antibody does not have any cross-reactivity to other closely related NLR family members, NLRC3 and NLRP13 (Figure 5.22). The characterization of antibodies to use it for immunofluorescence and immunoprecipitation needs to be done. As a further step, expression vectors for recombinant monoclonal antibody production can be generated after obtaining the gene fragments coding for antibody against NLRP7.

Finally, the relationship between inflammation and cancer has been studied for a long time. Especially, chronic inflammation has critical roles in cancer development and progression [77]. Since the innate immunity is the first line of defence in the female genital tract, it is important to understand the role of pattern recognition receptors in these sides. Besides cancer, it is important to understand the role of innate immunity in endometrium since improper inflammatory responses in the endometrium or ovary may cause infertility. Therefore, the link between NLRP7 and cancer can be examined considering the effect of chronic inflammation as a triggering factor of cancer development or progression.

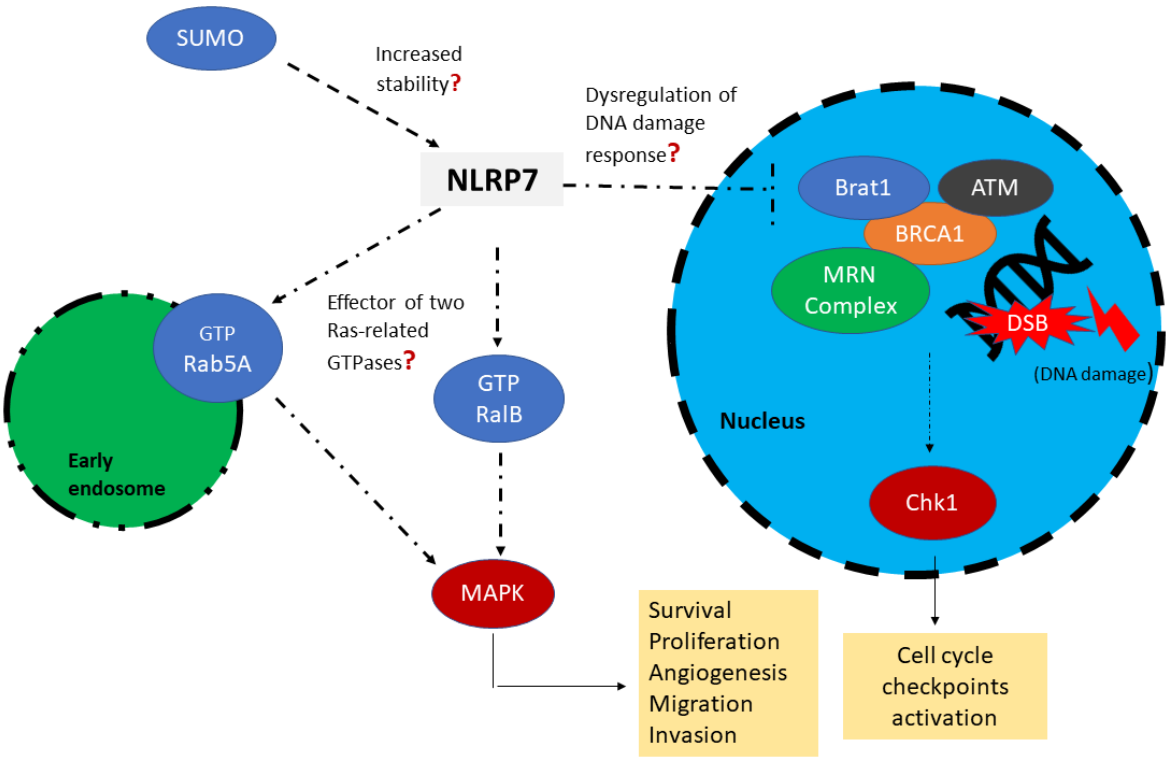

Figure 6.1. Proposed model for how NLRP7 may drive oncogenesis. NLRP7 upregulation may either trigger downstream pathways of two Ras-related GTPases (Rab5A or RalB) or disrupt proper DNA damage response via interfering with Brat1-ATM-Chk1 axis, all of which may result in cancer cell survival, proliferation, invasion or cell cycle dysregulation.

REFERENCES

1. Beutler, B., "Innate immunity: an overview", *Molecular Immunology*, Vol. 40, No. 12, pp. 845–859, 2 2004.

2. Gasteiger, G., A. D'Osualdo, D. A. Schubert, A. Weber, E. M. Bruscia and D. Hartl, "Cellular Innate Immunity: An Old Game with New Players", *Journal of Innate Immunity*, Vol. 9, No. 2, pp. 111–125, 2017.

3. Koenderman, L., W. Buurman and M. R. Daha, "The innate immune response", *Immunology Letters*, Vol. 162, No. 2, pp. 95–102, 12 2014.

4. Takeuchi, O. and S. Akira, "Pattern Recognition Receptors and Inflammation", *Cell*, Vol. 140, No. 6, pp. 805–820, 3 2010.

5. Pelka, K. and D. De Nardo, "Emerging Concepts in Innate Immunity", pp. 1–18, Humana Press, New York, NY, 2018.

6. Lamkanfi, M. and V. M. Dixit, "The inflammasomes.", *PLoS pathogens*, Vol. 5, No. 12, p. e1000510, 12 2009.

7. Kim, Y. K., J.-S. Shin and M. H. Nahm, "NOD-Like Receptors in Infection, Immunity, and Diseases", *Yonsei Medical Journal*, Vol. 57, No. 1, p. 5, 1 2016.

8. Lamkanfi, M. and V. M. Dixit, "Mechanisms and Functions of Inflammasomes", *Cell*, Vol. 157, No. 5, pp. 1013–1022, 5 2014.

9. Lamkanfi, M., L. Vande Walle and T.-D. Kanneganti, "Deregulated inflammasome signaling in disease.", *Immunological reviews*, Vol. 243, No. 1, pp. 163–73, 9 2011.

10. Okada, K., E. Hirota, Y. Mizutani, T. Fujioka, T. Shuin, T. Miki, Y. Nakamura and T. Katagiri, "Oncogenic role of NALP7 in testicular seminomas", *Cancer Science*,

Vol. 95, No. 12, pp. 949–954, 12 2004.

11. Slim, R., P. Coullin, A.-L. Diatta, W. Chebaro, D. Courtin, S. Abdelhak and A. Garcia, "NLRP7 and the genetics of post-molar choriocarcinomas in Senegal", *MHR: Basic science of reproductive medicine*, Vol. 18, No. 1, pp. 52–56, 1 2012.

12. Murdoch, S., U. Djuric, B. Mazhar, M. Seoud, R. Khan, R. Kuick, R. Bagga, R. Kircheisen, A. Ao, B. Ratti, S. Hanash, G. A. Rouleau and R. Slim, "Mutations in NALP7 cause recurrent hydatidiform moles and reproductive wastage in humans", *Nature Genetics*, Vol. 38, No. 3, pp. 300–302, 3 2006.

13. Kinoshita, T., Y. Wang, M. Hasegawa, R. Imamura and T. Suda, "PYPAF3, a PYRIN-containing APAF-1-like protein, is a feedback regulator of caspase-1-dependent interleukin-1beta secretion.", *The Journal of biological chemistry*, Vol. 280, No. 23, pp. 21720–5, 6 2005.

14. Radian, A. D., S. Khare, L. H. Chu, A. Dorfleutner and C. Stehlik, "ATP binding by NLRP7 is required for inflammasome activation in response to bacterial lipopeptides.", *Molecular immunology*, Vol. 67, No. 2 Pt B, pp. 294–302, 10 2015.

15. Khare, S., A. Dorfleutner, N. B. Bryan, C. Yun, A. D. Radian, L. de Almeida, Y. Rojanasakul and C. Stehlik, "An NLRP7-Containing Inflammasome Mediates Recognition of Microbial Lipopeptides in Human Macrophages", *Immunity*, Vol. 36, No. 3, pp. 464–476, 2012.

16. Zhou, Y., S. Z. A. Shah, L. Yang, Z. Zhang, X. Zhou and D. Zhao, "Virulent Mycobacterium bovis Beijing Strain Activates the NLRP7 Inflammasome in THP-1 Macrophages.", *PloS one*, Vol. 11, No. 4, p. e0152853, 2016.

17. Messaed, C., E. Akoury, U. Djuric, J. Zeng, M. Saleh, L. Gilbert, M. Seoud, S. Qureshi and R. Slim, "NLRP7, a nucleotide oligomerization domain-like receptor protein, is required for normal cytokine secretion and co-localizes with Golgi and the microtubule-organizing center.", *The Journal of biological chemistry*, Vol. 286,

No. 50, pp. 43313–23, 12 2011.

18. Abi Nahed, R., D. Reynaud, A. J. Borg, W. Traboulsi, A. Wetzel, V. Sapin, S. Brouillet, M. N. Dieudonné, M. Dakouane-Giudicelli, M. Benharouga, P. Murthi and N. Alfaidy, "NLRP7 is increased in human idiopathic fetal growth restriction and plays a critical role in trophoblast differentiation", *Journal of Molecular Medicine*, Vol. 97, No. 3, pp. 355–367, 3 2019.

19. Bednash, J. S., N. Weathington, J. Londino, M. Rojas, D. L. Gulick, R. Fort, S. Han, A. C. McKelvey, B. B. Chen and R. K. Mallampalli, "Targeting the deubiquitinase STAMBP inhibits NALP7 inflammasome activity", *Nature Communications*, Vol. 8, No. May, p. 15203, 2017.

20. Hanahan, D. and R. A. Weinberg, "Hallmarks of Cancer: The Next Generation", *Cell*, Vol. 144, No. 5, pp. 646–674, 3 2011.

21. Savage, K. J., "Primary Mediastinal Large B-Cell Lymphoma", *The Oncologist*, Vol. 11, No. 5, pp. 488–495, 5 2006.

22. Mottok A. et al., "Genomic Alterations in CIITA Are Frequent in Primary Mediastinal Large B Cell Lymphoma and Are Associated with Diminished MHC Class II Expression", *Cell Reports*, Vol. 13, No. 7, pp. 1418–1431, 11 2015.

23. Carreau, N. A. and C. S. Diefenbach, "Immune targeting of the microenvironment in classical Hodgkin's lymphoma: insights for the hematologist.", *Therapeutic advances in hematology*, Vol. 10, p. 2040620719846451, 2019.

24. Steidl C. et al., "MHC class II transactivator CIITA is a recurrent gene fusion partner in lymphoid cancers", *Nature*, Vol. 471, No. 7338, pp. 377–381, 3 2011.

25. Choi, J., Y. K. Hwang, Y. J. Choi, K. E. Yoo, J. H. Kim, S. J. Nam, J. H. Yang, S. J. Lee, K. H. Yoo, K. W. Sung, H. H. Koo and Y. H. Im, "Neuronal apoptosis inhibitory protein is overexpressed in patients with unfavorable prognostic factors

in breast cancer.", *Journal of Korean medical science*, Vol. 22 Suppl, No. Suppl, pp. 17–23, 9 2007.

26. Chiu, H. H. L., T. M. K. Yong, J. Wang, Y. Wang, R. L. Vessella, T. Ueda, Y.-Z. Wang and M. D. Sadar, "Induction of neuronal apoptosis inhibitory protein expression in response to androgen deprivation in prostate cancer.", *Cancer letters*, Vol. 292, No. 2, pp. 176–85, 6 2010.

27. Allam, R., M. H. Maillard, A. Tardivel, V. Chennupati, H. Bega, C. W. Yu, D. Velin, P. Schneider and K. M. Maslowski, "Epithelial NAIPs protect against colonic tumorigenesis.", *The Journal of experimental medicine*, Vol. 212, No. 3, pp. 369–83, 3 2015.

28. Kutikhin, A. G., "Role of NOD1/CARD4 and NOD2/CARD15 gene polymorphisms in cancer etiology", *Human Immunology*, Vol. 72, No. 10, pp. 955–968, 10 2011.

29. da Silva Correia, J., Y. Miranda, N. Austin-Brown, J. Hsu, J. Mathison, R. Xiang, H. Zhou, Q. Li, J. Han and R. J. Ulevitch, "Nod1-dependent control of tumor growth.", *Proceedings of the National Academy of Sciences of the United States of America*, Vol. 103, No. 6, pp. 1840–5, 2 2006.

30. da Silva Correia, J., Y. Miranda, N. Leonard, J. Hsu and R. J. Ulevitch, "Regulation of Nod1-mediated signaling pathways", *Cell Death & Differentiation*, Vol. 14, No. 4, pp. 830–839, 4 2007.

31. Velloso, F. J., M. C. Sogayar and R. G. Correa, "Expression and in vitro assessment of tumorigenicity for NOD1 and NOD2 receptors in breast cancer cell lines.", *BMC research notes*, Vol. 11, No. 1, p. 222, 4 2018.

32. Velloso, F. J., A. R. Campos, M. C. Sogayar and R. G. Correa, "Proteome profiling of triple negative breast cancer cells overexpressing NOD1 and NOD2 receptors unveils molecular signatures of malignant cell proliferation.", *BMC genomics*, Vol. 20,

No. 1, p. 152, 2 2019.

33. Li, Z.-X., Y.-M. Wang, F.-B. Tang, L. Zhang, Y. Zhang, J.-L. Ma, T. Zhou, W.-C. You and K.-F. Pan, "NOD1 and NOD2 Genetic Variants in Association with Risk of Gastric Cancer and Its Precursors in a Chinese Population.", *PloS one*, Vol. 10, No. 5, p. e0124949, 2015.

34. Asano, N., A. Imatani, T. Watanabe, J. Fushiya, Y. Kondo, X. Jin, N. Ara, K. Uno, K. Iijima, T. Koike, W. Strober and T. Shimosegawa, "Cdx2 Expression and Intestinal Metaplasia Induced by H. pylori Infection of Gastric Cells Is Regulated by NOD1-Mediated Innate Immune Responses.", *Cancer research*, Vol. 76, No. 5, pp. 1135–45, 3 2016.

35. Liu, R., A. D. Truax, L. Chen, P. Hu, Z. Li, J. Chen, C. Song, L. Chen and J. P.-Y. Ting, "Expression profile of innate immune receptors, NLRs and AIM2, in human colorectal cancer: correlation with cancer stages and inflammasome components.", *Oncotarget*, Vol. 6, No. 32, pp. 33456–69, 10 2015.

36. Udden, S. M. N., L. Peng, J.-L. Gan, J. M. Shelton, J. S. Malter, L. V. Hooper and M. H. Zaki, "NOD2 Suppresses Colorectal Tumorigenesis via Downregulation of the TLR Pathways.", *Cell reports*, Vol. 19, No. 13, pp. 2756–2770, 6 2017.

37. Karki, R., R. K. S. Malireddi, Q. Zhu and T.-D. Kanneganti, "NLRC3 regulates cellular proliferation and apoptosis to attenuate the development of colorectal cancer.", *Cell cycle (Georgetown, Tex.)*, Vol. 16, No. 13, pp. 1243–1251, 7 2017.

38. Kolb R. et al., "Obesity-associated NLRC4 inflammasome activation drives breast cancer progression.", *Nature communications*, Vol. 7, p. 13007, 2016.

39. Yoshihama, S., J. Roszik, I. Downs, T. B. Meissner, S. Vijayan, B. Chapuy, T. Sidiq, M. A. Shipp, G. A. Lizee and K. S. Kobayashi, "NLRC5/MHC class I transactivator is a target for immune evasion in cancer.", *Proceedings of the National Academy of Sciences of the United States of America*, Vol. 113, No. 21, pp.

5999–6004, 5 2016.

40. Du, Q., Q. Wang, H. Fan, J. Wang, X. Liu, H. Wang, Y. Wang and R. Hu, "Dietary cholesterol promotes AOM-induced colorectal cancer through activating the NLRP3 inflammasome", *Biochemical Pharmacology*, Vol. 105, pp. 42–54, 4 2016.

41. Zhao, Y., Q. Guo, K. Zhao, Y. Zhou, W. Li, C. Pan, L. Qiang, Z. Li and N. Lu, "Small molecule GL-V9 protects against colitis-associated colorectal cancer by limiting NLRP3 inflammasome through autophagy.", *Oncoimmunology*, Vol. 7, No. 1, p. e1375640, 2017.

42. Deng, Q., Y. Geng, L. Zhao, R. Li, Z. Zhang, K. Li, R. Liang, X. Shao, M. Huang, D. Zuo, Y. Wu and Q. Ma, "NLRP3 inflammasomes in macrophages drive colorectal cancer metastasis to the liver", *Cancer Letters*, Vol. 442, pp. 21–30, 2 2019.

43. Wang, H., Y. Wang, Q. Du, P. Lu, H. Fan, J. Lu and R. Hu, "Inflammasome-independent NLRP3 is required for epithelial-mesenchymal transition in colon cancer cells", *Experimental Cell Research*, Vol. 342, No. 2, pp. 184–192, 3 2016.

44. Zaki, M. H., P. Vogel, M. Body-Malapel, M. Lamkanfi and T.-D. Kanneganti, "IL-18 Production Downstream of the Nlrp3 Inflammasome Confers Protection against Colorectal Tumor Formation", *The Journal of Immunology*, Vol. 185, No. 8, pp. 4912–4920, 10 2010.

45. Dupaul-Chicoine, J., A. Arabzadeh, M. Dagenais, T. Douglas, C. Champagne, A. Morizot, I. G. Rodrigue-Gervais, V. Breton, S. L. Colpitts, N. Beauchemin and M. Saleh, "The Nlrp3 Inflammasome Suppresses Colorectal Cancer Metastatic Growth in the Liver by Promoting Natural Killer Cell Tumoricidal Activity", *Immunity*, Vol. 43, No. 4, pp. 751–763, 10 2015.

46. Normand, S., A. Delanoye-Crespin, A. Bressenot, L. Huot, T. Grandjean, L. Peyrin-Biroulet, Y. Lemoine, D. Hot and M. Chamaillard, "Nod-like receptor

pyrin domain-containing protein 6 (NLRP6) controls epithelial self-renewal and colorectal carcinogenesis upon injury.", *Proceedings of the National Academy of Sciences of the United States of America*, Vol. 108, No. 23, pp. 9601–6, 6 2011.

47. Zaki, M. H., P. Vogel, R. S. Malireddi, M. Body-Malapel, P. K. Anand, J. Bertin, D. R. Green, M. Lamkanfi and T.-D. Kanneganti, "The NOD-Like Receptor NLRP12 Attenuates Colon Inflammation and Tumorigenesis", *Cancer Cell*, Vol. 20, No. 5, pp. 649–660, 11 2011.

48. Allen, I. C., J. E. Wilson, M. Schneider, J. D. Lich, R. A. Roberts, J. C. Arthur, R.-M. T. Woodford, B. K. Davis, J. M. Uronis, H. H. Herfarth, C. Jobin, A. B. Rogers and J. P.-Y. Ting, "NLRP12 Suppresses Colon Inflammation and Tumorigenesis through the Negative Regulation of Noncanonical NF-κB Signaling", *Immunity*, Vol. 36, No. 5, pp. 742–754, 5 2012.

49. Pontillo, A., P. Bricher, V. Leal, S. Lima, P. Souza and S. Crovella, "Role of inflammasome genetics in susceptibility to HPV infection and cervical cancer development", *Journal of Medical Virology*, Vol. 88, No. 9, pp. 1646–1651, 9 2016.

50. He, A., J. Shao, Y. Zhang, H. Lu, Z. Wu, Y. Xu, A. He, J. Shao, Y. Zhang, H. Lu, Z. Wu and Y. Xu, "CD200Fc reduces LPS-induced IL-1b; activation in human cervical cancer cells by modulating TLR4-NFk-B and NLRP3 inflammasome pathway", *Oncotarget*, Vol. 8, No. 20, pp. 33214–33224, 5 2017.

51. Staff, T. P. O., "Correction: The NOD-Like Receptor Signalling Pathway in Helicobacter pylori Infection and Related Gastric Cancer: A Case-Control Study and Gene Expression Analyses", *PLOS ONE*, Vol. 10, No. 1, p. e0117870, 1 2015.

52. Li, S., X. Liang, L. Ma, L. Shen, T. Li, L. Zheng, A. Sun, W. Shang, C. Chen, W. Zhao and J. Jia, "MiR-22 sustains NLRP3 expression and attenuates H. pylori-induced gastric carcinogenesis", *Oncogene*, Vol. 37, No. 7, pp. 884–896, 2 2018.

53. Wang, H., G. Xu, Z. Huang, W. Li, H. Cai, Y. Zhang, D. Xiong, G. Liu,

S. Wang, Z. Xue and Q. Luo, "LRP6 targeting suppresses gastric tumorigenesis via P14ARF-Mdm2-P53-dependent cellular senescence.", *Oncotarget*, Vol. 8, No. 67, pp. 111597–111607, 12 2017.

54. Tarassishin, L., D. Casper and S. C. Lee, "Aberrant Expression of Interleukin-1β and Inflammasome Activation in Human Malignant Gliomas", *PLoS ONE*, Vol. 9, No. 7, p. e103432, 7 2014.

55. Yin, X.-F., Q. Zhang, Z.-Y. Chen, H.-F. Wang, X. Li, H.-X. Wang, H.-X. Li, C.-M. Kang, S. Chu, K.-F. Li, Y. Li and Y.-R. Qiu, "NLRP3 in human glioma is correlated with increased WHO grade, and regulates cellular proliferation, apoptosis and metastasis via epithelial-mesenchymal transition and the PTEN/AKT signaling pathway.", *International journal of oncology*, Vol. 53, No. 3, pp. 973–986, 9 2018.

56. Li, L. and Y. Liu, "Aging-related gene signature regulated by Nlrp3 predicts glioma progression.", *American journal of cancer research*, Vol. 5, No. 1, pp. 442–9, 2015.

57. Shang, S., L. Wang, Y. Zhang, H. Lu and X. Lu, "The Beta-Hydroxybutyrate Suppresses the Migration of Glioma Cells by Inhibition of NLRP3 Inflammasome", *Cellular and Molecular Neurobiology*, Vol. 38, No. 8, pp. 1479–1489, 11 2018.

58. Ding, Q., L. Shen, X. Nie, B. Lu, X. Pan, Z. Su, A. Yan, R. Yan, Y. Zhou, L. Li and J. Xu, "MiR-223-3p overexpression inhibits cell proliferation and migration by regulating inflammation-associated cytokines in glioblastomas", *Pathology - Research and Practice*, Vol. 214, No. 9, pp. 1330–1339, 9 2018.

59. Kashyap, M., S. Pore, Z. Wang, J. Gingrich, N. Yoshimura and P. Tyagi, "Inflammasomes are important mediators of prostatic inflammation associated with BPH", *Journal of Inflammation*, Vol. 12, No. 1, p. 37, 12 2015.

60. Zhong F. et al., "Germline NLRP1 Mutations Cause Skin Inflammatory and Cancer Susceptibility Syndromes via Inflammasome Activation", *Cell*, Vol. 167, No. 1, pp. 187–202, 9 2016.

61. Ohno, S., T. Kinoshita, Y. Ohno, T. Minamoto, N. Suzuki, M. Inoue and T. Suda, "Expression of NLRP7 (PYPAF3, NALP7) protein in endometrial cancer tissues", *Anticancer Research*, Vol. 28, No. 4 C, pp. 2493–2497, 2008.

62. Velloso, F. J., M. Trombetta-Lima, V. Anschau, M. C. Sogayar and R. G. Correa, "NOD-like receptors: major players (and targets) in the interface between innate immunity and cancer", *Bioscience Reports*, Vol. 9, No. 39, 2019.

63. Livak, K. J. and T. D. Schmittgen, "Analysis of Relative Gene Expression Data Using Real-Time Quantitative PCR and the $2-\Delta\Delta$CT Method", *Methods*, Vol. 25, No. 4, pp. 402–408, 12 2001.

64. Bernhofer, M., T. Goldberg, S. Wolf, M. Ahmed, J. Zaugg, M. Boden and B. Rost, "NLSdb-major update for database of nuclear localization signals and nuclear export signals.", *Nucleic acids research*, Vol. 46, No. D1, pp. D503–D508, 1 2018.

65. Aglipay, J. A., S. A. Martin, H. Tawara, S. W. Lee and T. Ouchi, "ATM activation by ionizing radiation requires BRCA1-associated BAAT1.", *The Journal of biological chemistry*, Vol. 281, No. 14, pp. 9710–8, 4 2006.

66. Pichler, A., C. Fatouros, H. Lee and N. Eisenhardt, "SUMO conjugation – a mechanistic view", *Biomolecular Concepts*, Vol. 8, No. 1, pp. 13–36, 1 2017.

67. Barry, R., S. W. John, G. Liccardi, T. Tenev, I. Jaco, C.-H. Chen, J. Choi, P. Kasperkiewicz, T. Fernandes-Alnemri, E. Alnemri, M. Drag, Y. Chen and P. Meier, "SUMO-mediated regulation of NLRP3 modulates inflammasome activity", *Nature Communications*, Vol. 9, No. 1, p. 3001, 12 2018.

68. Seeler, J.-S. and A. Dejean, "SUMO and the robustness of cancer", *Nature Reviews Cancer*, Vol. 17, No. 3, pp. 184–197, 3 2017.

69. Fernández-Medarde, A. and E. Santos, "Ras in cancer and developmental diseases.", *Genes & cancer*, Vol. 2, No. 3, pp. 344–58, 3 2011.

70. Ma, X., C. X. Ma and J. Wang, "Endometrial Carcinogenesis and Molecular Signaling Pathways", *American Journal of Molecular Biology*, Vol. 4, pp. 134–149, 2014.

71. Gentry, L. R., T. D. Martin, D. J. Reiner and C. J. Der, "Ral small GTPase signaling and oncogenesis: More than just 15 minutes of fame", *Biochimica et Biophysica Acta (BBA) - Molecular Cell Research*, Vol. 1843, No. 12, pp. 2976–2988, 12 2014.

72. Zago, G., I. Veith, M. K. Singh, L. Fuhrmann, S. De Beco, A. Remorino, S. Takaoka, M. Palmeri, F. Berger, N. Brandon, A. El Marjou, A. Vincent-Salomon, J. Camonis, M. Coppey and M. C. Parrini, "RalB directly triggers invasion downstream Ras by mobilizing the Wave complex", *eLife*, Vol. 7, 10 2018.

73. Yan, C. and D. Theodorescu, "RAL GTPases: Biology and Potential as Therapeutic Targets in Cancer", *Pharmacological Reviews*, Vol. 70, No. 1, pp. 1–11, 1 2018.

74. Mantovani, A. and F. Balkwill, "RalB Signaling: A Bridge between Inflammation and Cancer", *Cell*, Vol. 127, No. 1, pp. 42–44, 2006.

75. Zhang, D., C. Lu and H. Ai, "Rab5a is overexpressed in oral cancer and promotes invasion through ERK/MMP signaling", *Molecular Medicine Reports*, Vol. 16, No. 4, pp. 4569–4576, 2017.

76. Basu, A. K., "DNA Damage, Mutagenesis and Cancer.", *International journal of molecular sciences*, Vol. 19, No. 4, 3 2018.

77. Saxena, M. and G. Yeretssian, "NOD-Like Receptors: Master Regulators of Inflammation and Cancer", *Frontiers in Immunology*, Vol. 5, p. 327, 7 2014.

APPENDIX A: SUPPLEMENTARY INFORMATION

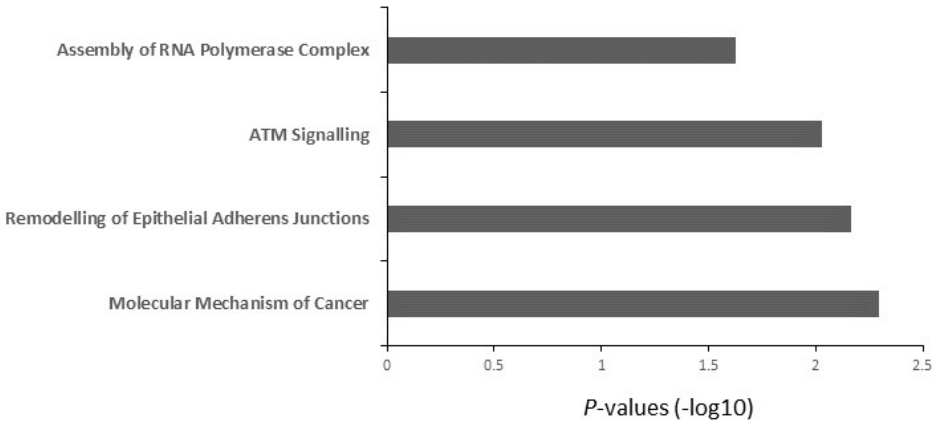

Figure A.1. Top canonical pathways of NLRP7 and its interactors determined via by IPA tool.

Table A.1: Mass Spectrometry results.

Protein Names	**Log2-rel-fc (NLRP7/Control1)**	**Log2-rel-fc (NLRP7/Control2)**
Methyltransferase-like protein 7B	9.58	10.81
Peroxisome biogenesis factor 1	6.19	7.46
DNA-directed RNA polymerase II subunit RPB1	2.08	2.91
Ig gamma-2 chain C region	4.11	12.78
Neuroblastoma-amplified sequence	8.59	5.64
von Willebrand factor A domain containing protein 8	2.63	3.22
Sulfatase-modifying factor 2	2.04	9.31
Prothymosin alpha	2.55	3.65
Eukaryotic translation elongation factor1 epsilon-1	2.16	12.87
Condensin complex subunit 2	9.27	9.88

Table A.1. Mass Spectrometry results (cont.).

Protein Names	**Log2-rel-fc (NLRP7/Control1)**	**Log2-rel-fc (NLRP7/Control2)**
Exocyst complex component 6	7.00	7.27
Cullin-9	3.16	6.91
Squalene synthase	2.26	9.82
DNA-binding protein SMUBP-2	10.12	10.04
DNA polymerase epsilon catalytic subunit A	6.97	4.27
Laminin subunit beta-1	4.48	2.66
Neurofibromin truncated	6.35	6.89
Nicastrin	4.20	9.34
Condensin-2 complex subunit G2	2.53	6.83
Liprin-beta-1	8.47	9.31
WD repeat-containing protein 61	10.48	10.39
Protein spinster homolog 1	11.39	10.51
Fanconi anemia group D2 protein	8.04	8.56
Bifunctional protein NCOAT	9.16	9.90
Proteasome-associated protein ECM29 homolog	6.71	6.03
Tubulin-folding cofactor B	2.70	9.54
Vacuole membrane protein 1	14.17	14.55
Glutaminyl-peptide cyclotransferase-like protein	9.84	11.98
Eukaryotic tranlation initiation factor 3 subunit K	9.78	9.41
Gamma-glutamylcyclotransferase	2.36	11.79
DNA-directed RNA polymerase mitochondrial	2.74	7.61

Table A.1. Mass Spectrometry results (cont.).

Protein Names	**Log2-rel-fc (NLRP7/Control1)**	**Log2-rel-fc (NLRP7/Control2)**
ANK repeat and PH domain-containing protein 2	11.20	11.31
Thiamine transporter 1	11.79	12.88
Pre-mRNA-splicing factor SPF27	11.30	13.87
Splicing factor, arginine/serine rich 15	6.73	8.13
Collagen alpha-1(I) chain	8.83	9.15
Ornithine aminotransferase	8.58	10.49
Glycogen phosphorylase	2.89	8.09
Ras-related protein Ral-B	11.81	10.97
Histone H1.2	2.28	12.45
Ras-related protein Rab-5A	10.36	8.80
Peptidyl-prolyl cis-trans isomerase FKBP2	2.03	13.02
Carbamoyl-phosphate synthase	2.68	4.57
Serine hydroxymethyltransferase	2.60	10.68
Short/chain branch specific acyl-CoA dehydrogenase	9.96	9.06
Double-strand break repair protein MRE11A	5.85	11.50
E3 ubiquitin-protein ligase TRIM32	6.60	4.01
Ribosomal RNA processing protein 1 homolog B	10.10	8.96
Probable E3 ubiquitin-protein ligase HERC1	6.03	8.57
Melanoma-associated antigen D2	8.68	2.81

Table A.1. Mass Spectrometry results (cont.).

Protein Names	**Log2-rel-fc (NLRP7/Control1)**	**Log2-rel-fc (NLRP7/Control2)**
E3 ubiquitin-protein ligase HECTD3	2.48	7.50
General transcription factor 3C polypeptide 5	8.50	7.40
Rho guanine nucleotide exchange factor 2	7.70	10.80
BRCA1-associated ATM activator 1	8.66	8.22
Rapamycin-insensitive companinon of mTOR	2.36	8.28
Eukaryotic translation initiation factor 3 subunit M	3.27	9.05
FAST kinase domian-containing protein 5	2.26	10.64
Protein MON2 homolog	6.13	8.94
Polyadenylate-binding protein 2	2.22	8.93
Transcriptional repressor p66-alpha	8.24	9.10
Hermansky-Pudlak syndrome 6 protein	7.08	7.68
Integrator complex subunit 1	7.16	4.93
Zinc finger protein 511	9.42	8.55
RNA polymerase-associated protein LEO1	6.71	8.73
DNA repair protein RAD50	2.14	3.30
Serine/threonine-protein phosphatase PGAM5	8.58	12.75
Exocyst complex component 2	7.37	6.36

Table A.1. Mass Spectrometry results (cont.).

Protein Names	**Log2-rel-fc (NLRP7/Control1)**	**Log2-rel-fc (NLRP7/Control2)**
Glutamate-rich WD repeat-containing protein 1	13.40	3.40
Partner of Y14 and mago	8.23	13.63
UPF0488 protein C8orf33	5.34	3.50
GrpE protein homolog 1	11.06	7.01
GPN-loop GTPase 1	2.31	9.96
Kinesin-like protein KIF13B	6.88	5.63
L-aminoadipate-semialdehyde dehydrogenase-phosphopantetheinyl transferase	9.73	7.71
Endoplasmic reticulum aminopeptidase 1	2.26	7.75
Poly [ADP-ribose] polymerase 4	7.80	5.66
General transcription factor 3C polypeptide 4	5.29	8.09
Pre-mRNA-processing factor 19	5.49	6.96
Endoribonuclease Dicer	4.28	5.83
General transcription factor 3C polypeptide 3	8.28	2.98

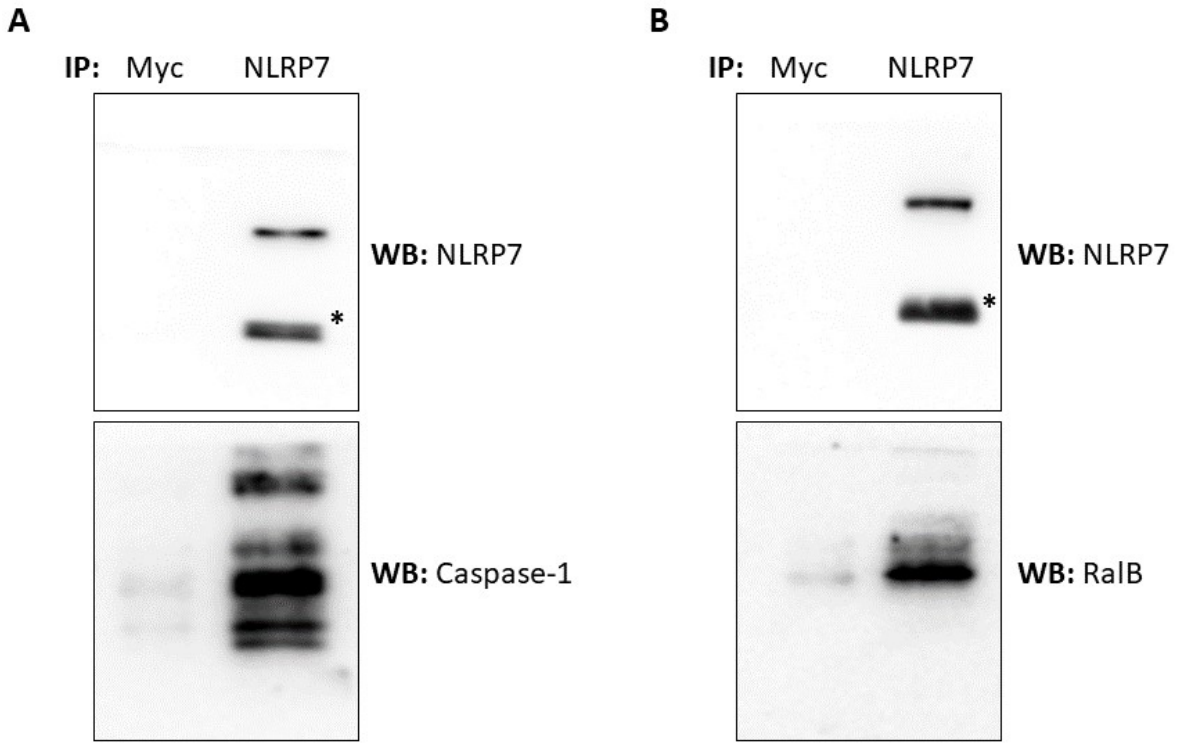

Figure A.2. NLRP7 interacts with RalB in THP-1 cells. A) NLRP7 interaction with endogeneous Caspase-1 were used as a positive control. B) Endogeneous RalB interacts with NLRP7 in THP-1 cells. Co-IP experiment was performed as previously described. Myc pull-down was performed for negative control. Asterisks denote heavy chains.

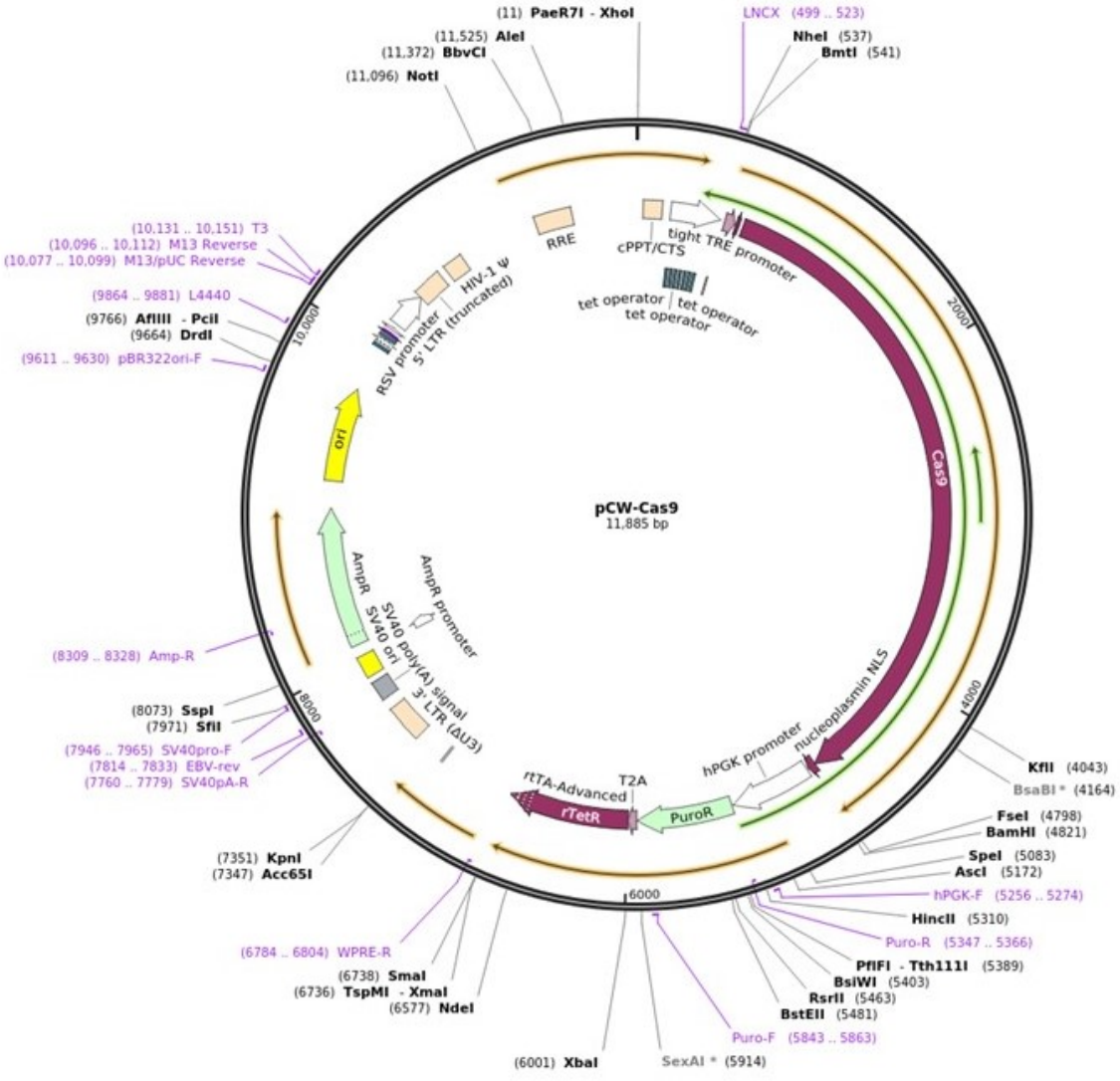

Figure A.3. Addgene Full Sequence Map for pCW-Cas9.

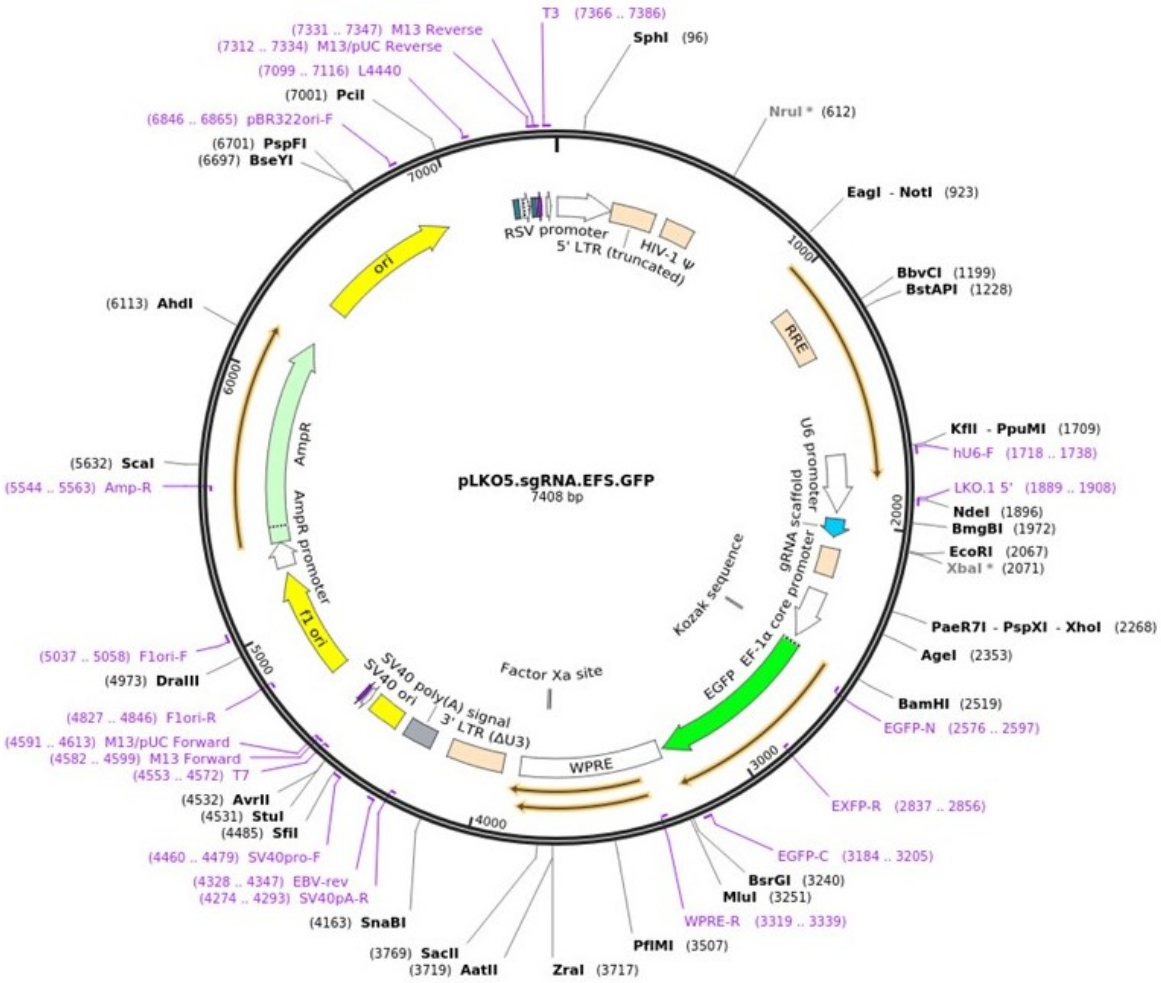

Figure A.4. Addgene Full Sequence Map for pLKO5.sgRNA.

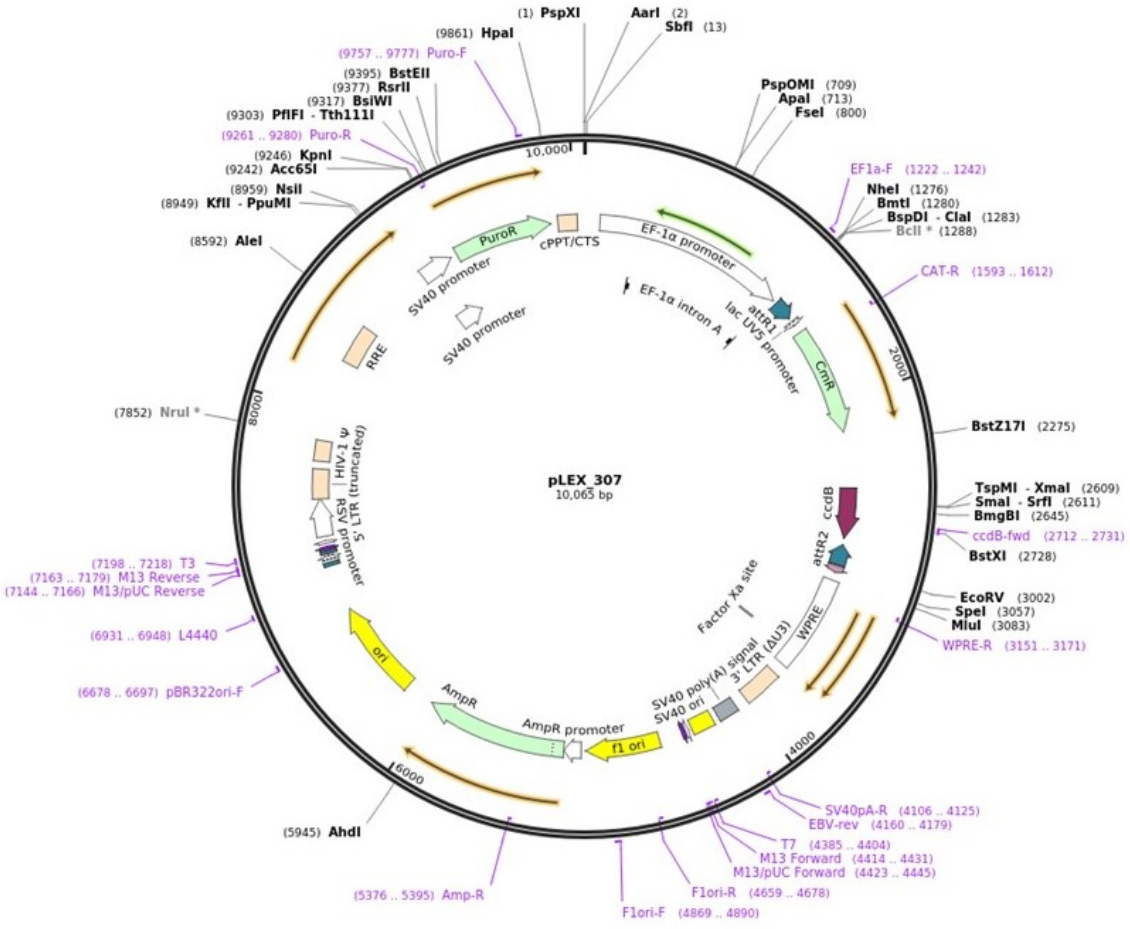

Figure A.5. Addgene Full Sequence Map for pLEX307.